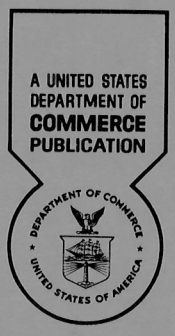

WEATHER BUREAU
Office of Systems Development
Techniques Development Laboratory
Silver Spring, Md.

September 1969

Charts Giving Station Precipitation in the Plateau States from 850- and 500-Millibar Lows During Winter

Technical Memorandum WBTM TDL 25

U.S. DEPARTMENT OF COMMERCE / ENVIRONMENTAL SCIENCE SERVICES ADMINISTRATION

ESSA TECHNICAL MEMORANDA

Weather Bureau, Techniques Development Laboratory Series

The primary purpose of the Techniques Development Laboratory of the Office of Systems Development is to translate increases in basic knowledge in meteorology and allied disciplines into improved operating techniques and procedures. To achieve this goal, TDL conducts and sponsors applied research and development aimed at improvement of diagnostic and prognostic methods for producing weather information. The laboratory carries out studies both for the general improvement of prediction methodology used in the National Meteorological Service System and for more effective utilization of weather forecasts by the ultimate user.

ESSA Technical Memoranda in the Weather Bureau Techniques Development Laboratory series facilitate rapid distribution of material which may be preliminary in nature and which may be published formally elsewhere at a later date. The first five papers in the TDL series are part of the former Weather Bureau Technical Notes series.

Papers listed below are available from the Clearinghouse for Federal Scientific and Technical Information, U.S. Department of Commerce, Sills Bldg., 5285 Port Royal Road, Springfield, Va. 22151. Price: $3.00 hard copy; $0.65 microfiche. Order by accession number shown in parentheses at end of each entry.

TN 10 TDL 1 Objective Prediction of Daily Surface Temperature. William H. Klein, Curtis W. Crockett, and Carlos R. Dunn, October 1965. (PB-168 590)

TN 11 TDL 2 Hurricane Cindy Galveston Bay Tides. N. A. Pore, A. T. Angelo, and J. G. Taylor, September 1965. (PB-168 608)

TN 29 TDL 3 Atmospheric Effects on Re-Entry Vehicle Dispersions. Karl R. Johannessen, December 1965. (PB-169 381)

TN 45 TDL 4 A Synoptic Climatology of Winter Precipitation from 700-mb. Lows for the Intermountain Areas of the West. D. L. Jorgensen, W. H. Klein, and A. F. Korte, May 1966. (PB-170 635)

TN 47 TDL 5 Hemispheric Specification of Sea Level Pressure from Numerical 700-mb. Height Forecasts. William H. Klein and Billy M. Lewis, June 1966. (PB-173 091)

WBTM TDL 6 A Fortran Program for the Calculation of Hourly Values of Astronomical Tide and Time and Height of High and Low Water. N. A. Pore and R. A. Cummings, January 1967. (PB-174 660)

WBTM TDL 7 Numerical Experiments Leading to the Design of Optimum Global Meteorological Networks. M. A. Alaka and F. Lewis, February 1967. (PB-174 497)

WBTM TDL 8 An Experiment in the Use of the Balance Equation in the Tropics. M. A. Alaka, D. T. Rubsam, and G. E. Fisher, March 1967. (PB-174 501)

WBTM TDL 9 A Survey of Studies of Aerological Network Requirements. M. A. Alaka, May 1967. (PB-174 984)

WBTM TDL 10 Objective Determination of Sea Level Pressure from Upper Level Heights. William Klein, Frank Lewis, and John Stackpole, May 1967. (PB-179 949)

WBTM TDL 11 Short Range, Subsynoptic Surface Weather Prediction. H. R. Glahn and D. A. Lowry, July 1967. (PB-175 772)

WBTM TDL 12 Charts Giving Station Precipitation in the Plateau States from 700-Mb. Lows During Winter. D. L. Jorgensen, A. F. Korte, and J. A. Bunce, Jr., October 1967. (PB-176 742)

(Continued on inside back cover)

U.S. DEPARTMENT OF COMMERCE
Environmental Science Services Administration
Weather Bureau

ESSA Technical Memorandum WBTM TDL 25

CHARTS GIVING STATION PRECIPITATION IN THE PLATEAU STATES FROM 850- AND 500-MILLIBAR LOWS DURING WINTER

August F. Korte, Donald L. Jorgensen,
and
William H. Klein

OFFICE OF SYSTEMS DEVELOPMENT
TECHNIQUES DEVELOPMENT LABORATORY

SILVER SPRING, MD.
September 1969

UDC 551.589.1:551.577.36:551.515.12(78)"324"

551.5	Meteorology
.589.1	Synoptic climatology
.577.36	Precipitation frequencies
.515	Distribution of elements in
.12	extratropical cyclones
(78)	Plateau States
"324"	Winter

CONTENTS

CHARTS GIVING STATION PRECIPITATION IN THE PLATEAU STATES FROM 850- AND 500-MB LOWS DURING WINTER

August F. Korte, Donald L. Jorgensen, and William H. Klein

ABSTRACT

Probabilities of precipitation from 850-mb and 500-mb lows are derived for selected stations in the Intermountain West during winter. It is found that the precipitation generally appears to be best specified at the lower levels and by the most intense lows. Considerable variability is found between stations, partly as a result of differences in their elevation, surrounding topography, and latitude. The relative effectiveness of each level in specifying precipitation is illustrated for several stations with varying characteristics. The application of these charts as forecast aids is presented.

INTRODUCTION

This study presents concluding results of the development of a synoptic climatology for the intermountain region of the West relating precipitation to cyclones in the lower troposphere during winter. Earlier studies [2, 5] described the manner in which winter precipitation was generally distributed relative to the position and intensity of low centers at several levels. A later study [3] gave the observed precipitation in terms of frequency of occurrence and amounts for selected stations resulting from cyclones at the 700-mb level. The present investigation extends the study of individual stations to the 850- and 500-mb levels.

In the earlier studies, a moving grid centered on the cyclone at a particular atmospheric level was used to obtain the precipitation pattern relative to the storm center at that level [1]. This pattern could then be applied to any station coming under the influence of the storm. This approach tended to average out the orographic effects, while maintaining the dynamic factors of the storm system. The use of a stationary grid, on the other hand, takes into account the topography surrounding the station as well as the dynamics of the storm. The moving grid was found useful for generalized studies of a large area [2, 5], while the stationary grid gave more useful results for specific station locations [3].

In both the moving and stationary grid approach, the precipitation occurring in the grid area was processed and summarized by computer. Analysis of the results produced synoptic climatological charts of measurable precipitation frequencies. These frequencies, when used in a forecasting sense, can be interpreted as representing the probabilities of occurrence of the precipitation event. Averaged precipitation amounts were also derived

for both methods.

The present study uses the stationary grid approach. Charts are presented which describe the frequency (probability) of occurrence of precipitation associated with the 850-mb and 500-mb atmospheric levels for 35 stations in the western Plateau area. Expected average amounts are also indicated for the various frequency levels.

Our earlier study [5] shows that the lows over the area studied were concentrated in the southern sector; hence the average data there are more reliable. It was also found that lows at the lower levels generally have a larger maximum frequency of precipitation, located nearer their center, than those at the upper levels. Similar characteristics can be observed in some of the station charts shown in Appendix B.

ACQUISITION AND ANALYSIS OF DATA

The winter period investigated included the months of December, January, and February for the years 1951 through 1964.

Figure 1 shows the area of study (enclosed by heavy dashed lines) that included all of the lows observed from 90° to 125°W. Longitude and 25° to

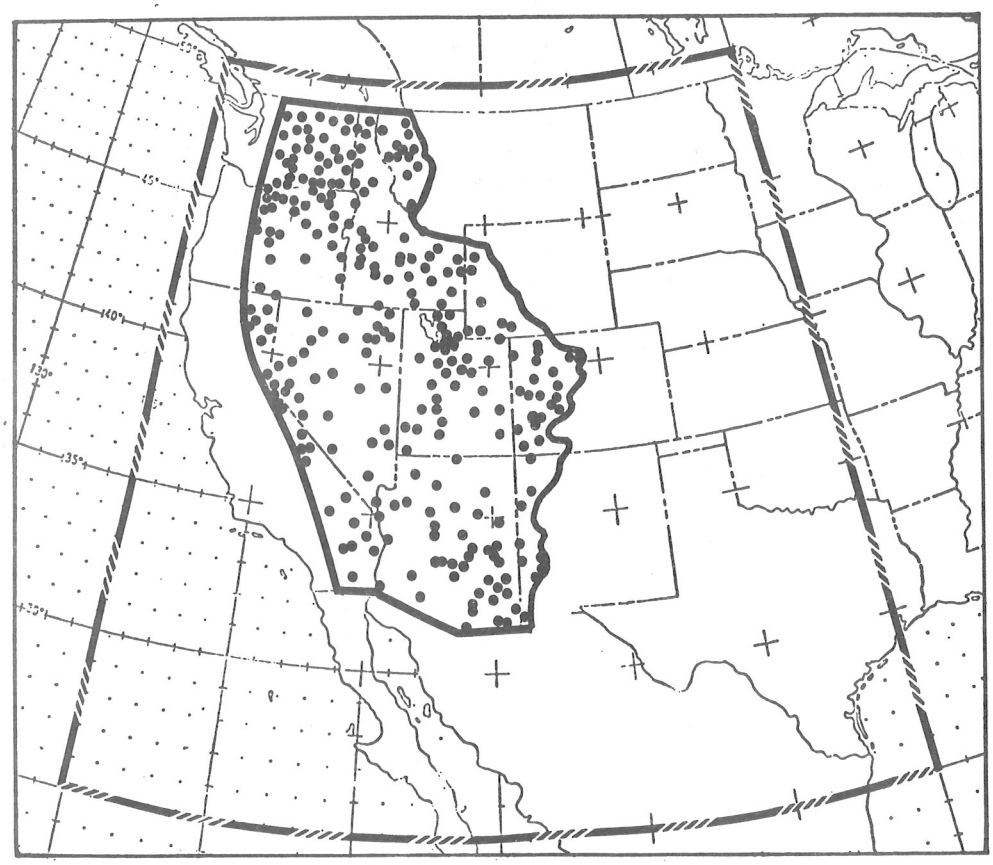

Figure 1.--Chart showing observational area (enclosed by heavy lines) from which upper low data were obtained and precipitation station network (black dots).

50°N. Latitude. The black dots represent the observational network of 280 precipitation stations in the Plateau region of the United States between the Continental Divide and the Cascade-Sierra Nevada Mountains.

The positions of the 850- and 500-mb low centers were obtained from microfilm copies of manuscript maps analyzed by the National Meteorological Center (NMC), Suitland, Md. The labeled center of the low was recorded to the nearest half degrees of latitude and longitude.

For this study the National Weather Records Center (NWRC), Asheville, North Carolina, provided hourly precipitation data in the form of twelve-hourly amounts centered at the upper-air observation time of each low.

The methods used to obtain, process, and analyze these data were similar to those described in earlier studies. The grid used is illustrated in figure 2. It consists of a grid area essentially 18 degrees latitude on a side with the area coinciding with the spherical surface of the earth. The precipitation (including zero amounts) received by the station located at the origin of the grid was assigned to the cell in which the associated low was located. The percentage of precipitation occurrences ($\geq .01$") falling within the grid cell then gave the probability that the station would receive precipitation when the low was in this position. The average precipitation of all cases occurring within the cell gave the average amount received by the station. Considerable smoothing was necessary in analyzing the probability of occurrence patterns. Precipitation amounts were averaged by combining all cases falling within given probability of occurrence ranges.

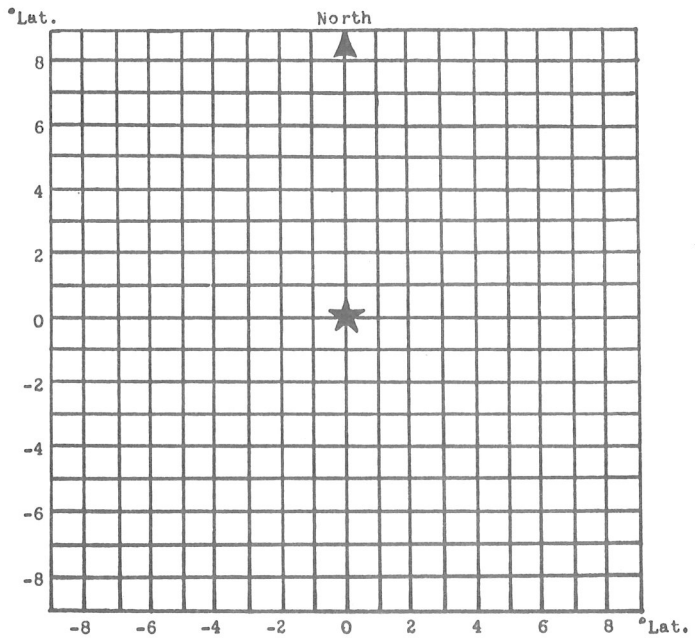

Figure 2.--Grid representation on plane surface. Grid system consists of great circles on the spherical earth with dimensional units equivalent to latitude degrees along the two axes.

As in earlier studies, the lows were grouped into three intensity classes depending upon the departure of the central height from the local normal. (See Appendix A for the classification procedure.) The lows were then categorized into three nearly equal ranges of departure from normal (DN) values, with Class I representing the weak, Class II the moderate, and Class III the most intense cases based on the DN criterion. Table 1 gives the class limits of the DN values for the two pressure levels, and table 2 gives the number of cases occurring in each class, indicating more lows at 850 mb than at 500 mb [5].

Table 1.--Class limits (in meters) of departures from normal of central heights for lows at the two levels.

Level in mb	Class I	Class II	Class III
850	> -45	-45 to -120	< -120
500	> -60	-60 to -242	< -242

Table 2.--The number of lows studied at each level and in each intensity category.

Level in mb	Class I	Class II	Class III	All Classes
850	316	509	285	1110
500	220	483	172	875

RESULTS OF THE INVESTIGATION

In this section charts for selected stations will be discussed to illustrate the differing frequency patterns. Charts for all stations are given in Appendix B.

(a) Flagstaff, Arizona - Class I maps for this station (charts 13-Ia and 13-Ib) show that precipitation from weak lows has a relatively small frequency of occurrence which decreases with height of the lows. Maxima of precipitation frequency occur at 850 mb (i.e., 30 percent) with lows to the northeast and at 500 mb with lows to the north of the station. This may be a favorable location for lows when a trailing moist front or trough occurs near the station.

Class II situations at Flagstaff (charts 13-IIa and 13-IIb) show a marked increase in the frequency of precipitation with lows, again with the maximum frequency generally decreasing with height of the lows from 80 percent at 850 mb to 60 percent at 500 mb. At each level the maximum occurs in a quadrant northwest of the station.

Charts 13-IIIa and 13-IIIb for Flagstaff show that the intense lows of Class III situations have two maxima. One shifts position with increasing height from eastern Utah to the Nevada area, while the other changes from a position over California to an area off the coast of southern California. Both areas are favorable locations for intense lows to be associated with precipitation at Flagstaff.

(b) Salt Lake City, Utah - The precipitation frequency at this station is shown in charts 30-Ia and 30-Ib for the Class I category. The larger frequencies at 850 mb than at 500 mb suggest that most of the weak lows that cause precipitation in this location are very shallow and related to cyclogenesis in southern Nevada, an area where surface storms frequently develop [4].

Chart 30-IIa indicates that, at 850 mb, three maxima are in an area within which some of the principal tracks of sea level lows are located [4]. It is noted that the maximum frequency of the station precipitation occurs when lows are over or adjacent to northeast Colorado. Such lows may be either directly or indirectly related to the precipitation at Salt Lake City. It is not necessarily true that the low directly causing the precipitation at the station is generally located where the maximum occurs. At 500 mb the maximum is located over northeast Oregon (chart 30-IIb).

The deep, or Class III lows, are shown in charts 30-IIIa and 30-IIIb. At 850 mb, the centroid of the frequency maxima is east of Salt Lake City. This is possibly due to orographic effects, as pointed out by Williams [7] who states: "Because of the high Wasatch Range to the east of Salt Lake City, post-cold frontal precipitation continues much longer than at stations with no orographic effect." At 500 mb. a double-maximum frequency area is noted northwest and southwest of the city.

Figure 3 shows a scatter-diagram of the probability of precipitation at Salt Lake City from 700-mb lows in combination with concurrent 850-mb lows. The black dots indicate measurable precipitation cases (often these are the Class III data) while the open circles (mostly Class I and some Class II data) indicate no measurable precipitation. A similar graphical-regression procedure is also applicable to three or more levels to obtain a combined probability value. The dashed area near the origin of figure 3 is intended to represent and enclose 9 closed and 179 open circles.

(c) El Centro, California - This station is located in an area where most of the 500-mb lows were concentrated but where only a few 850-mb lows were congregated [5]. Despite the smaller amount of data at 850 mb, the chart series (9a and 9b) for each class at the 850- and 500-mb levels show good agreement when the location of their corresponding maxima are compared. The frequencies of precipitation are shown to be greater for lows at the

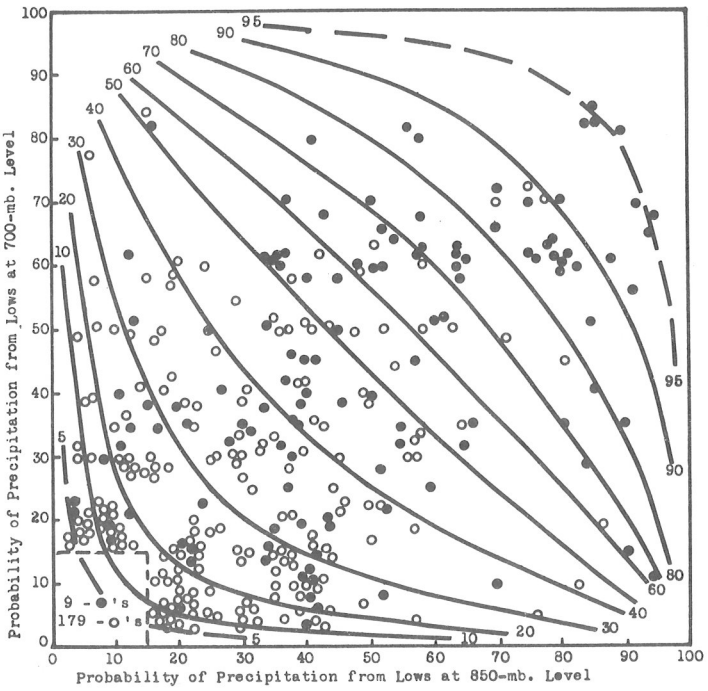

Figure 3.--Combined probability of precipitation from the 850-mb and 700-mb lows at Salt Lake City, Utah, for all classes of intensity. Analysis shows equal probability lines. Measurable precipitation is shown by a black dot; otherwise an open circle is used. Averaging the precipitation amounts substituted at each black dot between adjacent isopleths will yield the average precipitation amount for each range of combined probabilities.

lower than at the upper level.

(d) Craig, Colorado - At this station a maximum probability of 80 percent is shown on chart 5-Ia for weak 850-mb lows. No other mountain stations in this category had a maximum probability as large as 80 percent. The orographic component of this probability was found to be about 60 percent using the method described in an earlier study [3].

One of the weak 850-mb lows contributing to this high probability was observed about 1/2 degree of latitude and longitude southwest of Craig on January 19, 1962 at 1200 GMT. During the 12-hour period centered at this time, 0.11 inch of precipitation was recorded. No upper lows were observed at the 700-, 500-, and 300-mb levels in the grid area. Therefore no probability of precipitation at and above 700 mb could be inferred from our charts at these levels. It is evident that this weak low at the relatively low level of 850 mb did cause considerable precipitation at Craig, which again shows the importance of the lower level. A recent study by Weaver [6] describes the orographic factors related to precipitation in this area.

(e) Tonopah, Nevada - This station (elevation 5426 ft.) is on the lee side of the Sierra Nevada and therefore is in a very dry location. Charts 32-a and 32-b for this station reflect the dry climate of the area. The precipitation probability, considering all classes of lows, has a maximum value slightly over 40 percent, and the highest average precipitation goes up to only 0.07 inch.

(f) Ouray, Colorado - At this mountain station (elevation 7740 ft.), considerable moisture is observed in charts 21-a and 21-b. The precipitation probability reaches a value of over 90 percent, and the average precipitation goes up to 0.22 inch for the most intense lows. The station is on the windward slopes for a northerly flow of air.

The derived charts show the considerable variety in precipitation probability patterns between the various stations and emphasize the preferability of adapting the large-scale forecast to the local station features, using charts such as those in Appendix B as an initial forecast aid.

Generally the average precipitation, and its relationship to the frequency of occurrence of measurable precipitation for each station, is similar to that shown by an earlier study [3] concerning 700-mb lows. The average amount related to each range of frequencies of measurable precipitation represented by a corresponding contour interval on the station chart generally increases with increasing frequency and more intense class of low.

APPLICATION OF THE DERIVED CHARTS

It was shown in an earlier study [3] that probability charts for 700-mb lows at a station could be used as a forecast aid and for weather-modification research. The charts presented in Appendix B can be used in a similar fashion. They give a first estimate of the average measurable precipitation and the related probability from lows at either the 850- or 500-mb level.

It is suggested that the charts in Appendix B may be applied using the following procedure; but the forecaster's best judgment is always an overriding consideration:

1. Using numerical prognostic charts transmitted over facsimile or other sources of forecast information, plot the corresponding position of the major low within the grid area centered on the station. If more than one concurrent low exists in the grid area at a selected level, choose the preferred low as:

(a) the deepest one present. If these lows are of equal intensity,

(b) select the low nearest to the station in the grid area. If both lows are equidistant from the station,

(c) select the most persistent low with the greatest forecast period while it is expected to affect the station and is in the grid area.

2. Obtain the DN (Departure from Normal) height using the appropriate normal height maps in Appendix A and the forecast position of the low center.

3. Using table 1, determine the intensity class of the selected low and then obtain the related probability and average amount of precipitation from the corresponding intensity chart for the station.

4. Choose the largest probability available if probabilities exist derived from more than one concurrent level and class of low.

The derived charts have been provided to the headquarters of the Western Region of the Weather Bureau in Salt Lake City, Utah, for operational tests and evaluation. Similar charts are being derived for the spring and fall seasons. The summer season may require a different approach because considerable precipitation in the Plateau may occur from convective activity unrelated to a low center.

ACKNOWLEDGMENTS

This investigation was accomplished through the financial support of the Bureau of Reclamation, U. S. Department of the Interior. Computer processing of data was handled by the National Weather Records Center, Asheville, North Carolina. Normal maps at 850 and 500 mb were calculated by Messrs. Frank Lewis and Clifton K. S. Chun of Techniques Development Laboratory. Assistance in manually processing data was provided by Messrs. James A. Bunce, Jr., James R. Noffsinger, and Miss Margaret A. Dalton, also of Techniques Development Laboratory.

REFERENCES

1. Jorgensen, D. L., 1963: "A Computer Derived Synoptic Climatology of Precipitation from Winter Storms." Journal of Applied Meteorology, vol. 2, No. 2, pp. 226-234.

2. Jorgensen, D. L., Klein, W. H., and Korte, A. F., 1967: "A Synoptic Climatology of Winter Precipitation from 700-mb Lows for Intermountain Areas of the West." Journal of Applied Meteorology, vol. 6, No. 5, pp. 782-790.

3. Jorgensen, D. L., Korte, A. F., and Bunce, J. A., Jr., 1967: "Charts Giving Station Precipitation in the Plateau States from 700-mb Lows During Winter." Technical Memorandum WBTM TDL-12, U. S. Department of Commerce, ESSA, Weather Bureau, Silver Spring, Md., 18 pp + 34 charts.

4. Klein, W. H., 1957: "Principal Tracks and Mean Frequencies of Cyclones and Anticyclones in the Northern Hemisphere." Research Paper No. 40, U. S. Department of Commerce, Weather Bureau, Extended Forecast Section, Washington, D. C., 62 pp.

5. Klein, W. H., Jorgensen, D. L., and Korte, A. F., 1968: "Relation Between Upper Air Lows and Winter Precipitation in the Western Plateau States." Monthly Weather Review, vol. 96, No. 3, pp. 162-168.

6. Weaver, R. L., 1968: "Meteorology of Major Storms in Western Colorado and Eastern Utah." Technical Memorandum WBTM HYDRO-7, U. S. Department of Commerce, ESSA, Weather Bureau, Washington, D. C., 75 pp.

7. Williams, P., Jr., 1967 (rev): "Station Descriptions of Local Effects on Synoptic Weather Patterns." Technical Memorandum WBTM WR-5 (revised), U. S. Department of Commerce, ESSA, Weather Bureau, Western Region, Salt Lake City, Utah, 63 pp.

APPENDIX A

PROCEDURE FOR DETERMINING DEPARTURE FROM NORMAL CLASSIFICATION OF UPPER LOWS

The 850-mb and 500-mb lows used in this investigation have been classified according to the departure from normal of the central height. Normal charts used for this purpose were calculated from NMC grid point data by means of harmonic analysis and are given in figures 4 and 5. These charts comprise normals for whole months and mid-month to mid-month periods, based on 7 years of data. Dates applied to the individual charts are indicated by table 3.

Table 3.--Dates applicable to normal charts in figure 4 and 5.

Inclusive Dates	Chart	Period
Nov. 23 - Dec. 7	(a)	Nov. - Dec.
Dec. 8 - Dec. 22	(b)	Dec.
Dec. 23 - Jan. 7	(c)	Dec. - Jan.
Jan. 8 - Jan. 22	(d)	Jan.
Jan. 23 - Feb. 7	(e)	Jan. - Feb.
Feb. 8 - Feb. 22	(f)	Feb.
Feb. 23 - Mar. 7	(g)	Feb. - Mar.

The position of the upper low is located on the appropriate normal chart for the given date, and the normal height at this point is read off. The difference between the observed and normal heights (observed minus normal) in meters gives the departure from normal (DN) values which are then used to classify the individual situations according to the class intervals in table 1.

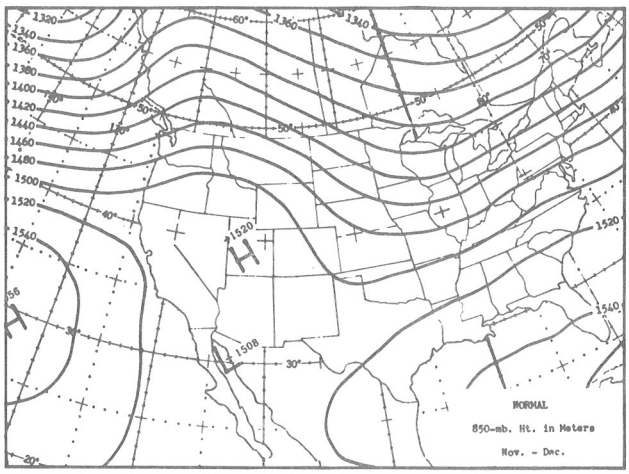

(a)

Figure 4.--Harmonically smoothed 850-mb normal charts [5].

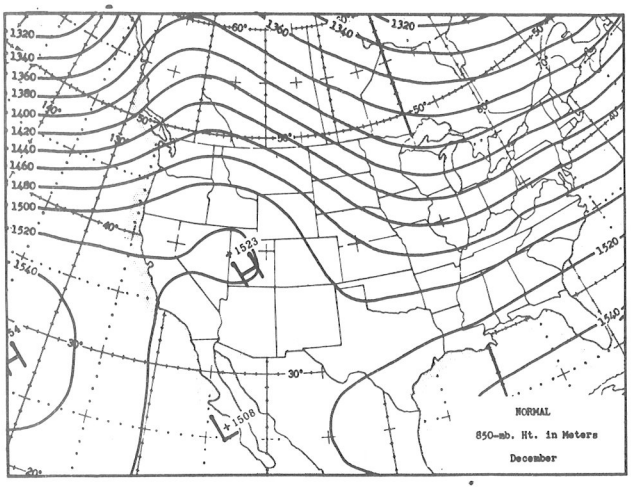

(b)

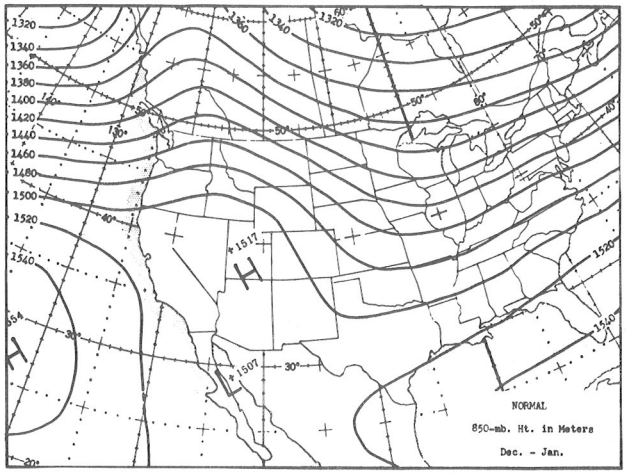

(c)

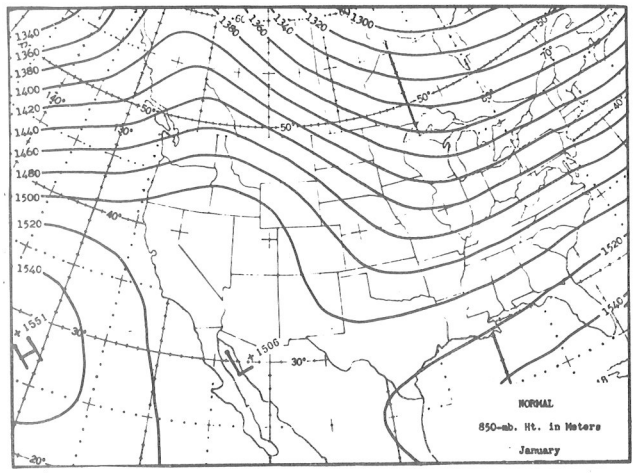

(d)

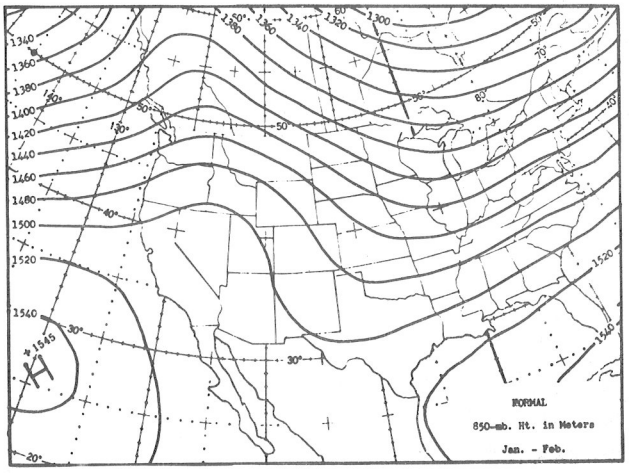

(e)

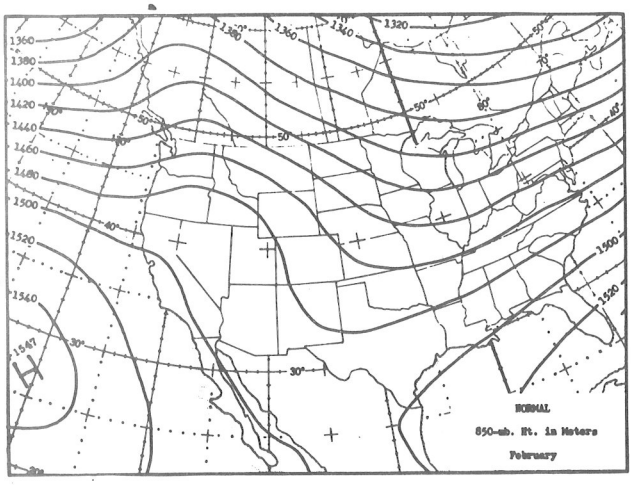

(f)

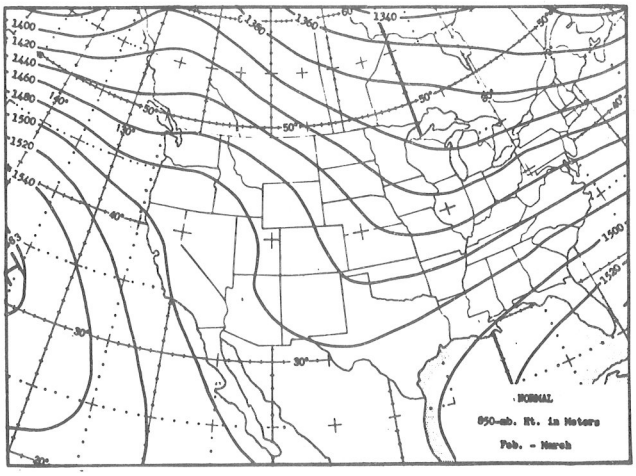

(g)

(Figure 4, continued)

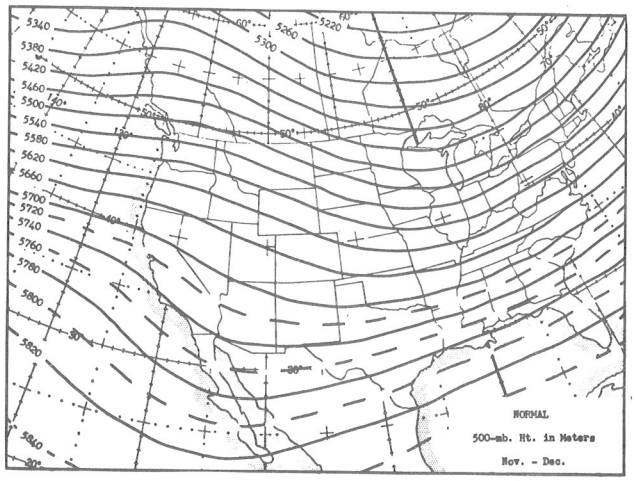

(a)

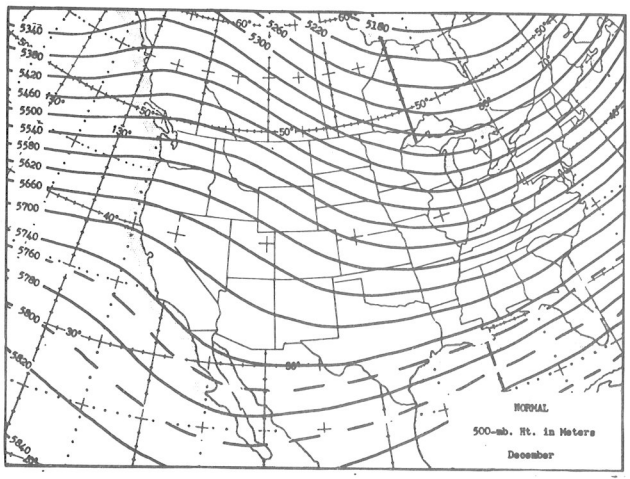

(b)

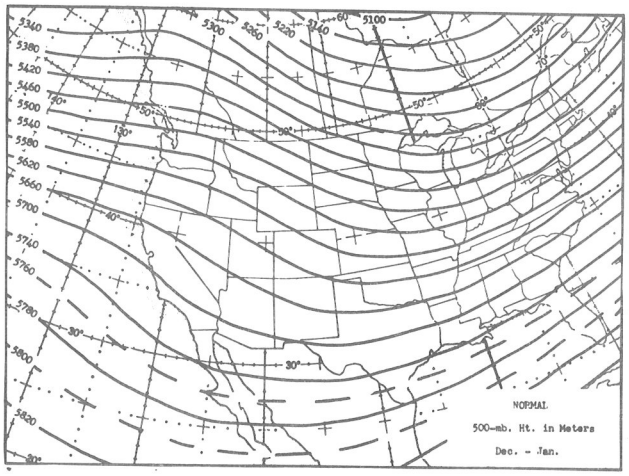

(c)

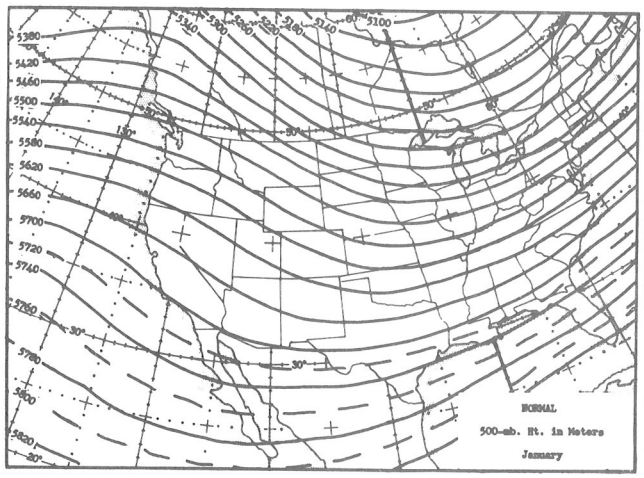

(d)

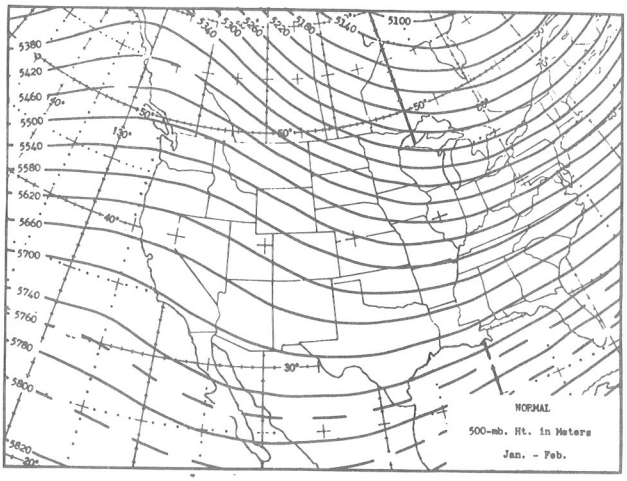

(e)

Figure 5.--Harmonically smoothed 500-mb normal charts [5].

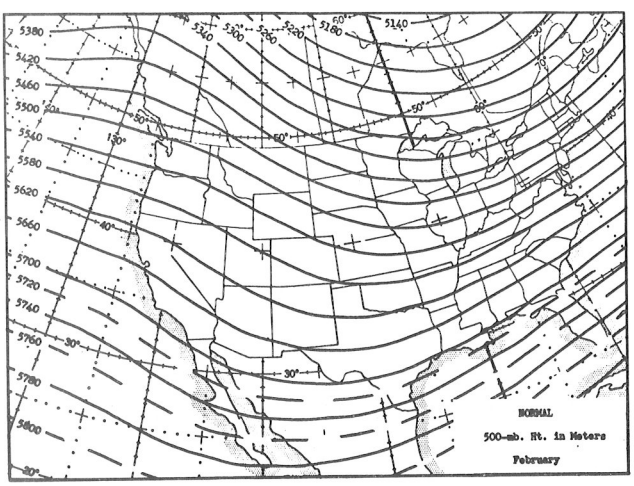

(f)

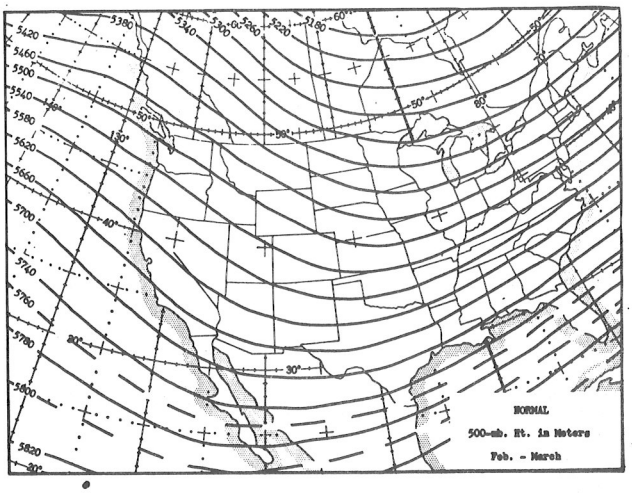

(g)

(Figure 5, continued)

APPENDIX B

OPERATIONAL CHARTS

In the intermountain region with its varied and rugged terrain, each individual station will exhibit a unique topographic effect. As has been shown in the body of this report, the patterns giving the frequency of occurrence of precipitation for several stations show significant individual station characteristics. In order to illustrate further these characteristics and to make station charts available for operational use, charts have been prepared for a selection of 35 stations out of the 280 for which data are available. These stations have been chosen on the completeness of their precipitation records and to give a sampling of the various sections of the observing station network area.

Charts at both the 850-mb and 500-mb levels for each of the three intensity classes, Class I, II, and III, are given for each station. The stations for which charts have been prepared are given in the following list with corresponding chart numbers. Station elevations are indicated in feet within parenthesis.

1. Antimony, Utah (6460')
2. Boise, Idaho (2842')
3. Bryce Canyon, Utah (7900')
4. Cedar City, Utah (5980')
5. Craig, Colo. (6280')
6. Crownpoint, N. Mex. (6978')
7. Durango, Colo. (6550')
8. Eagle, Colo. (6497')
9. El Centro, Calif. (30')
10. Elko, Nev. (5075')
11. Ely, Nev. (6257')
12. Farmington, N. Mex. (5395')
13. Flagstaff, Ariz. (6993')
14. Grand Junction, Colo. (4849')
15. Green River, Utah (4070')
16. Iron Mountain, Calif. (922')
17. Jackson, Wyo. (6244')
18. Las Vegas, Nev. (2162')
19. Mogollon, N. Mex. (6795')
20. Ogden, Utah (4280')
21. Ouray, Colo. (7740')
22. Parker Reservoir, Calif. (738')
23. Phoenix, Ariz. (1083')
24. Pocatello, Idaho (4444')
25. Prescott, Ariz. (5014')
26. Price, Utah (5580')
27. Reno, Nev. (4404')
28. Rifle, Colo. (5319')
29. Rock Springs, Wyo. (6367')
30. Salt Lake City, Utah (4220')
31. Silver Lake Brighton, Utah (8700')
32. Tonopah, Nev. (5426')
33. Tucson, Ariz. (2584')
34. Winslow, Ariz. (4880')
35. Yuma, Ariz. (199')

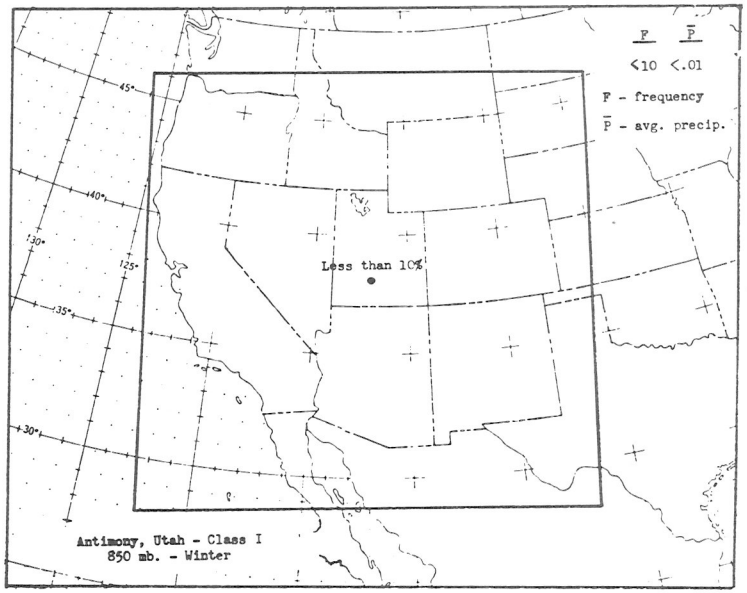

Chart 1 - Ia

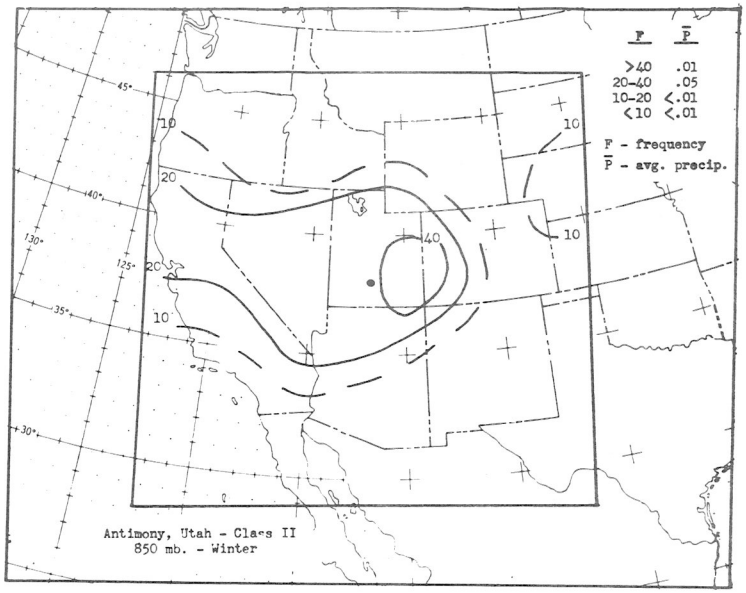

Chart 1 - IIa

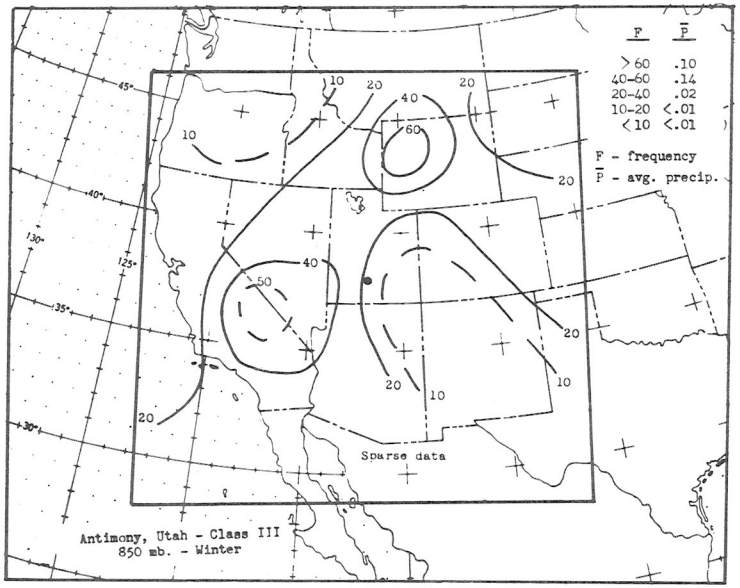

Chart 1 - IIIa

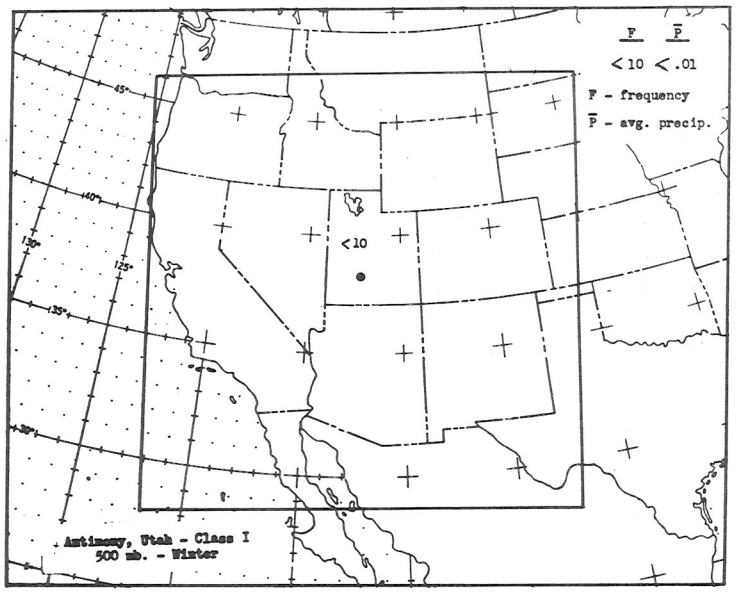

Chart 1 - Ib

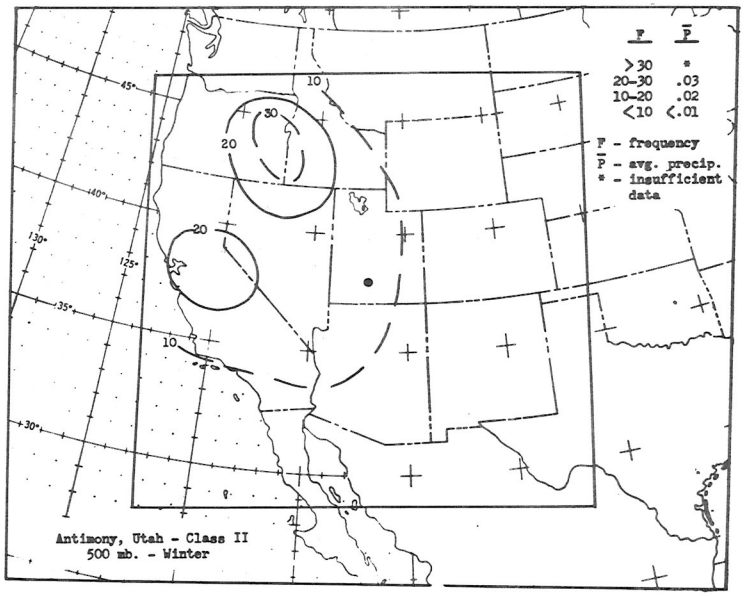

Chart 1 - IIb

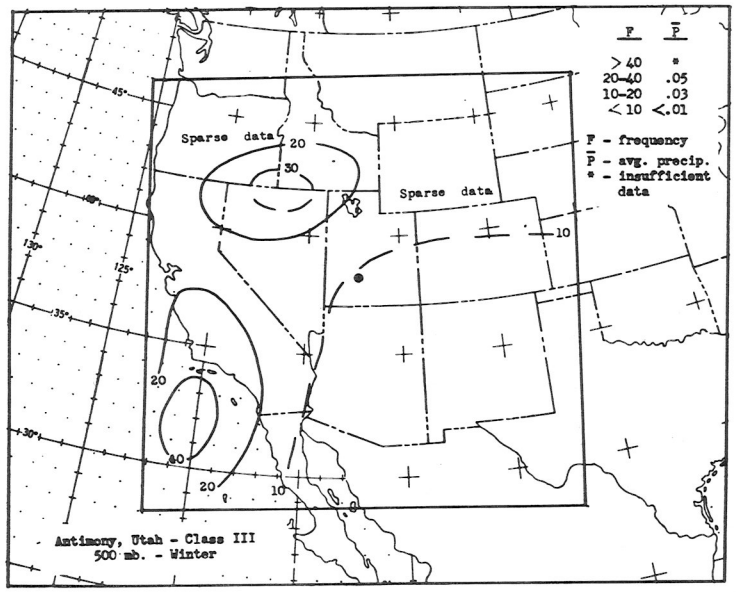

Chart 1 - IIIb

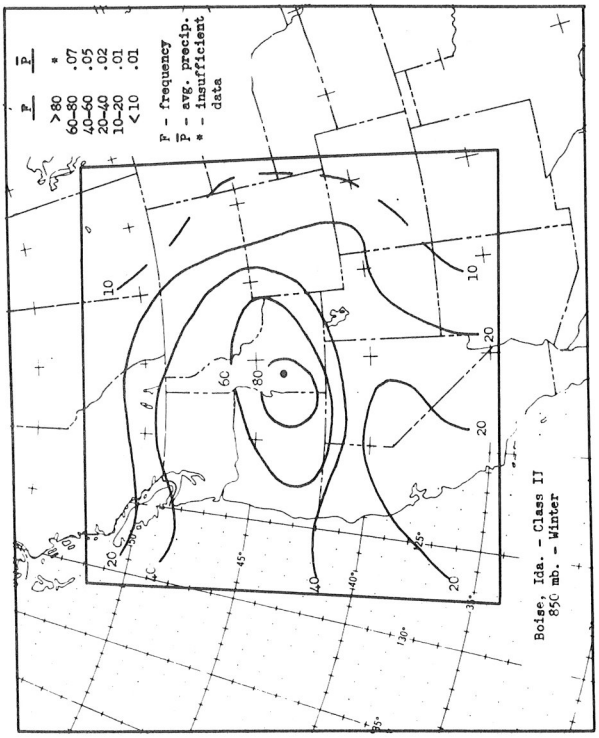

Chart 2 - IIa

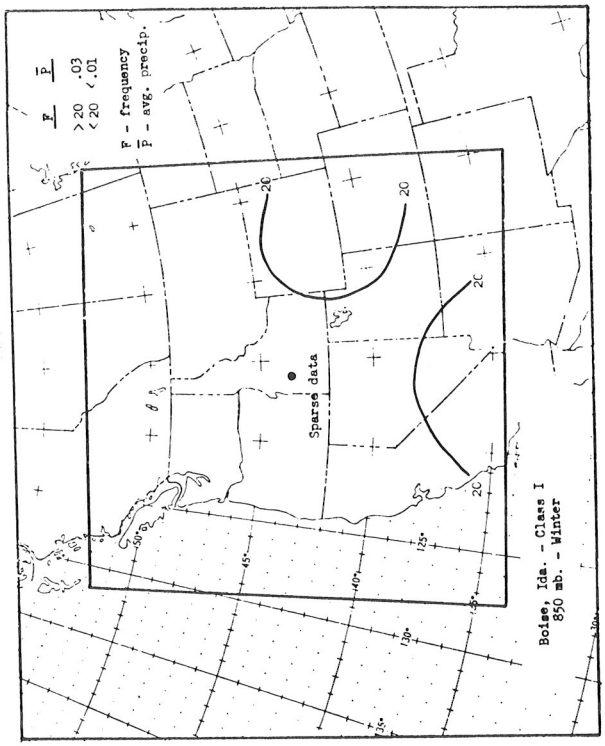

Chart 2 - Ia

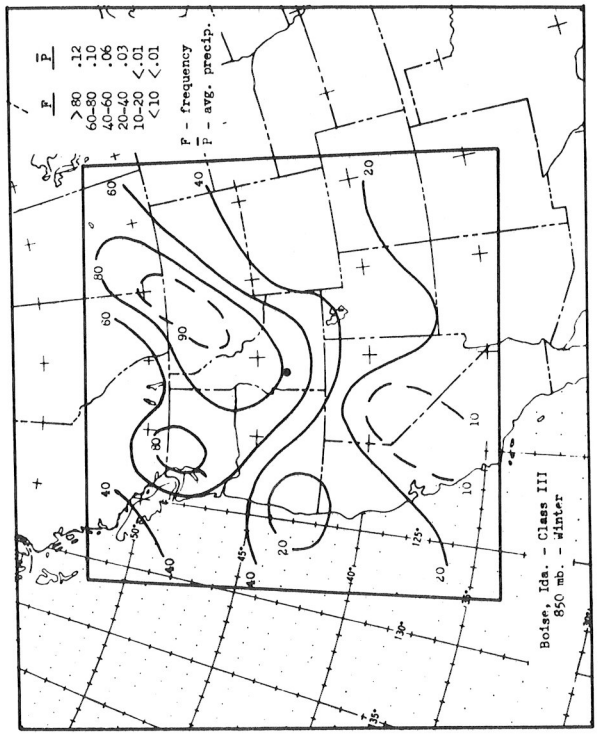

Chart 2 - IIIa

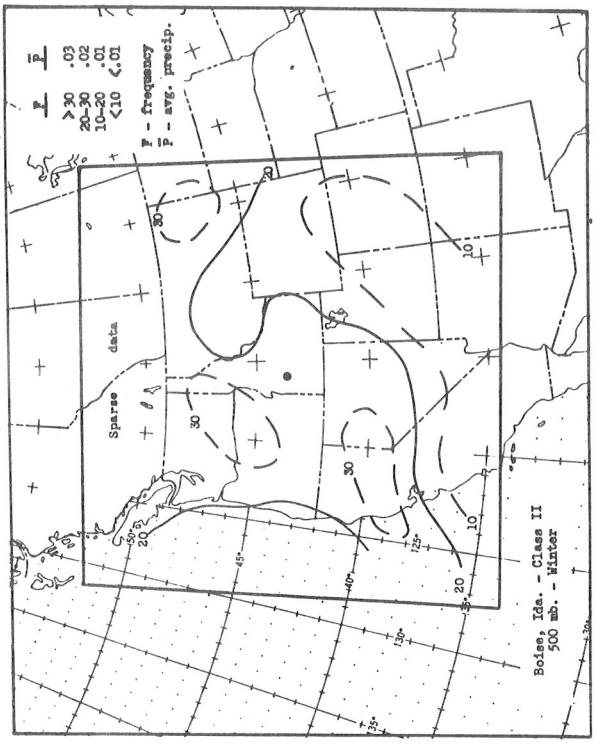

Chart 2 - IIb

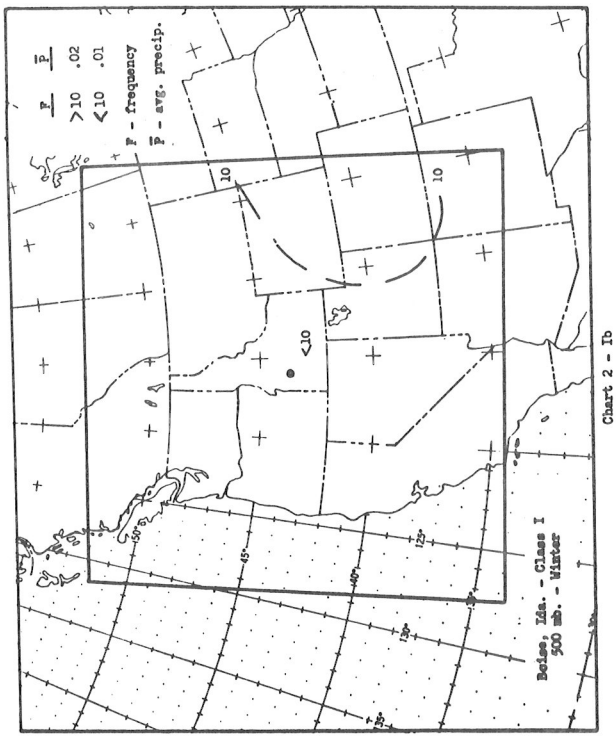

Chart 2 - Ib

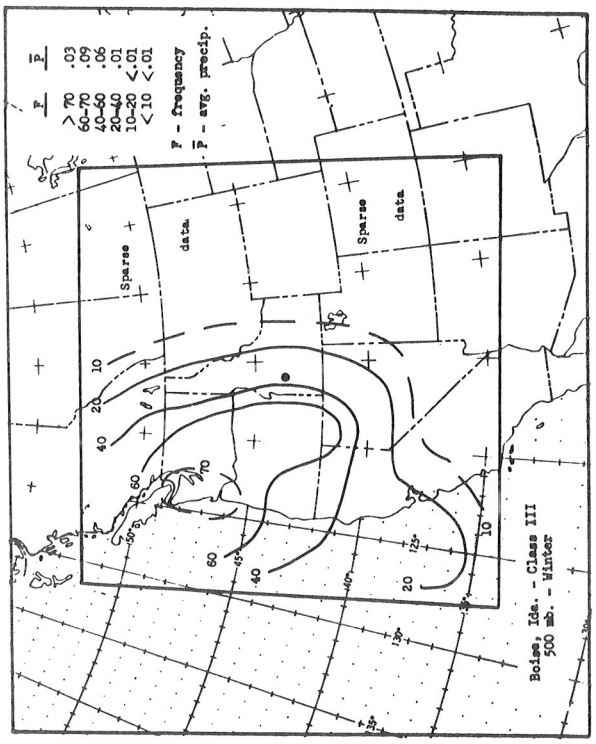

Chart 2 - IIIb

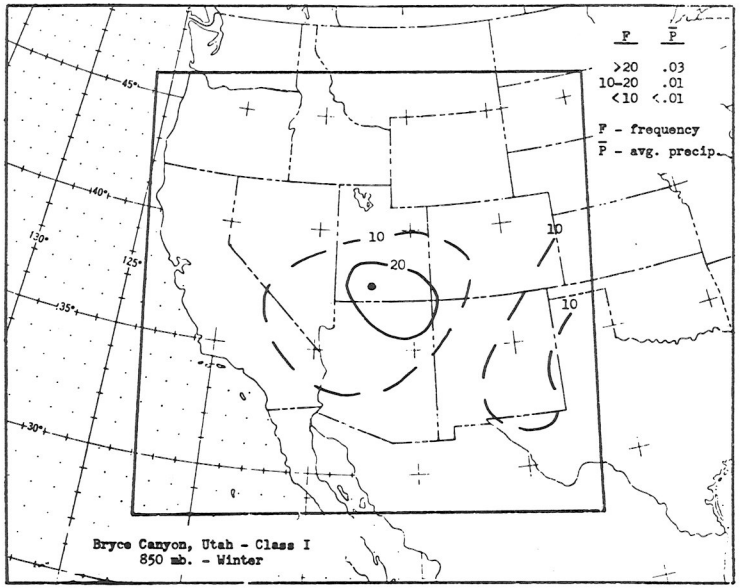

Chart 3 - Ia

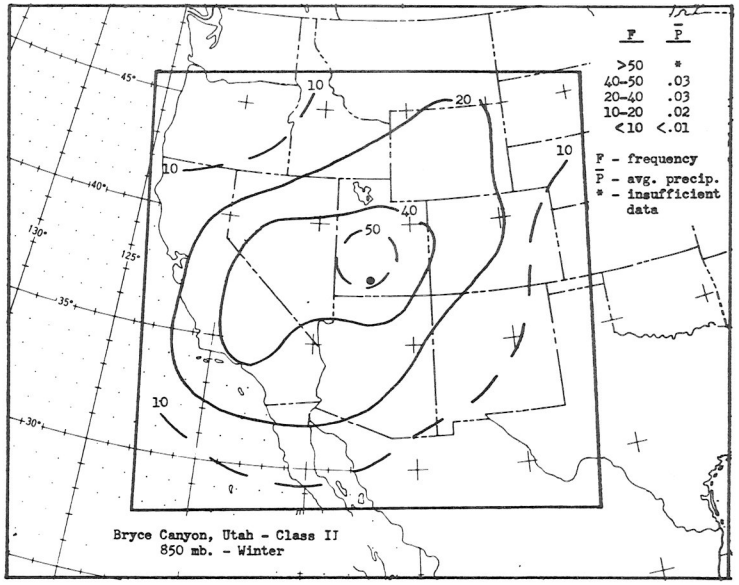

Chart 3 - IIa

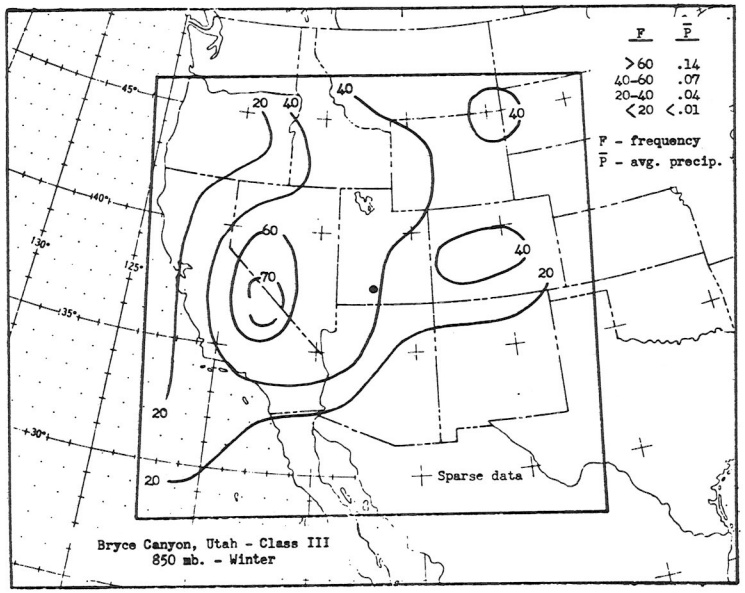

Chart 3 - IIIa

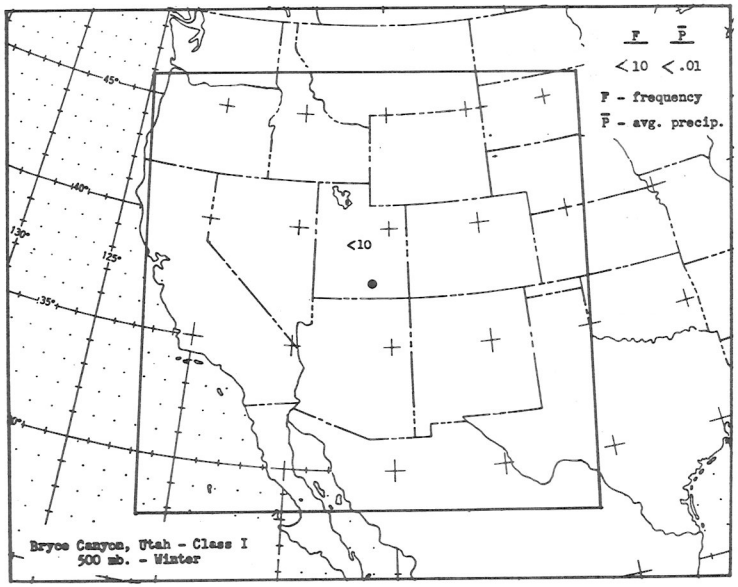

Chart 3 - Ib

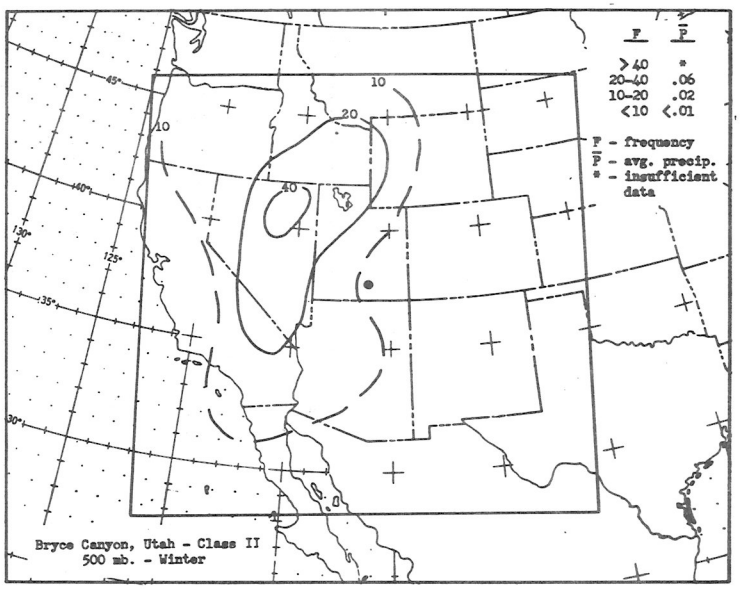

Chart 3 - IIb

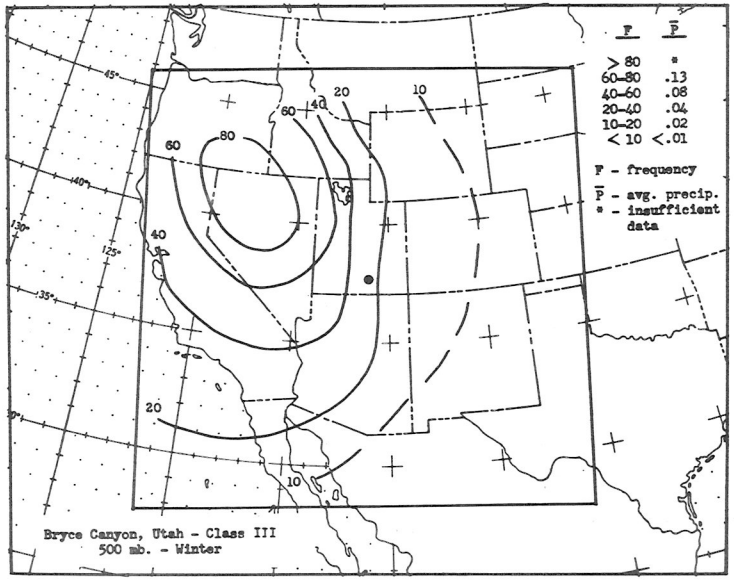

Chart 3 - IIIb

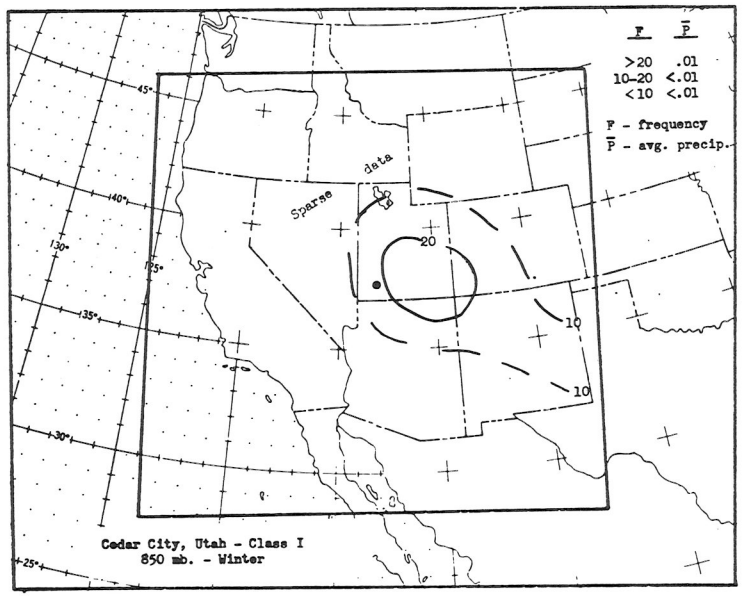

Chart 4 - Ia

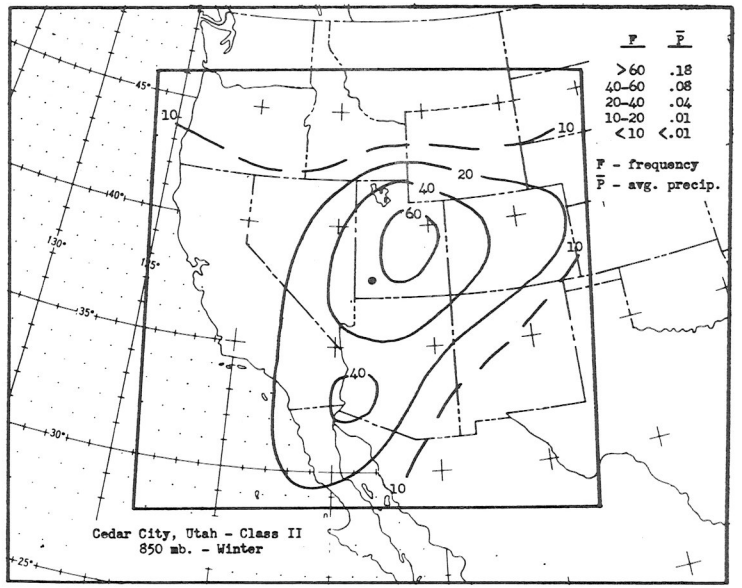

Chart 4 - IIa

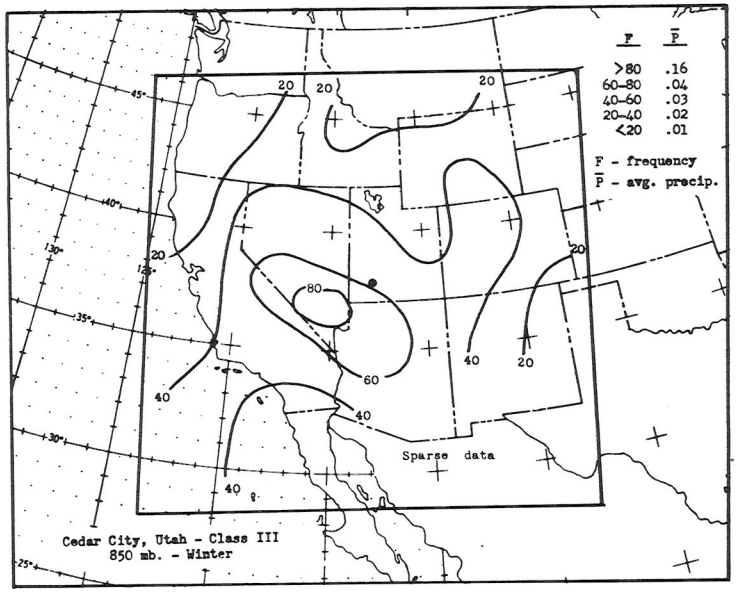

Chart 4 - IIIa

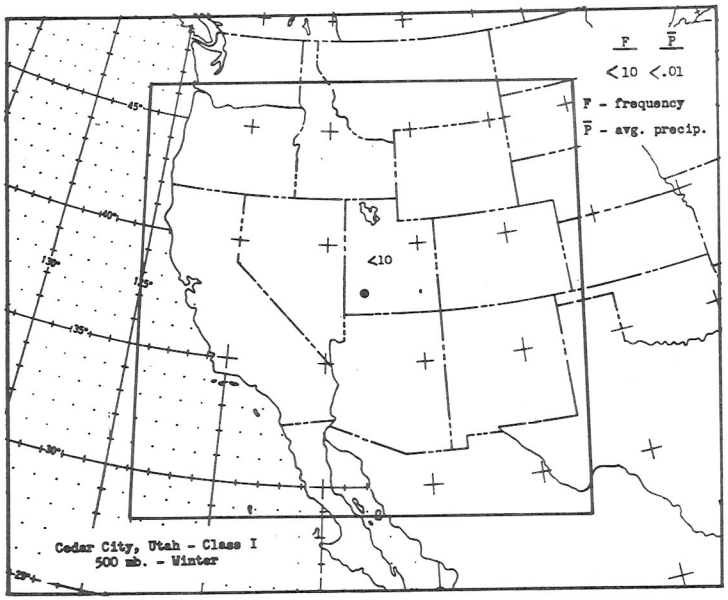

Chart 4 - Ib

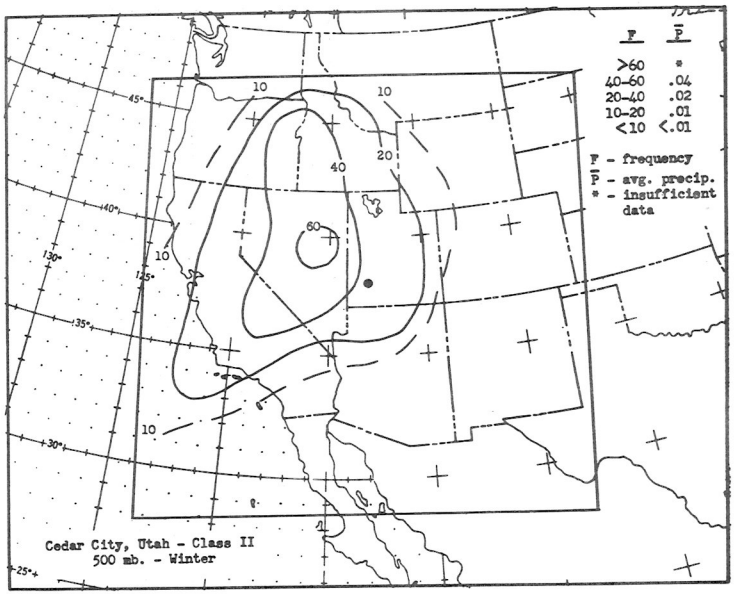

Chart 4 - IIb

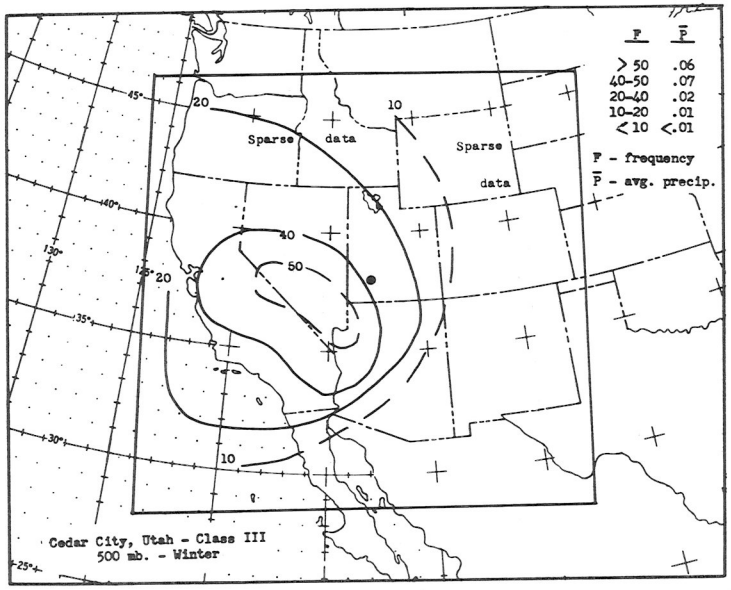

Chart 4 - IIIb

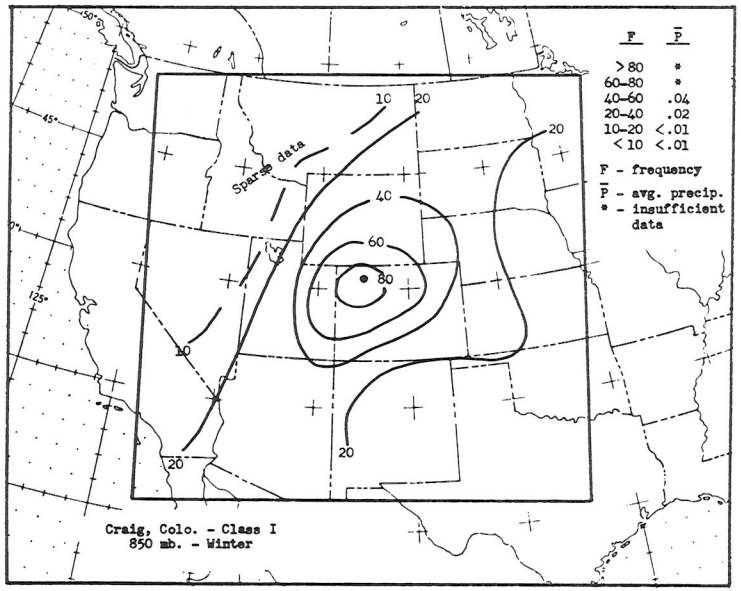

Chart 5 - Ia

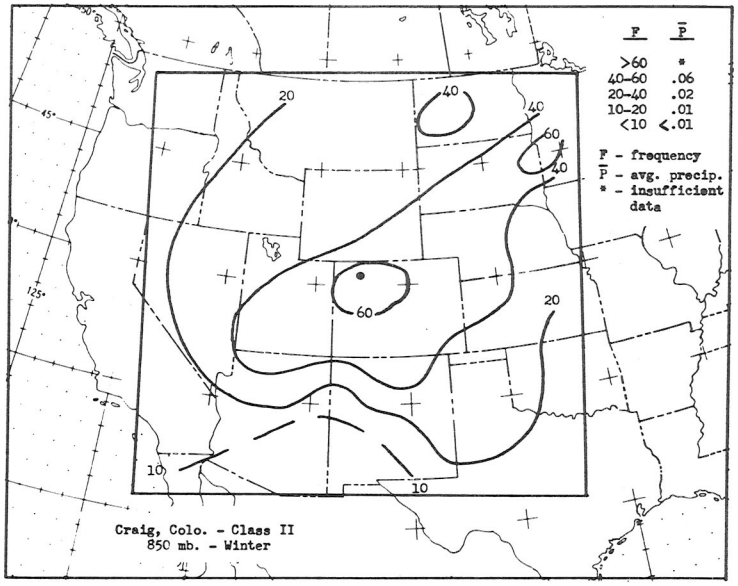

Chart 5 - IIa

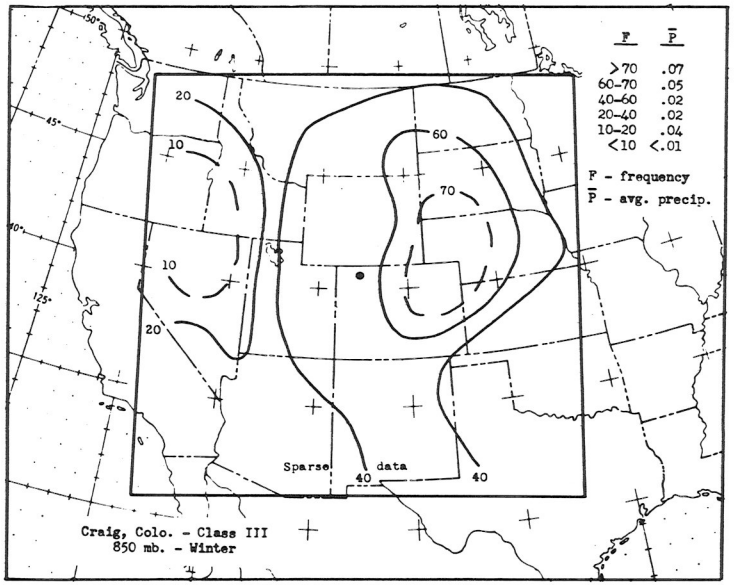

Chart 5 - IIIa

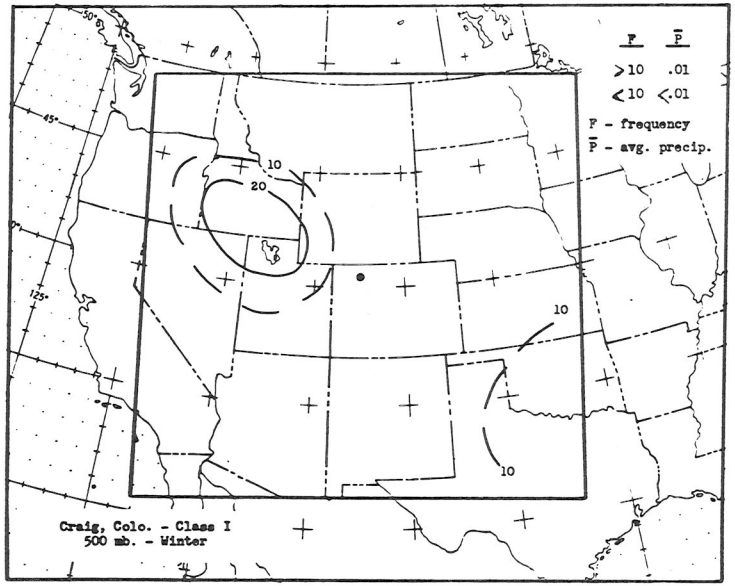

Chart 5 - Ib

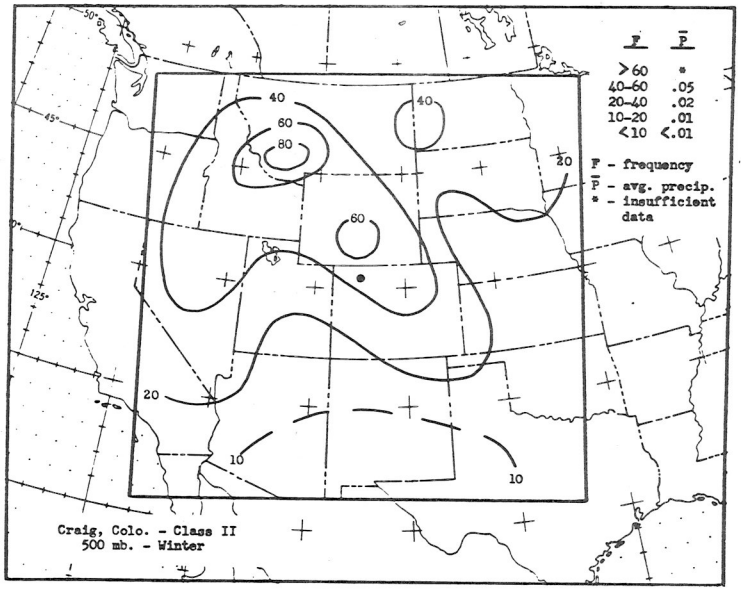

Chart 5 - IIb

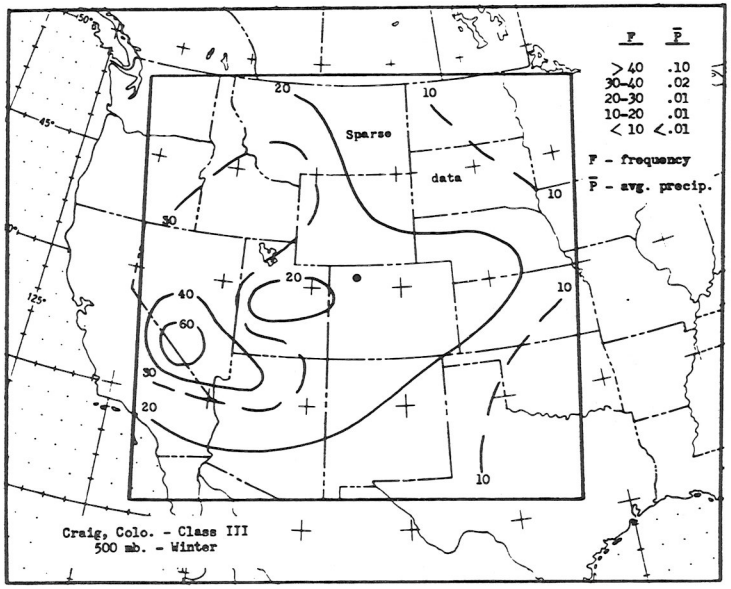

Chart 5 - IIIb

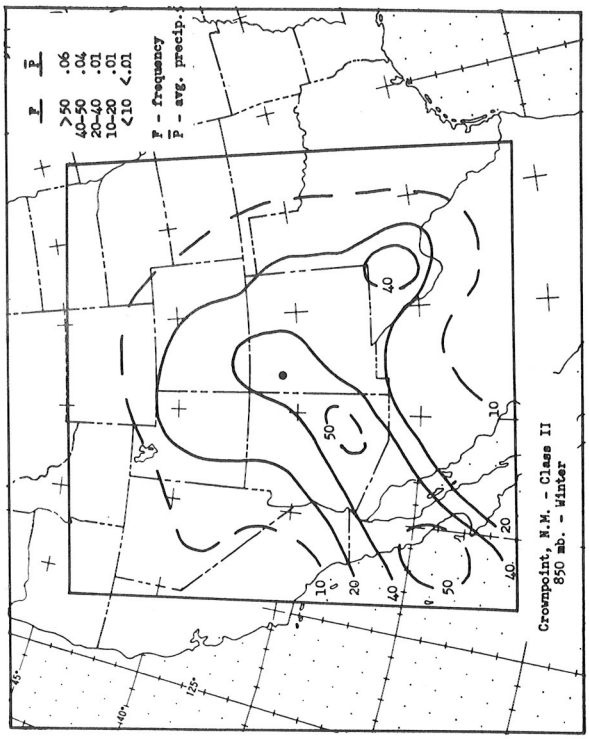

Chart 6 - IIa

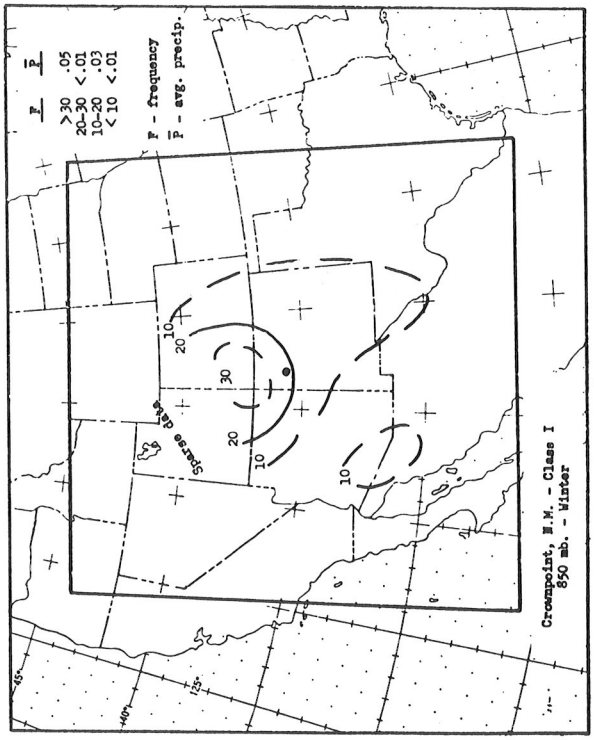

Chart 6 - Ia

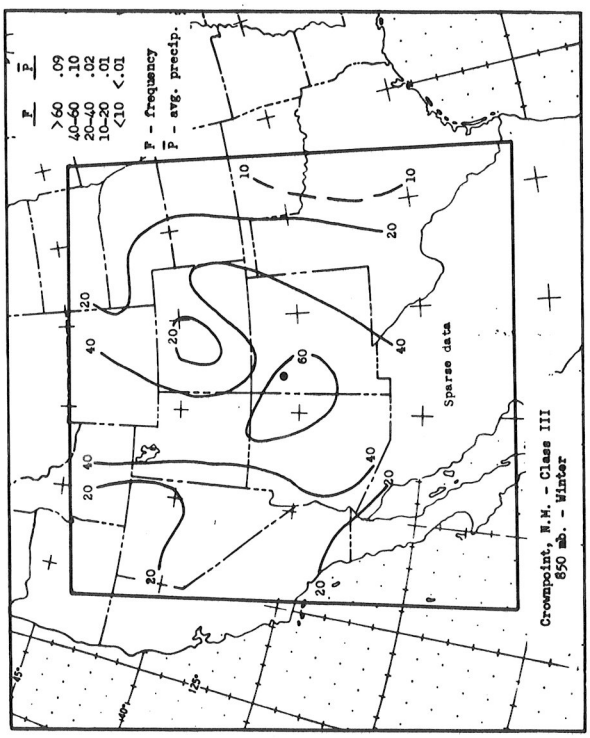

Chart 6 - IIIa

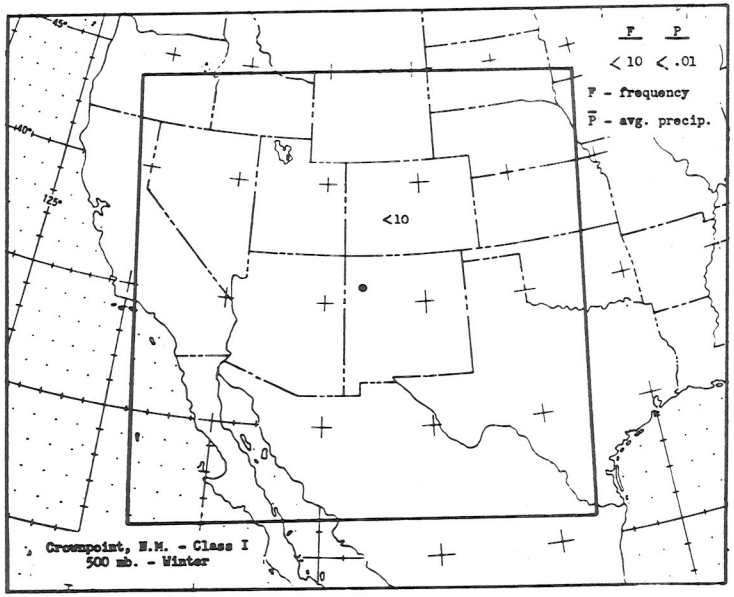

Chart 6 - Ib

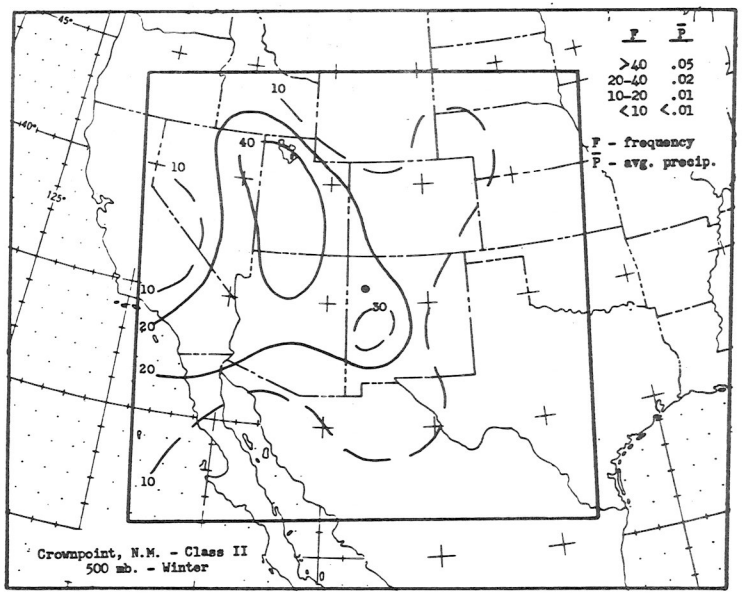

Chart 6 - IIb

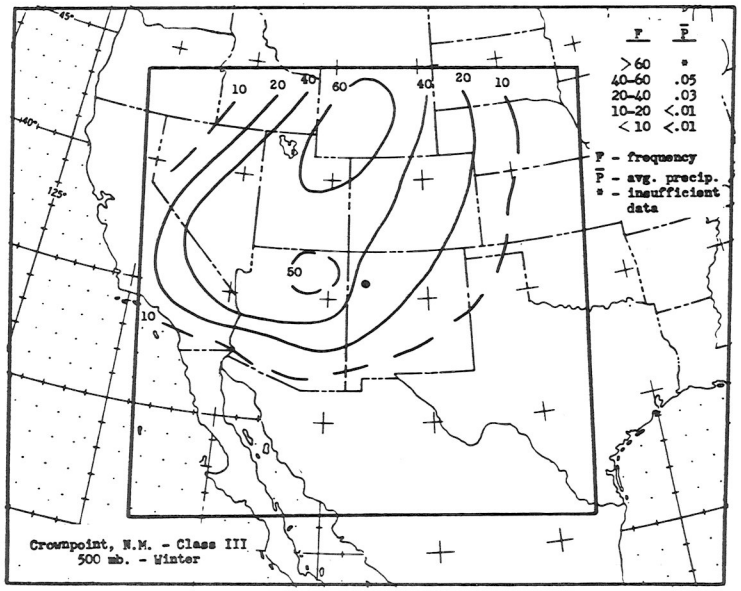

Chart 6 - IIIb

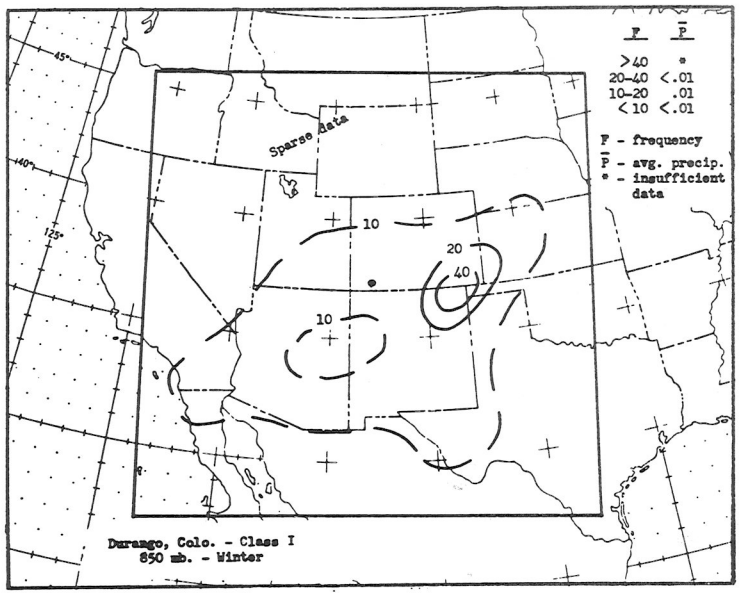

Chart 7 - Ia

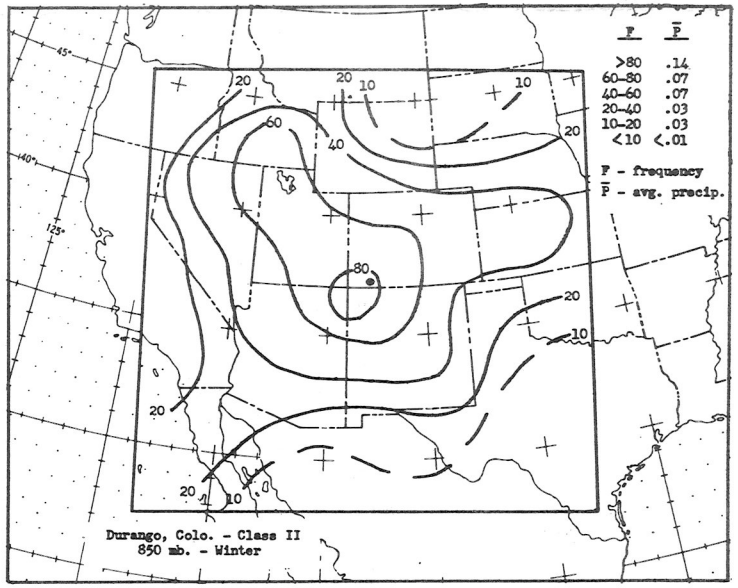

Chart 7 - IIa

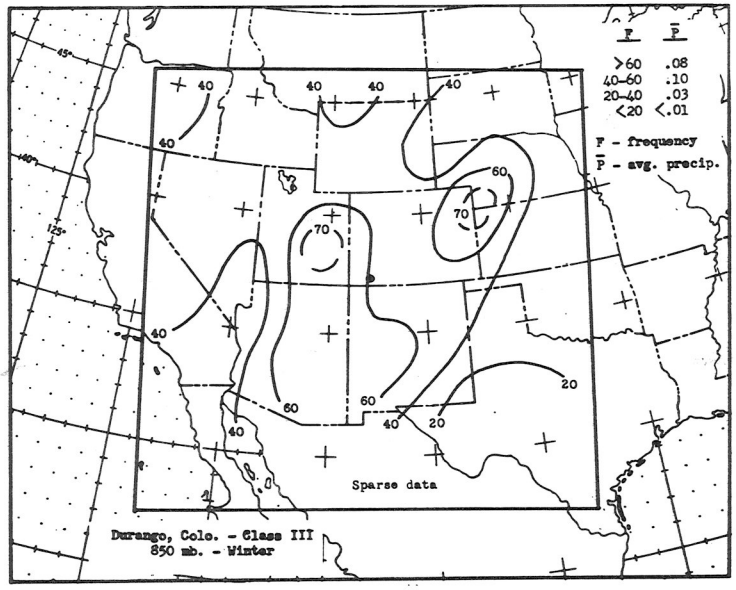

Chart 7 - IIIa

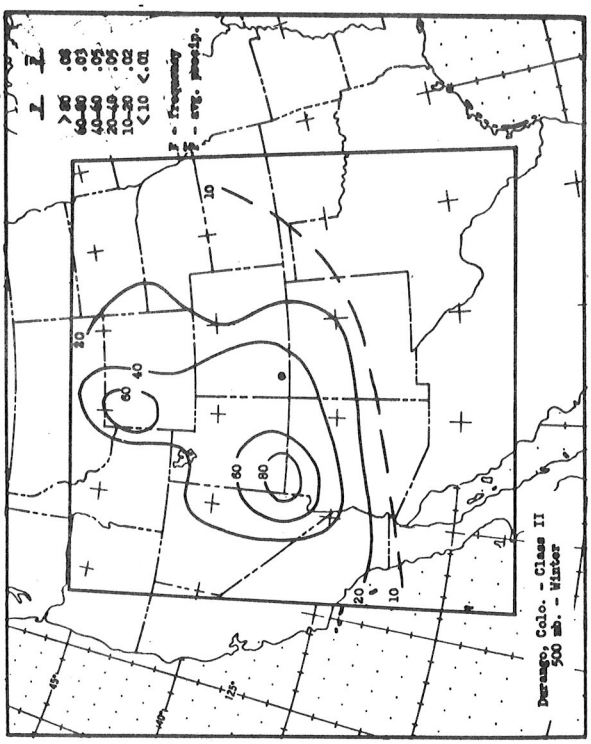

Chart 7 - IIb

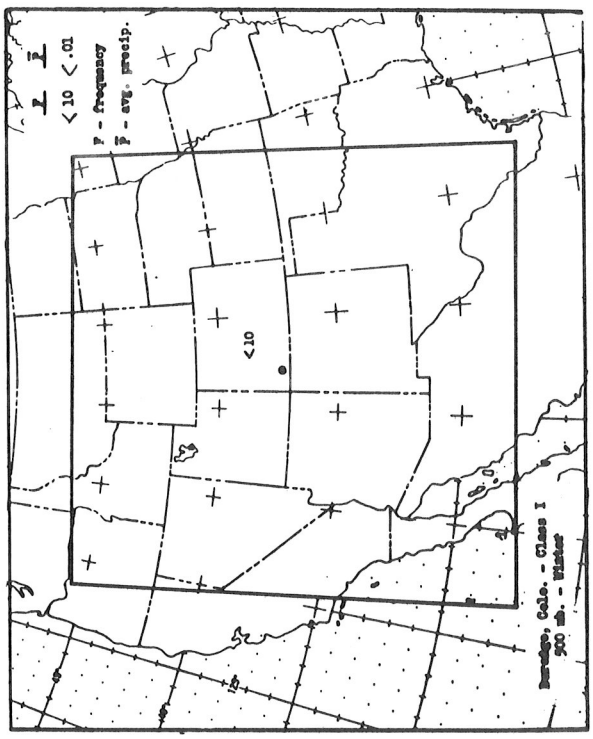

Chart 7 - Ib

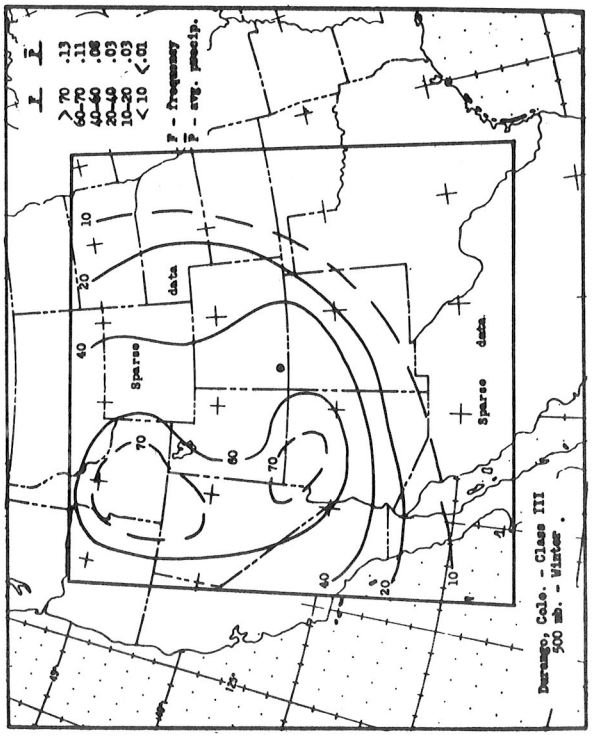

Chart 7 - IIIb

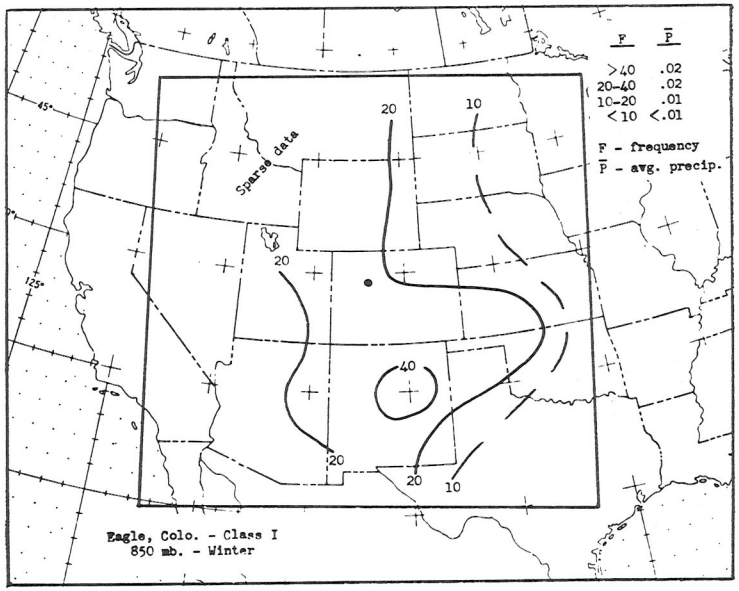

Chart 8 - Ia

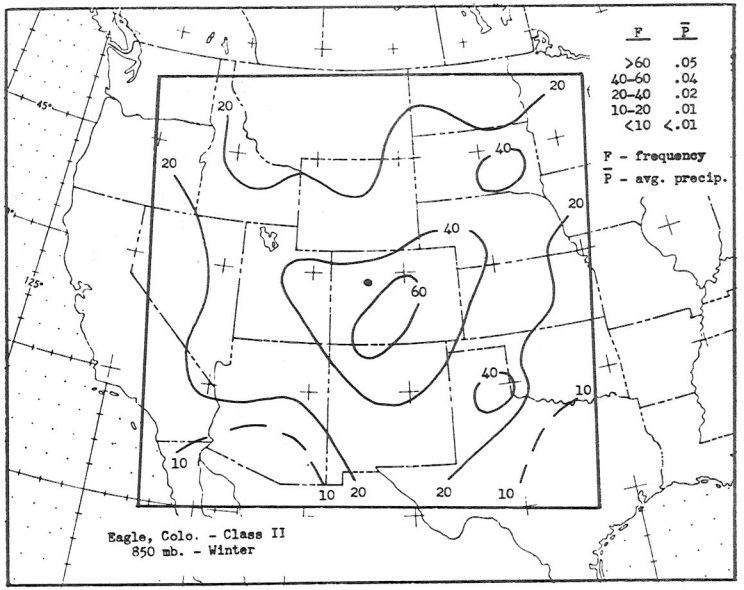

Chart 8 - IIa

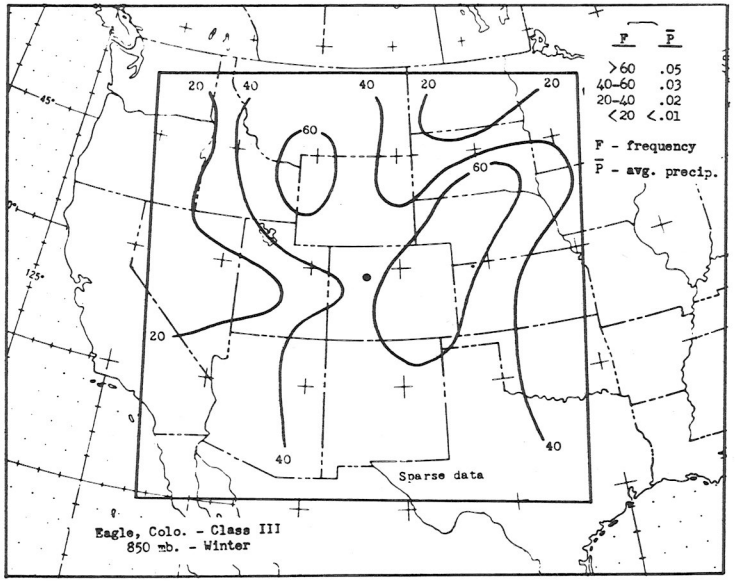

Chart 8 - IIIa

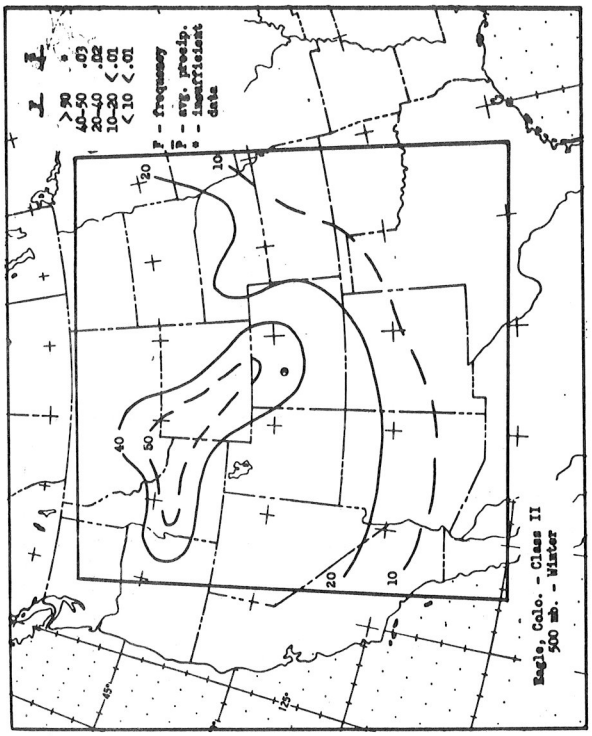

Chart 8 - Ib

Chart 8 - IIb

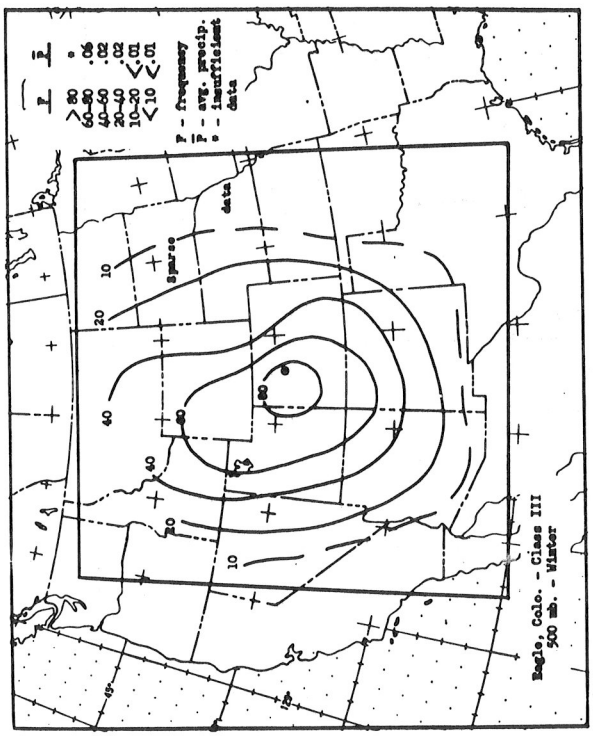

Chart 8 - IIIb

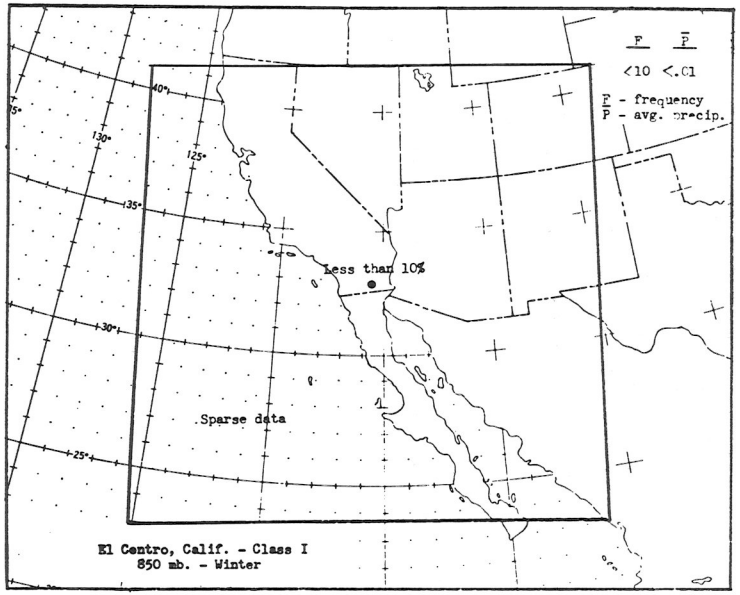

Chart 9 - Ia

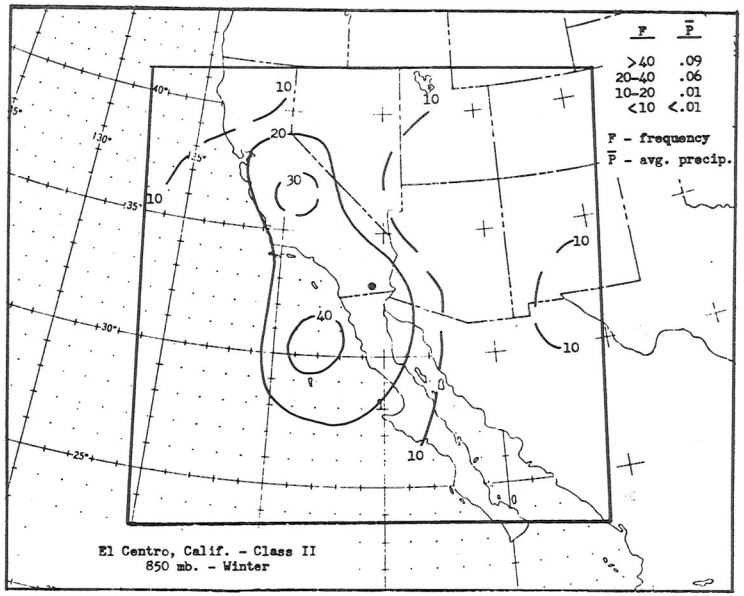

Chart 9 - IIa

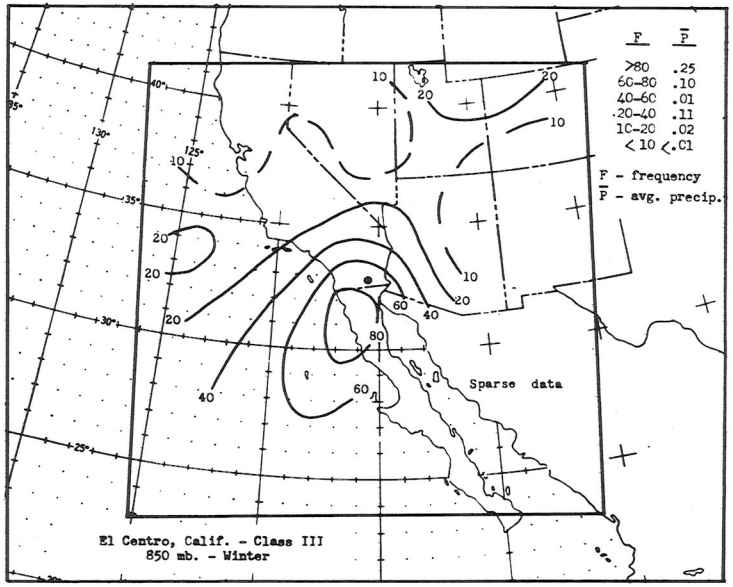

Chart 9 - IIIa

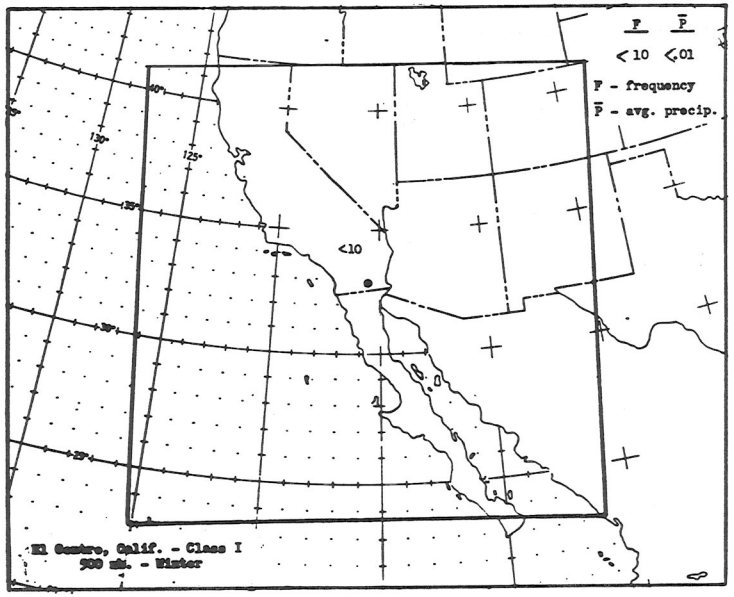

Chart 9 - Ib

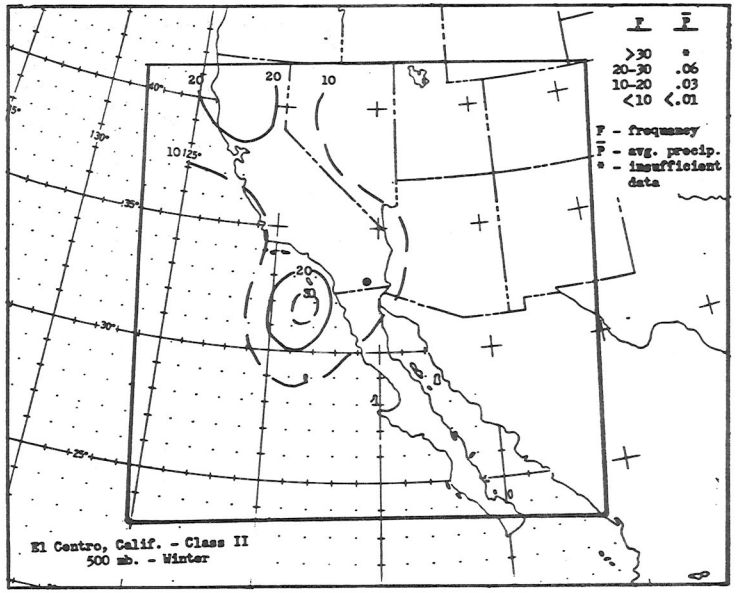

Chart 9 - IIb

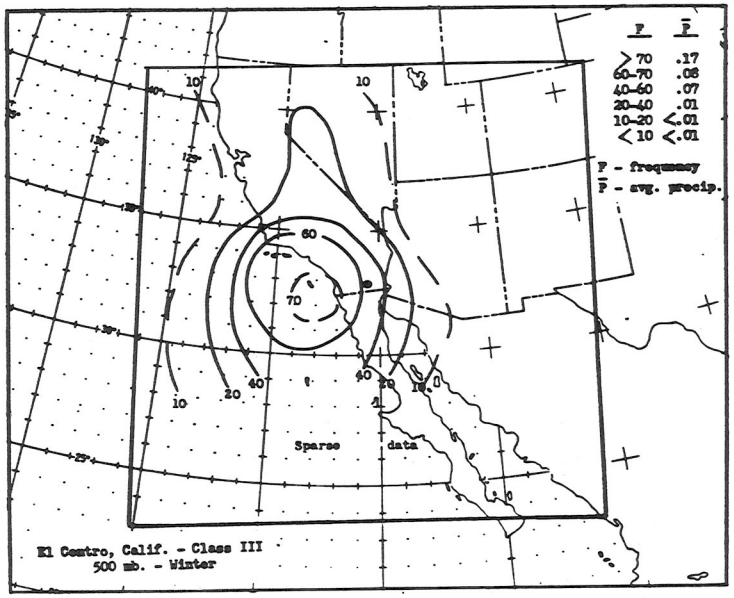

Chart 9 - IIIb

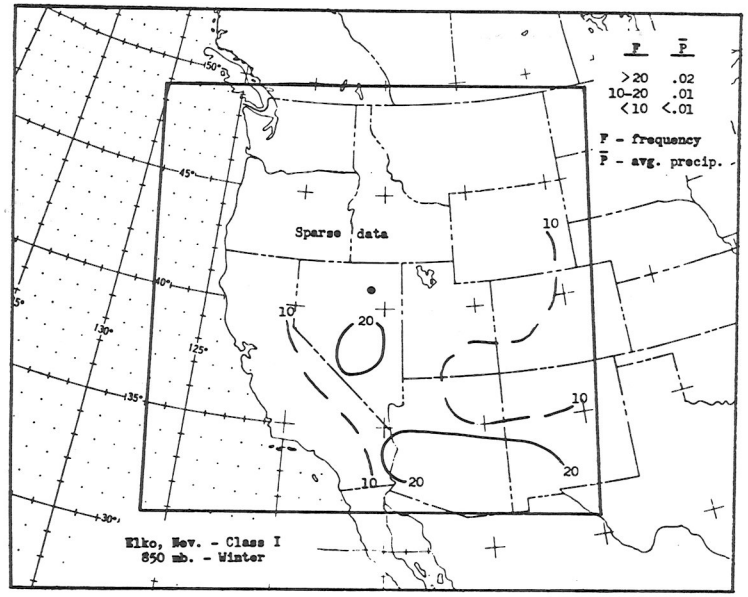

Chart 10 - Ia

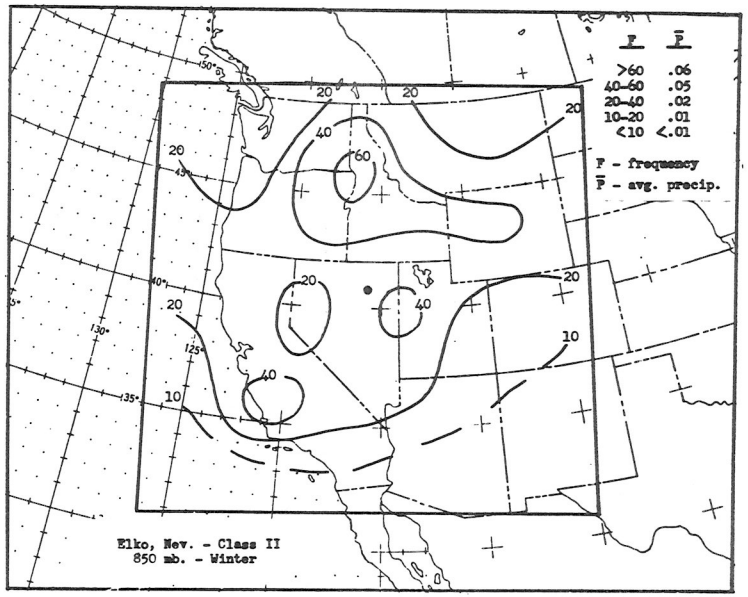

Chart 10 - IIa

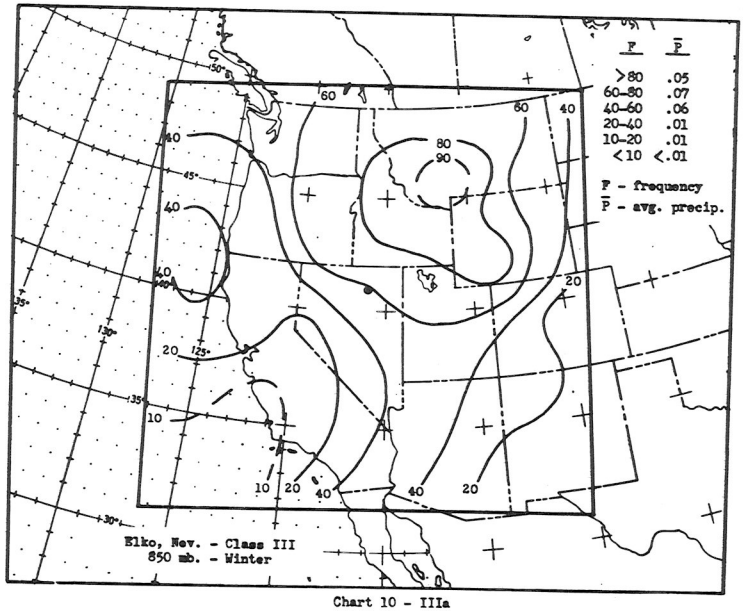

Chart 10 - IIIa

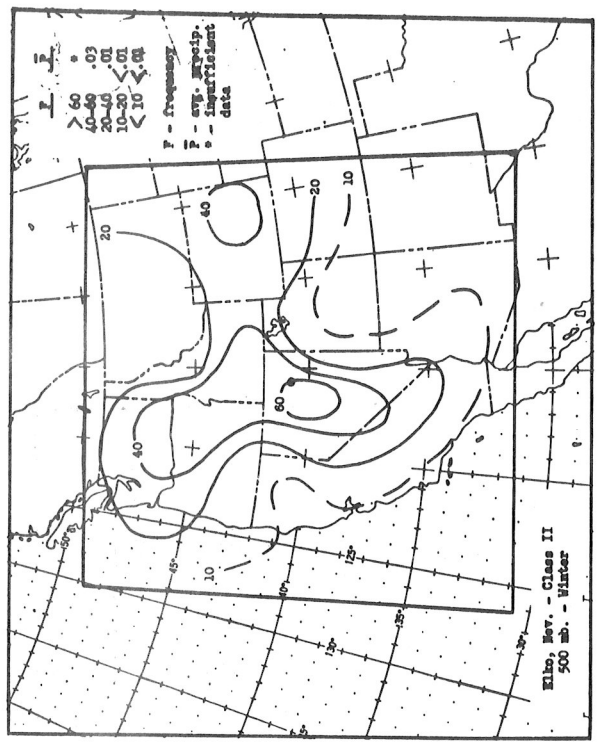

Chart 10 - IIb

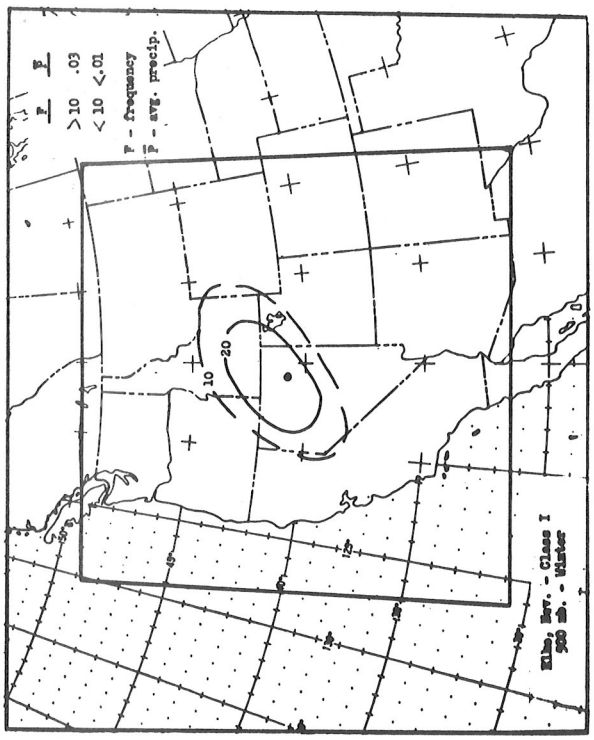

Chart 10 - Ib

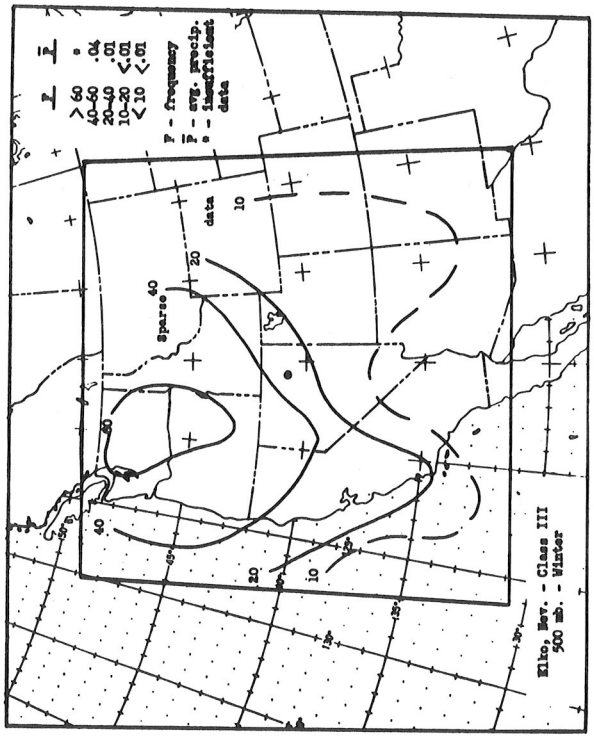

Chart 10 - IIIb

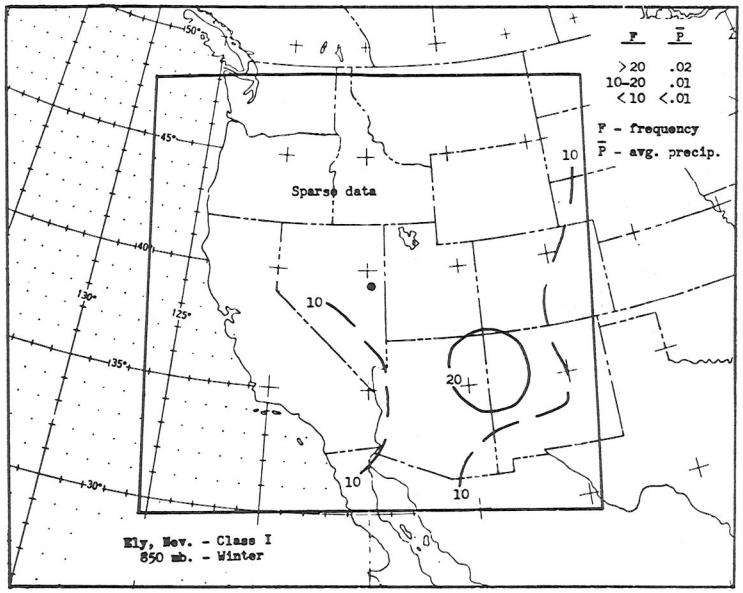

Chart 11 - Ia

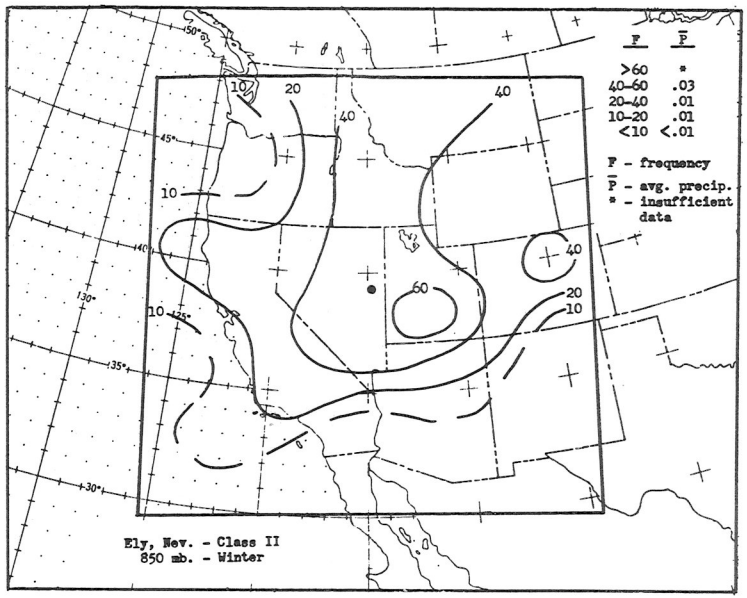

Chart 11 - IIa

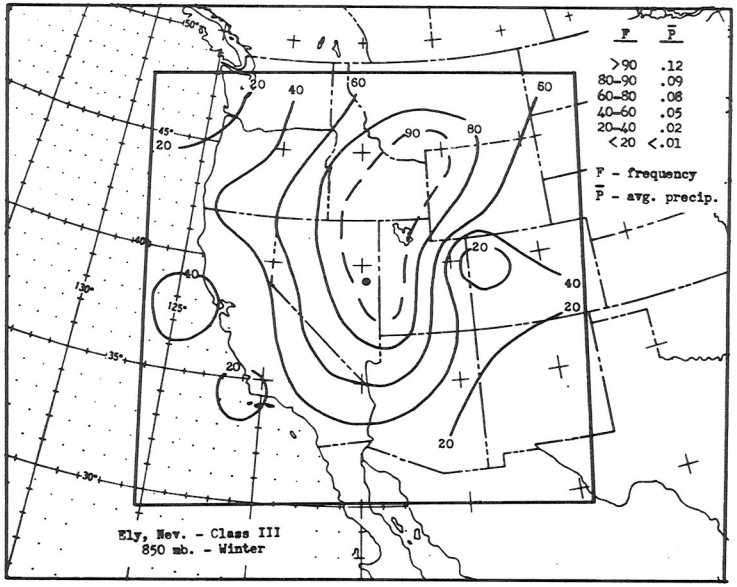

Chart 11 - IIIa

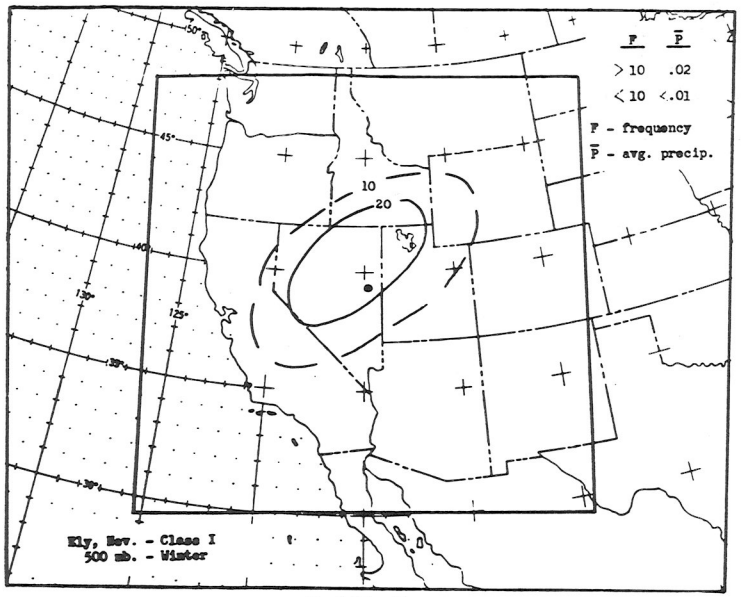

Chart 11 - Ib

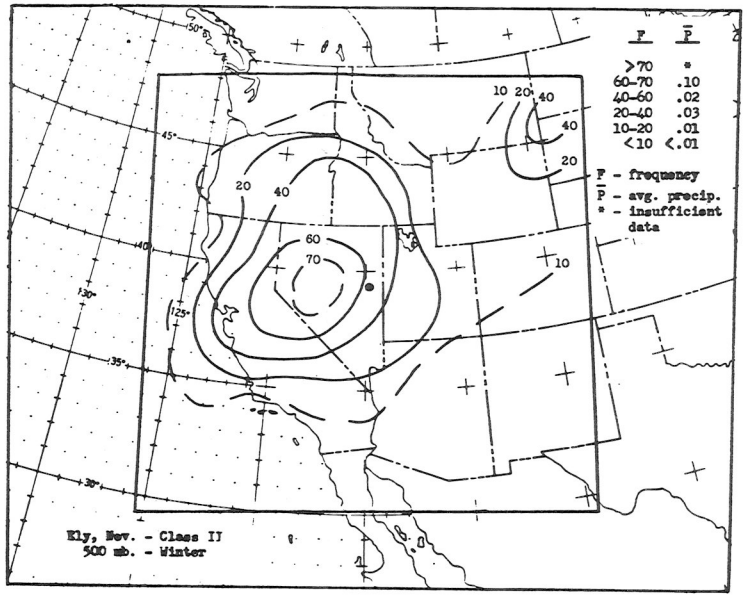

Chart 11 - IIb

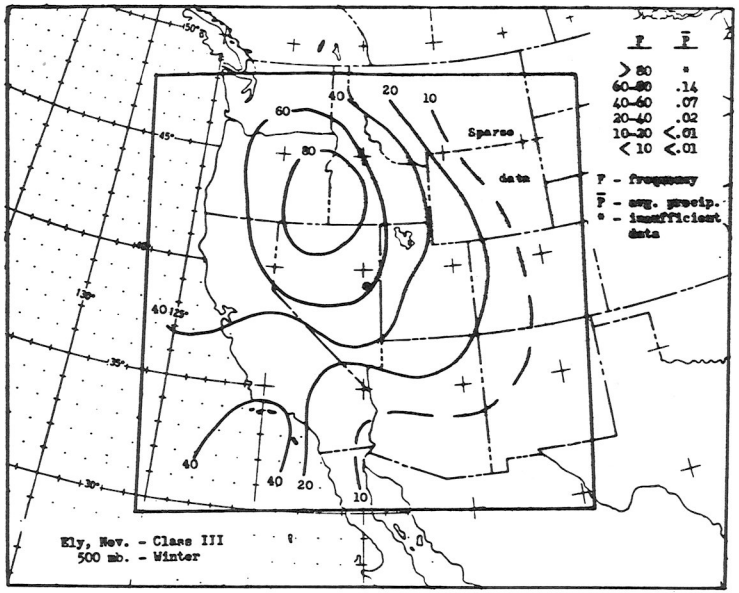

Chart 11 - IIIb

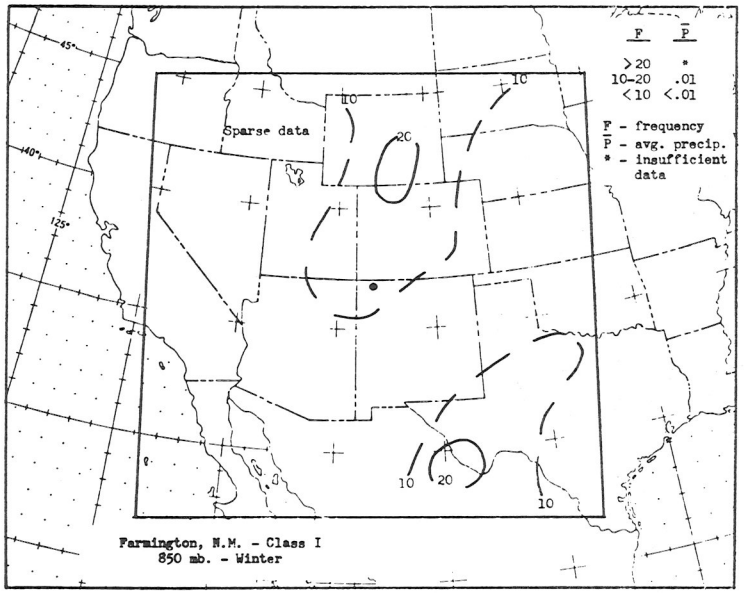

Chart 12 - Ia

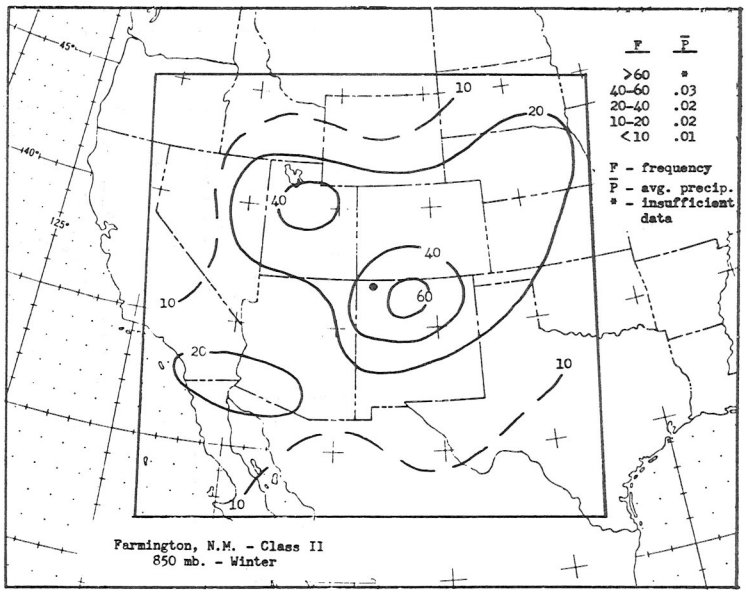

Chart 12 - IIa

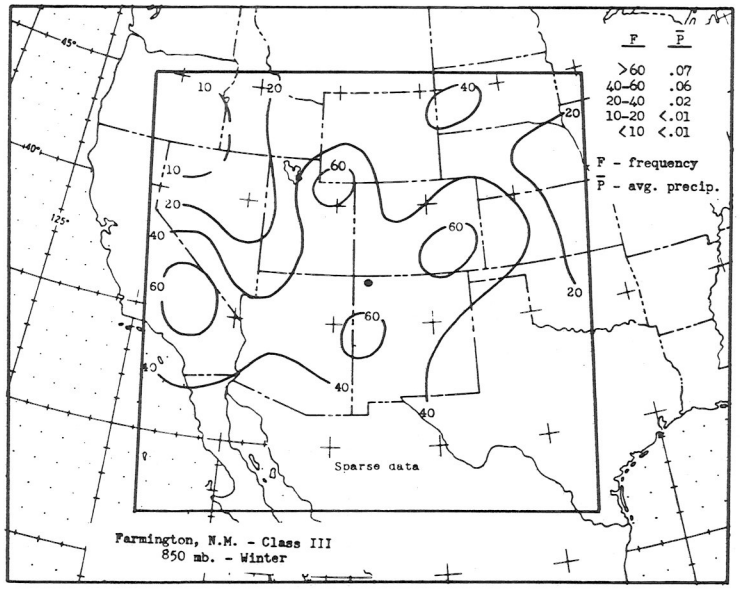

Chart 12 - IIIa

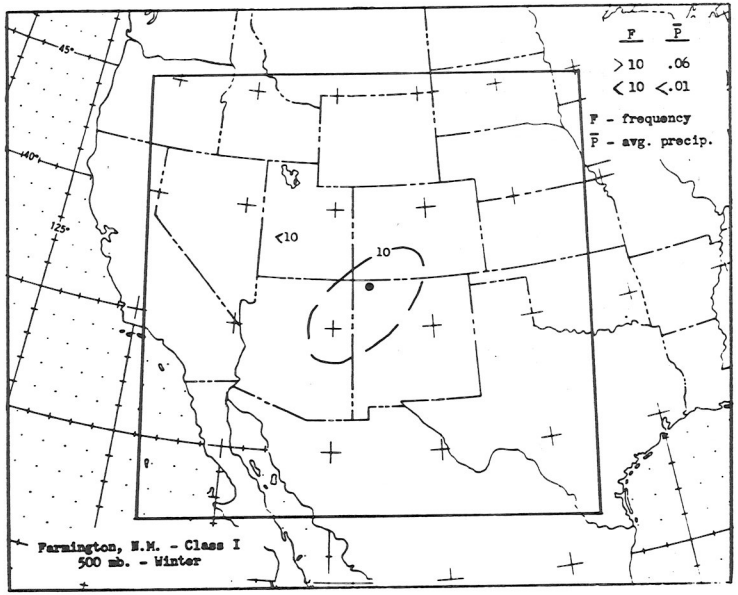

Chart 12 - Ib

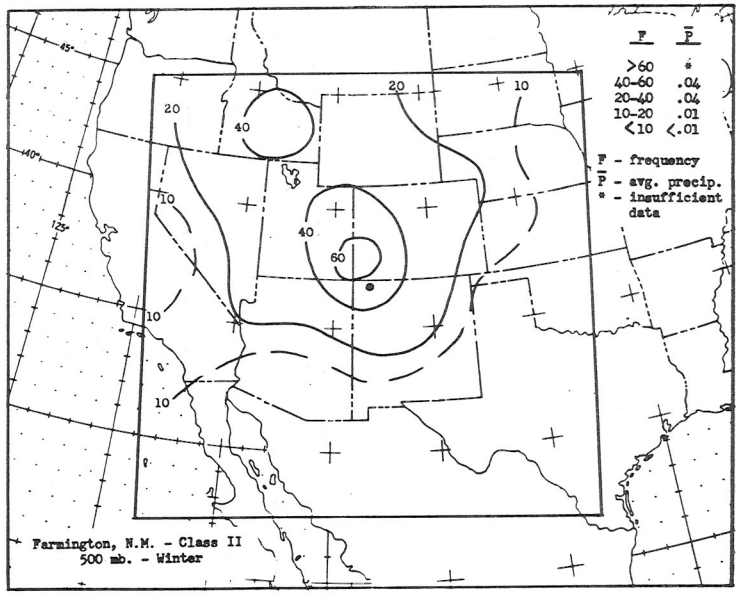

Chart 12 - IIb

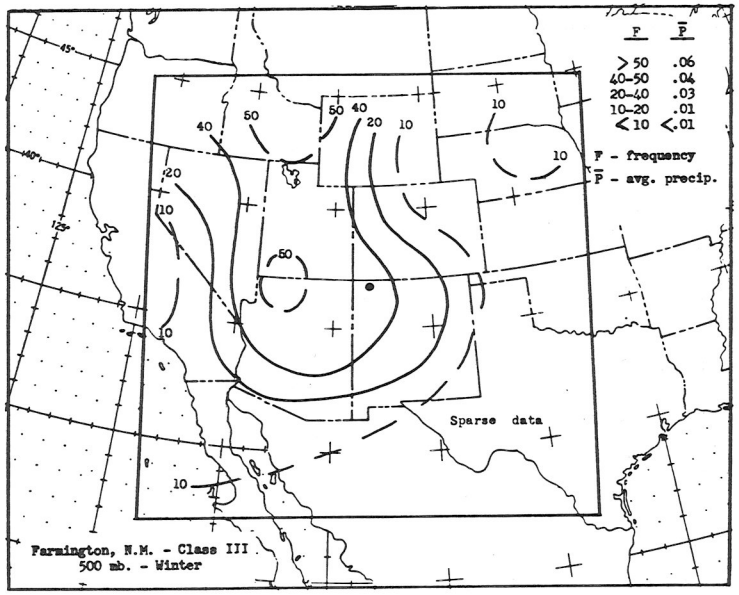

Chart 12 - IIIb

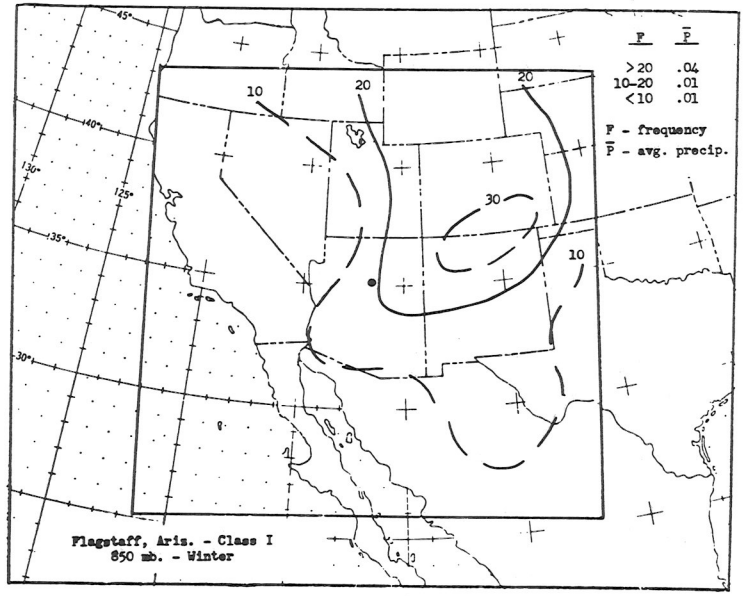

Chart 13 - Ia

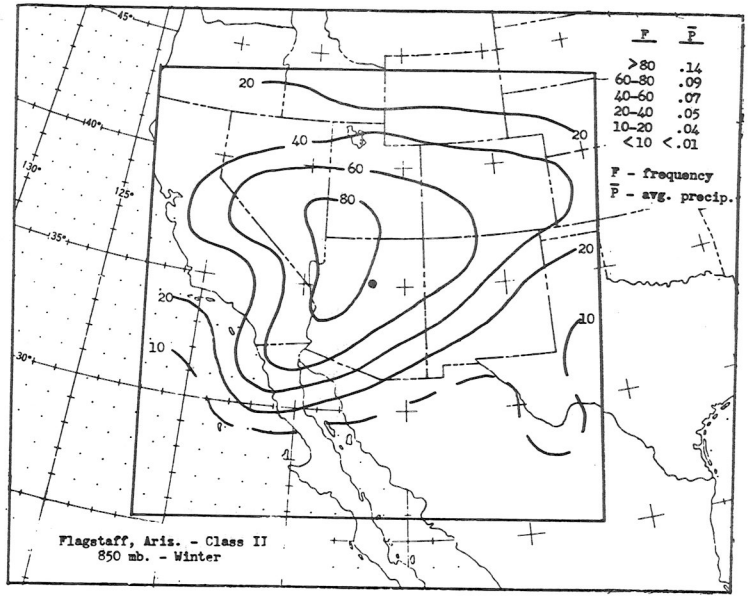

Chart 13 - IIa

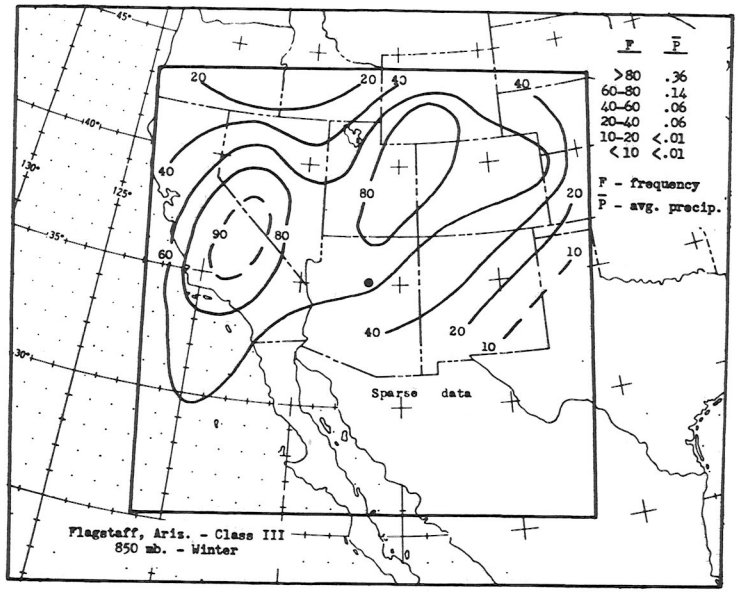

Chart 13 - IIIa

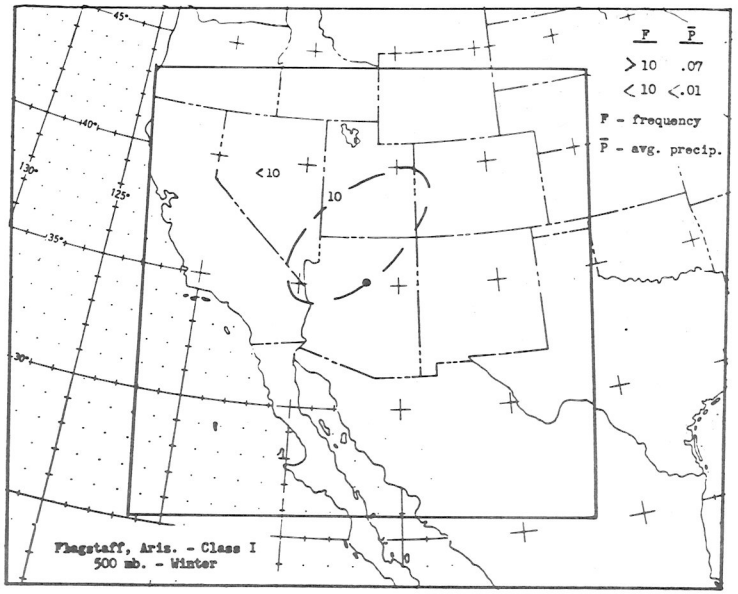

Chart 13 - Ib

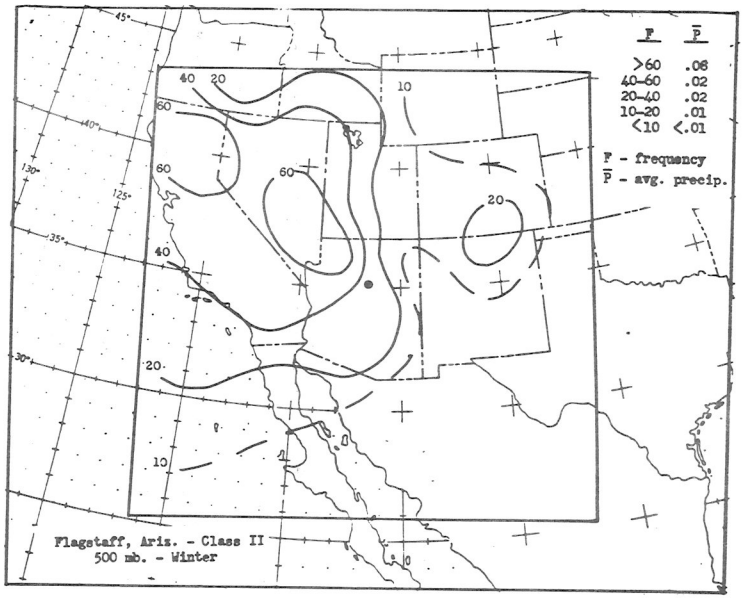

Chart 13 - IIb

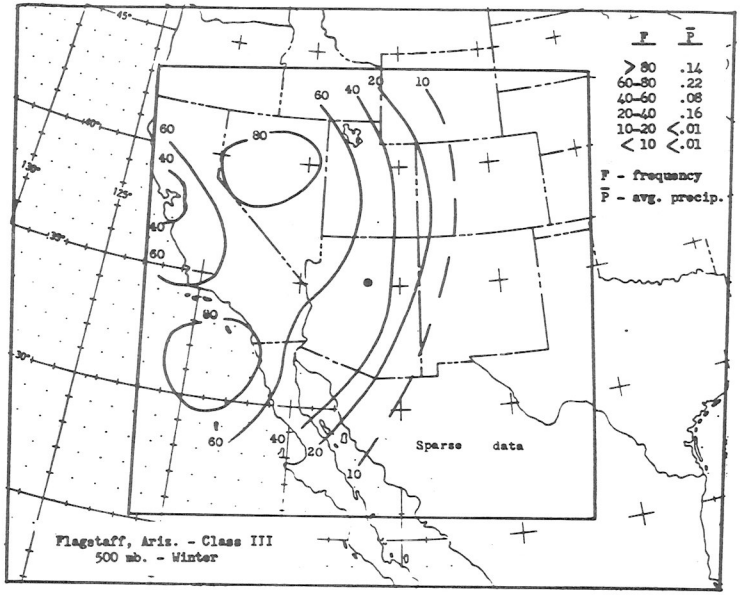

Chart 13 - IIIb

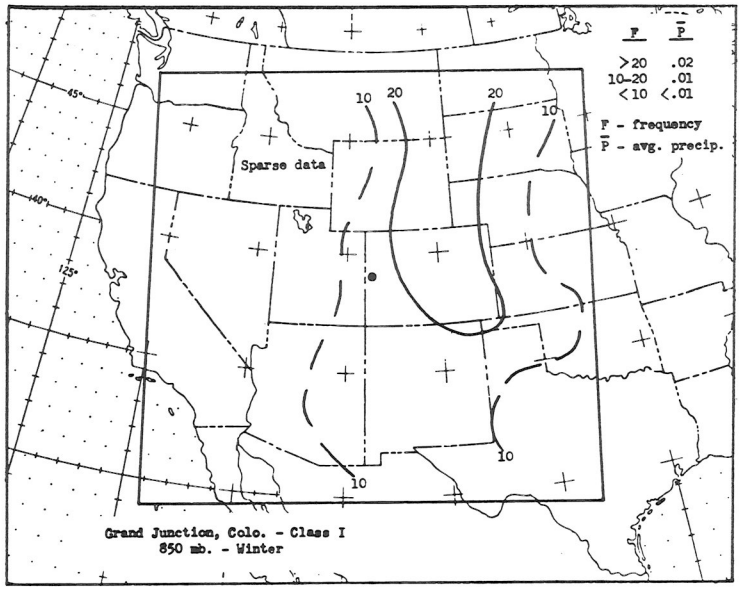

Chart 14 - Ia

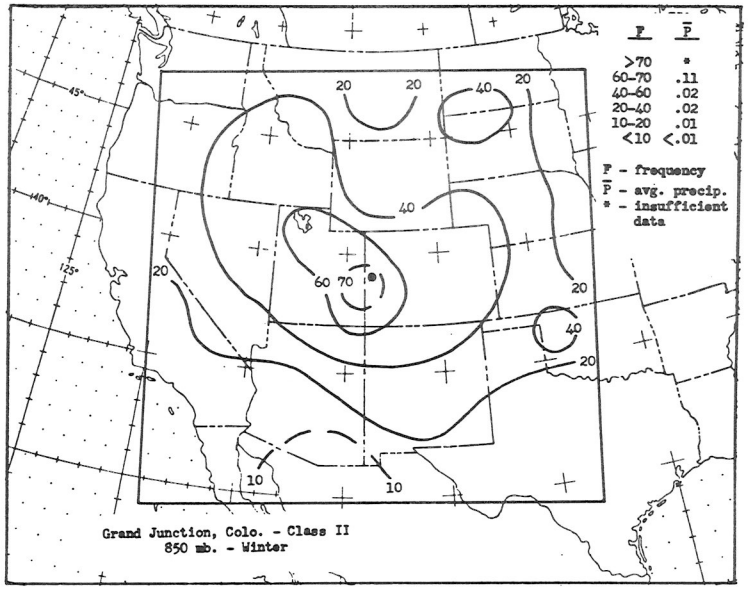

Chart 14 - IIa

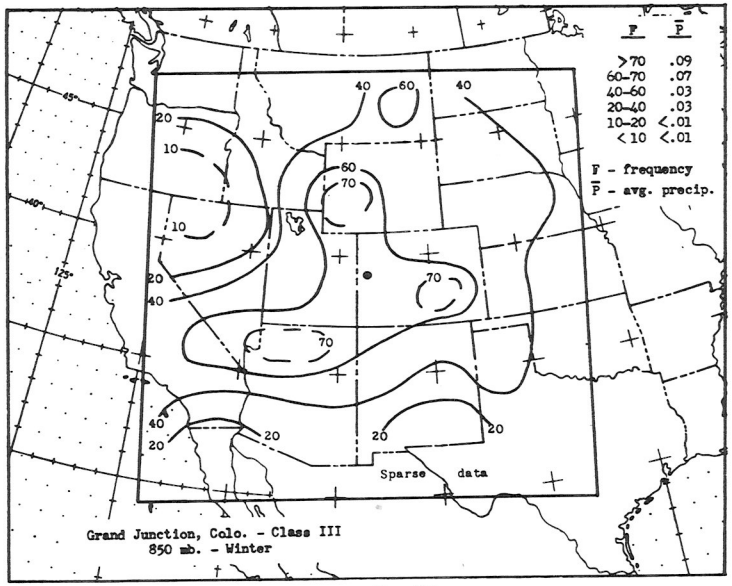

Chart 14 - IIIa

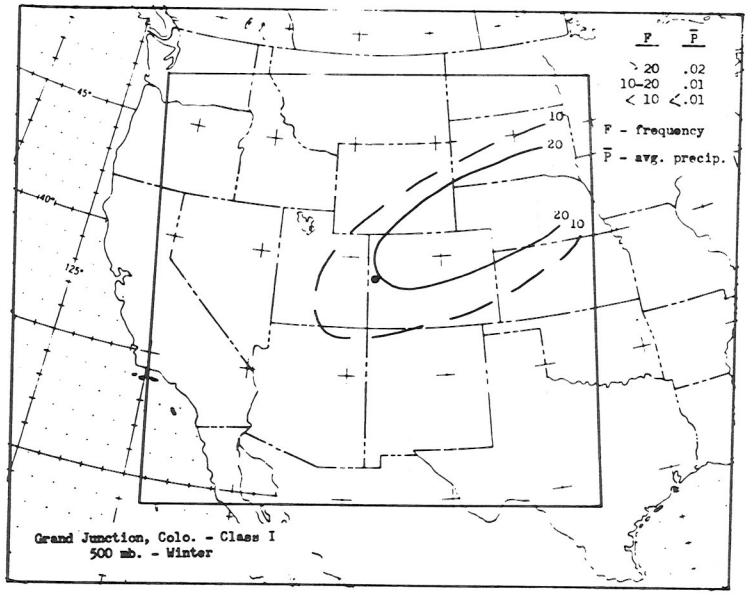

Chart 14 - Ib

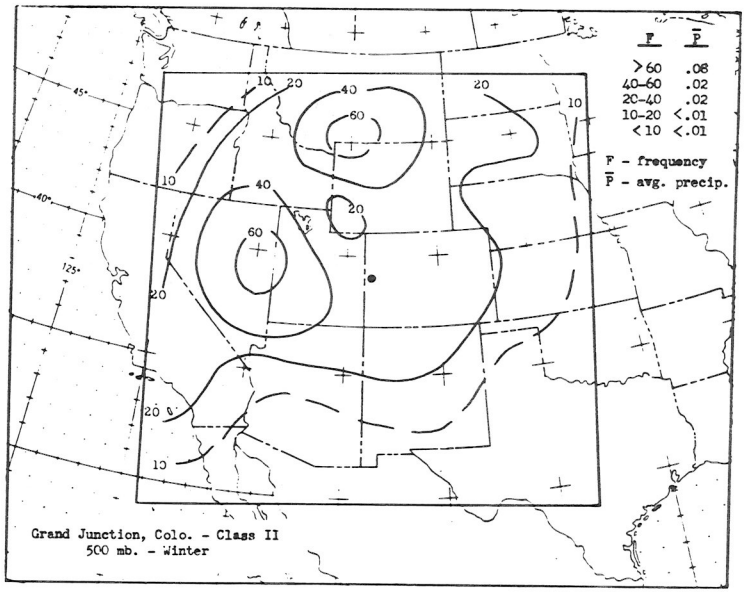

Chart 14 - IIb

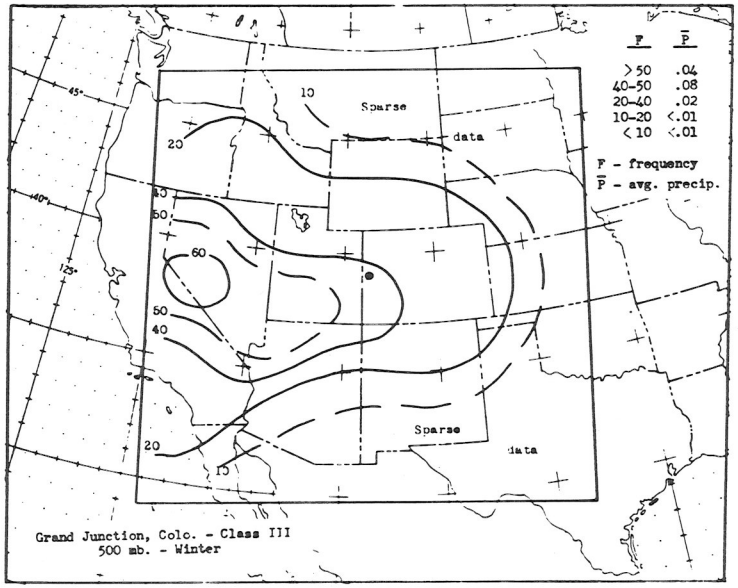

Chart 14 - IIIb

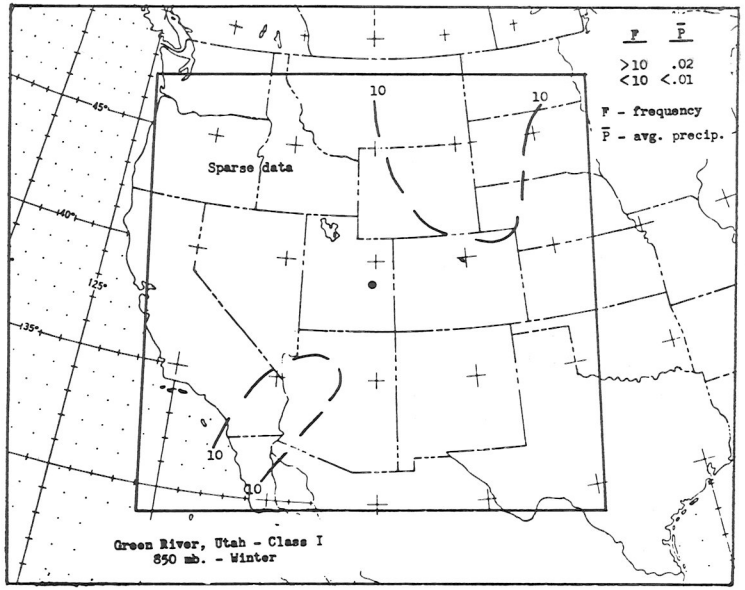

Chart 15 - Ia

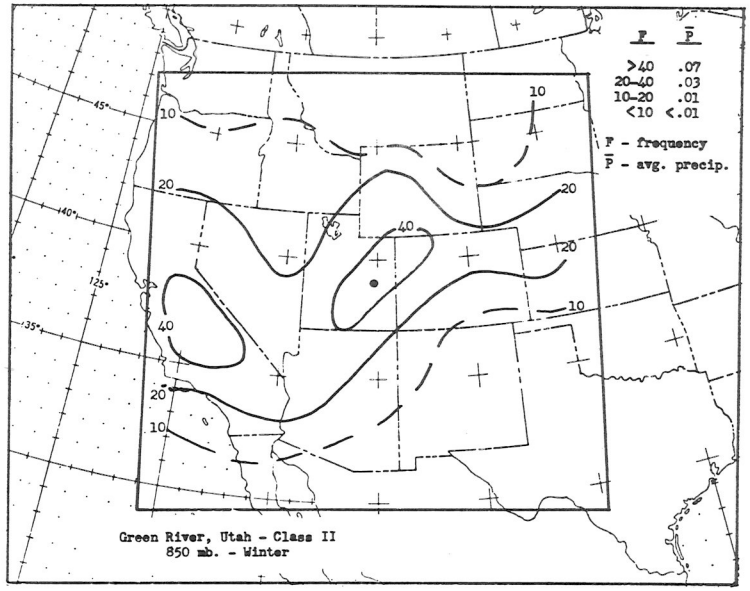

Chart 15 - IIa

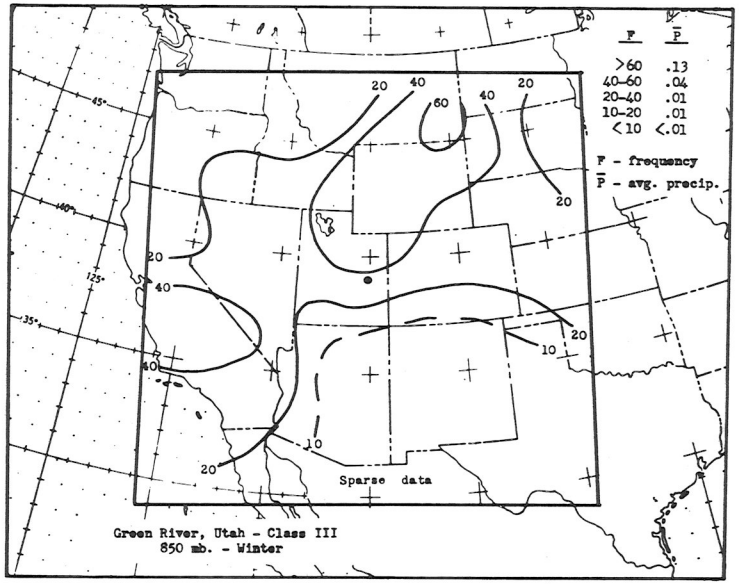

Chart 15 - IIIa

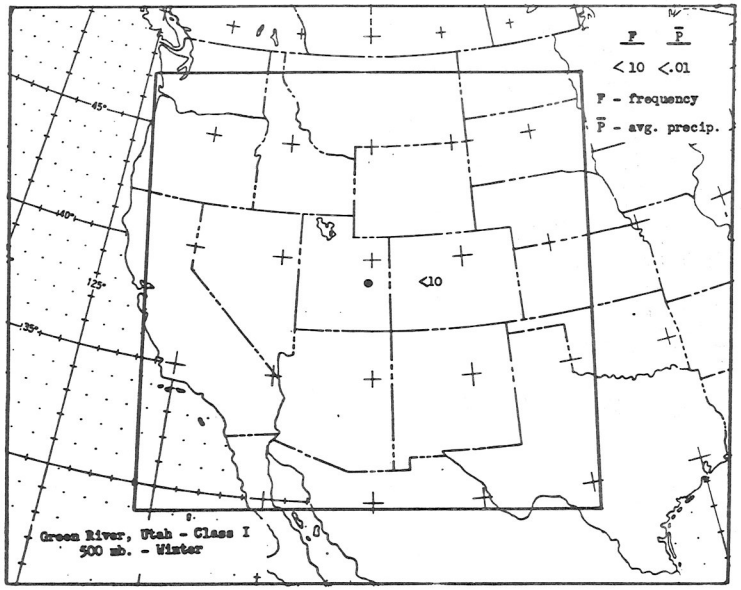

Chart 15 - Ib

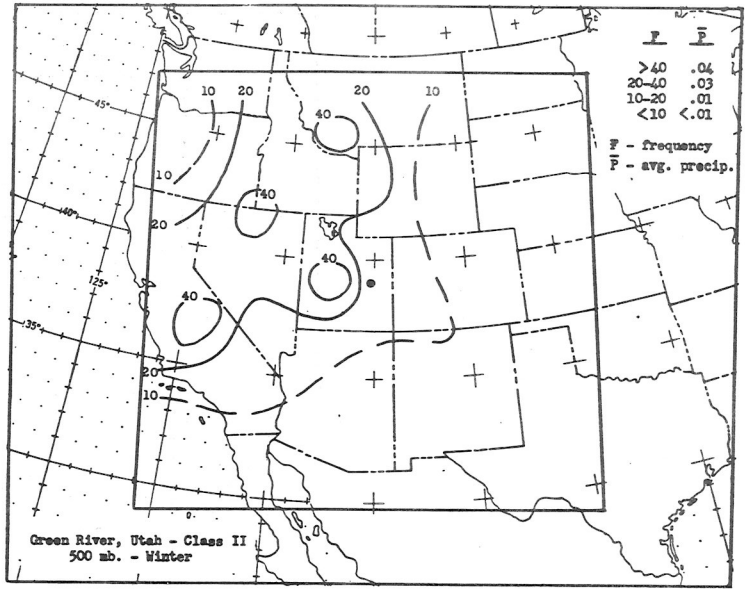

Chart 15 - IIb

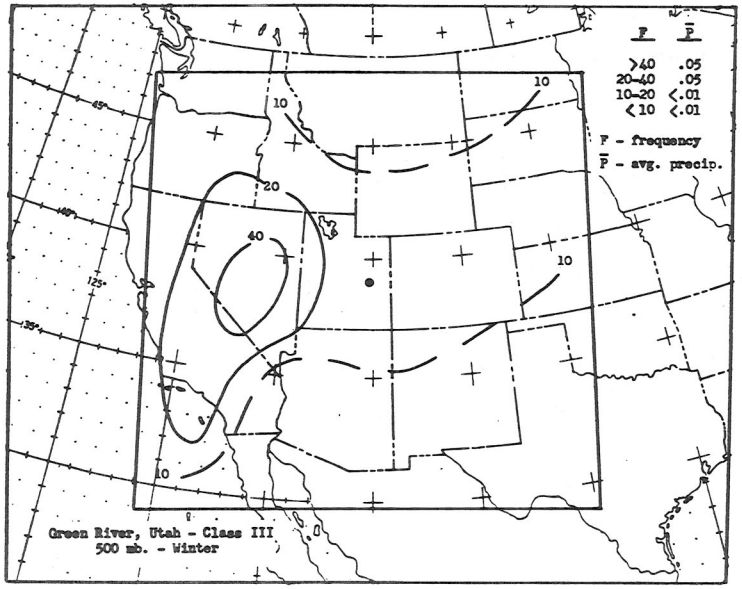

Chart 15 - IIIb

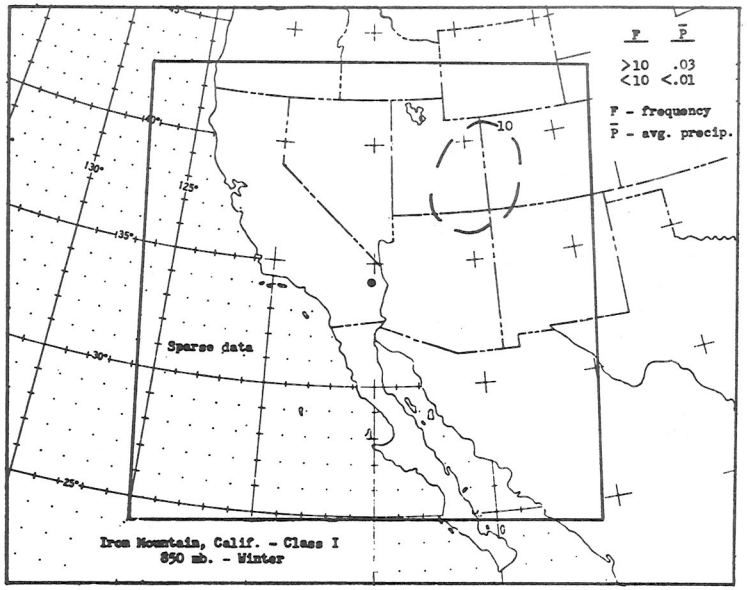

Chart 16 - Ia

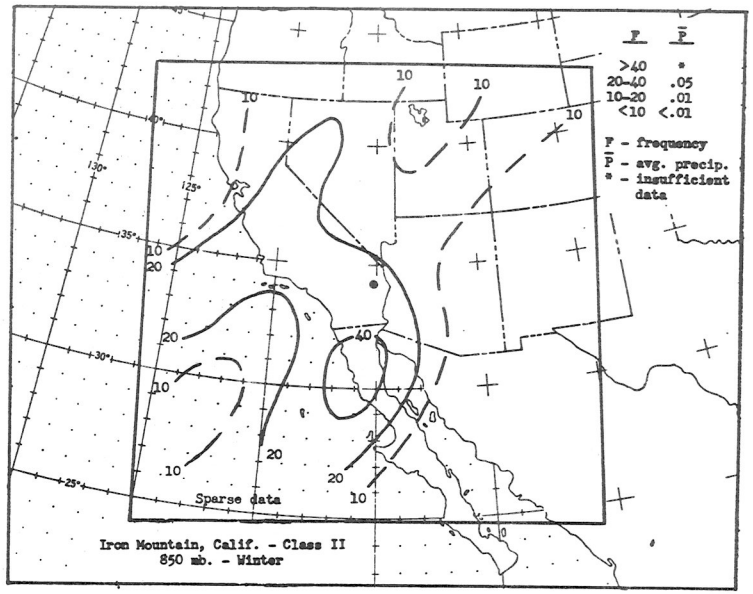

Chart 16 - IIa

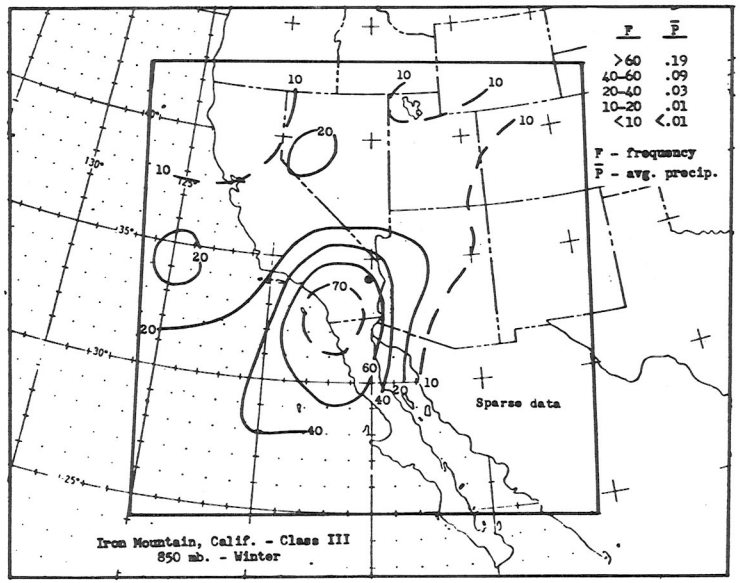

Chart 16 - IIIa

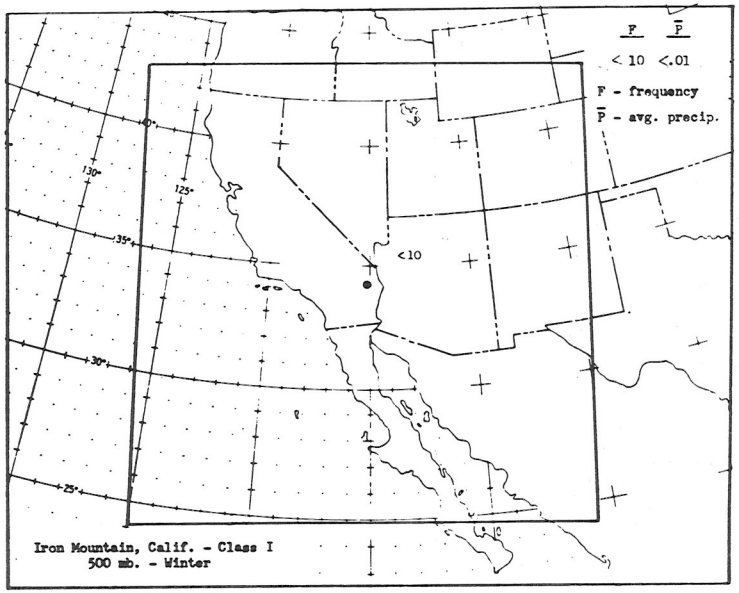

Chart 16 - Ib

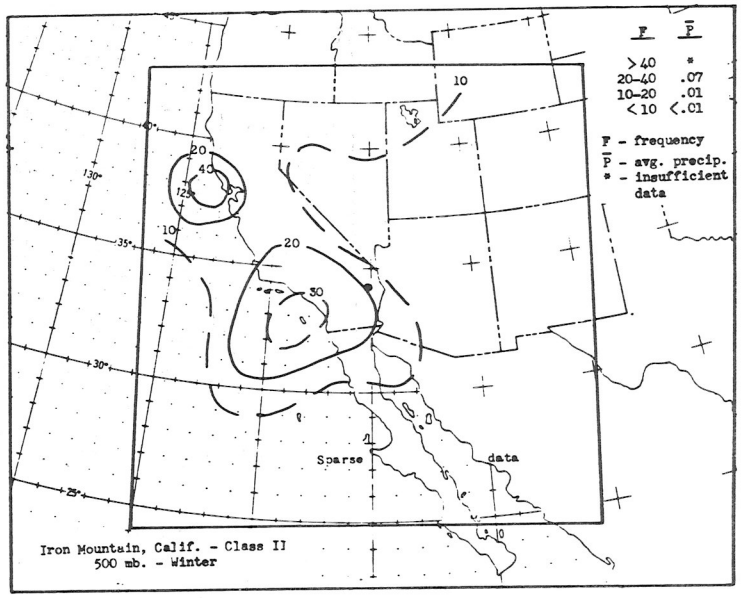

Chart 16 - IIb

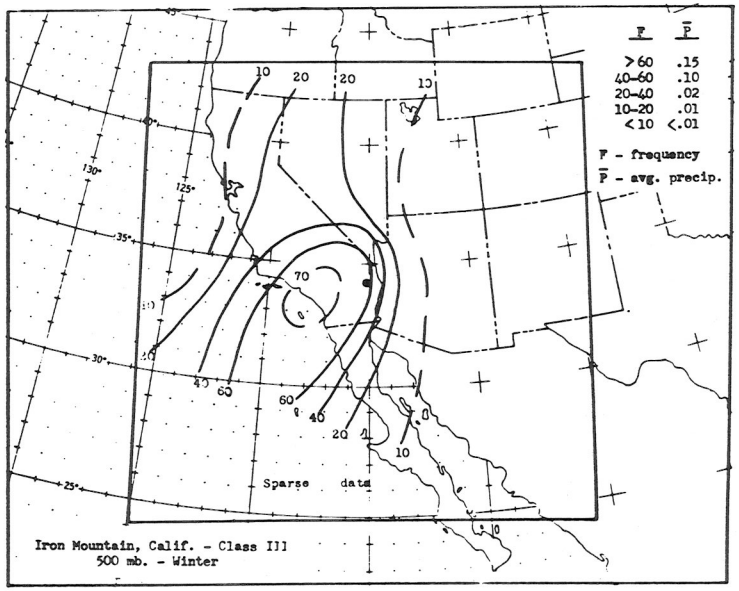

Chart 16 - IIIb

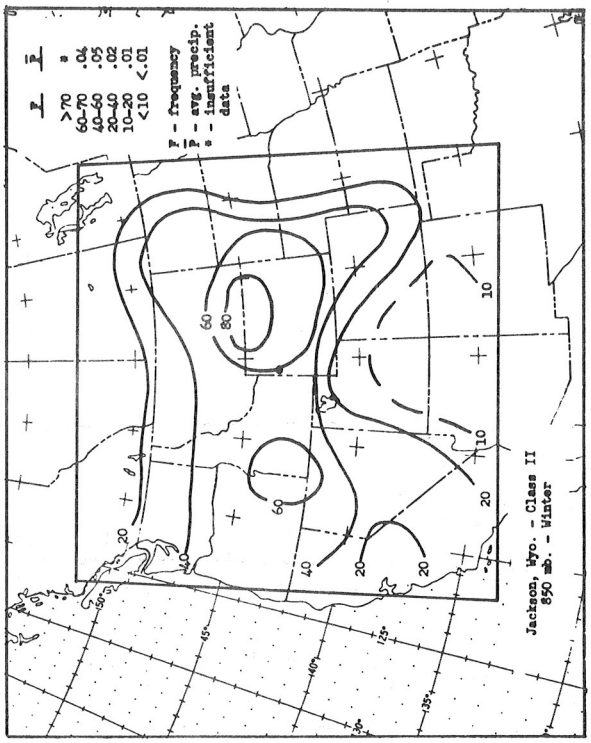

Chart 17 - IIa

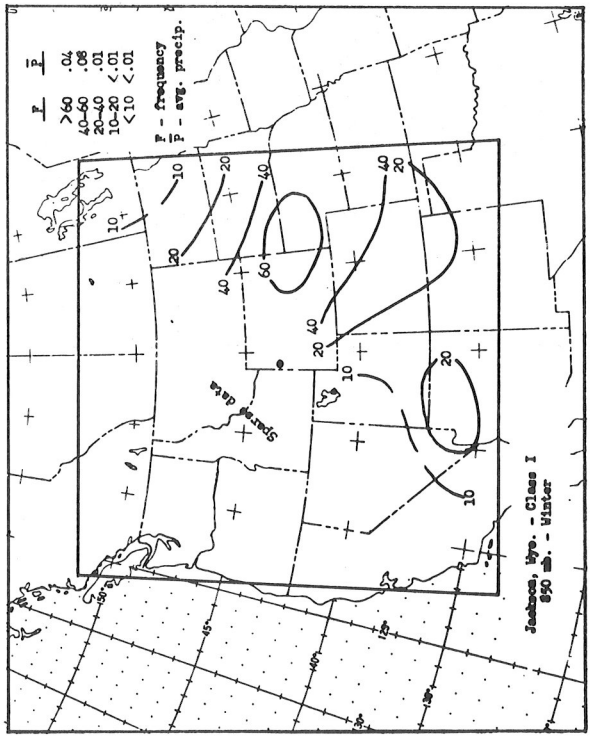

Chart 17 - Ia

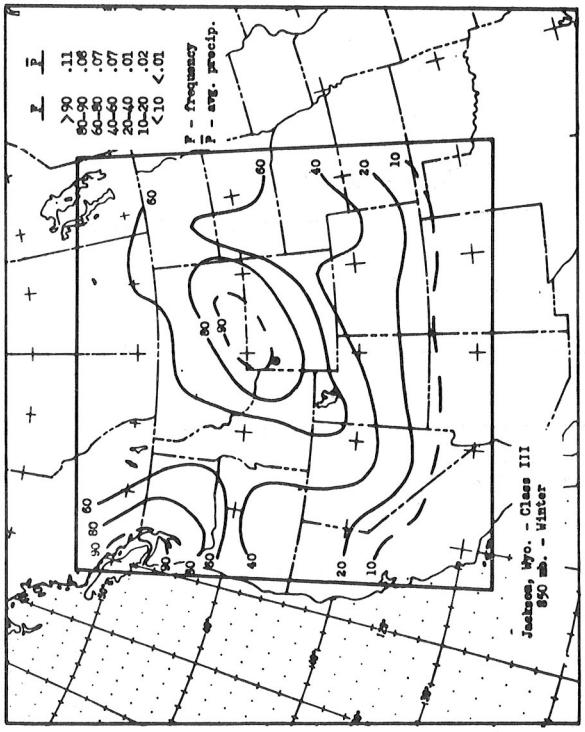

Chart 17 - IIIa

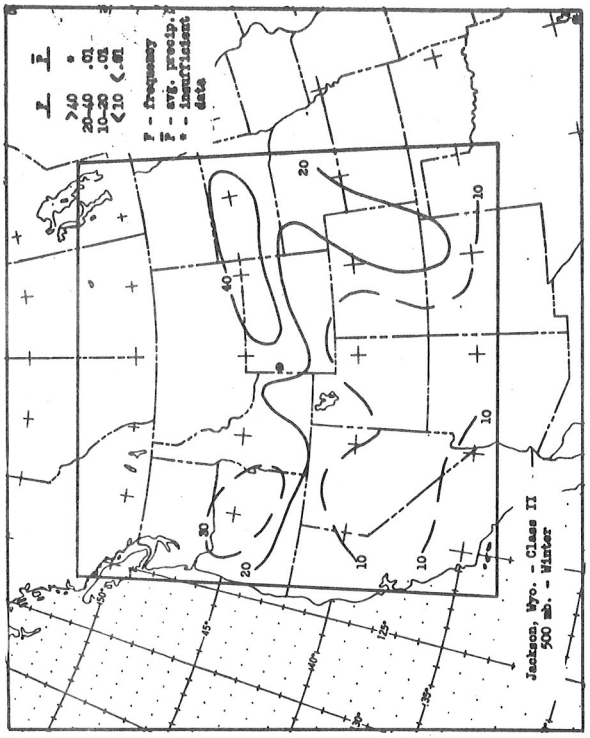

Chart 17 - IIb

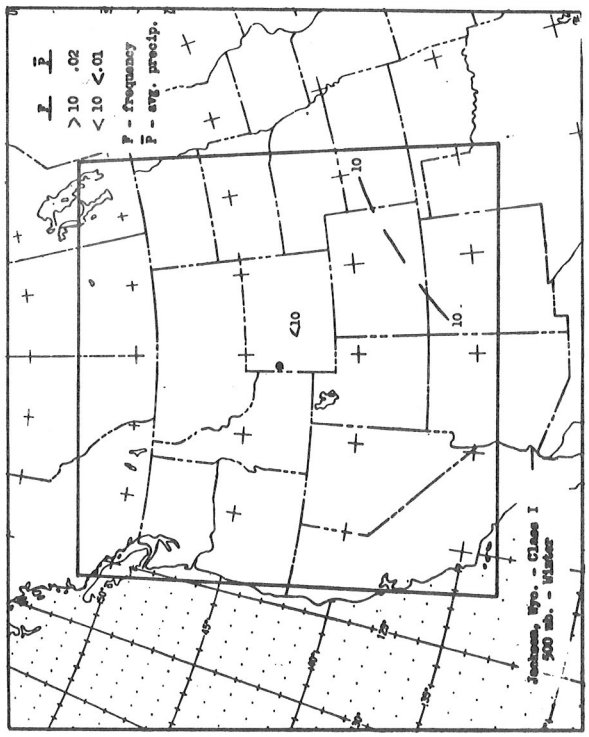

Chart 17 - Ib

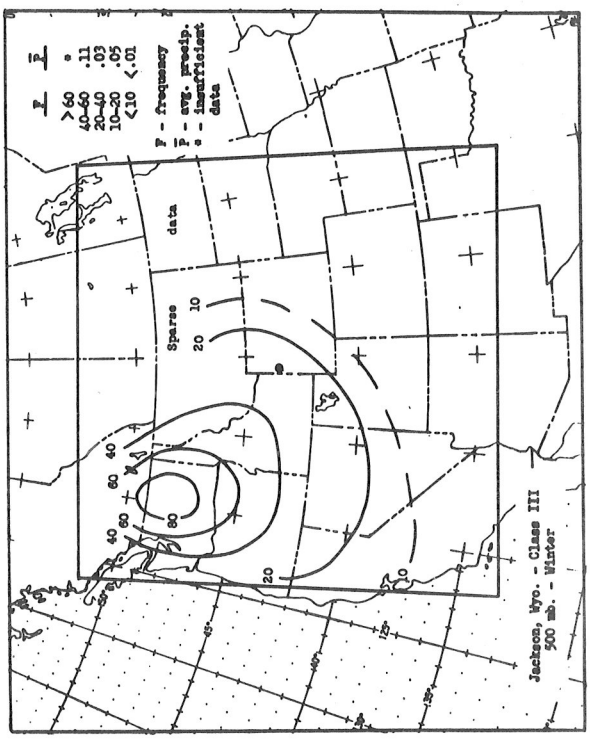

Chart 17 - IIIb

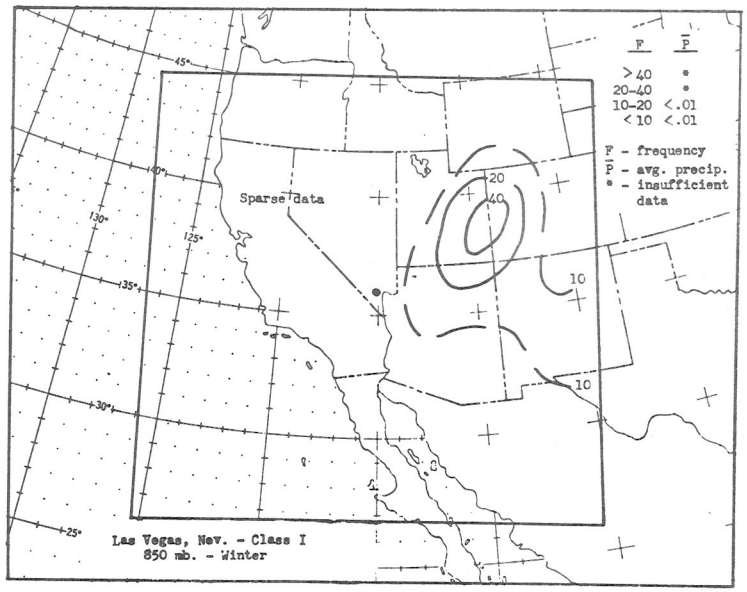

Chart 18 - Ia

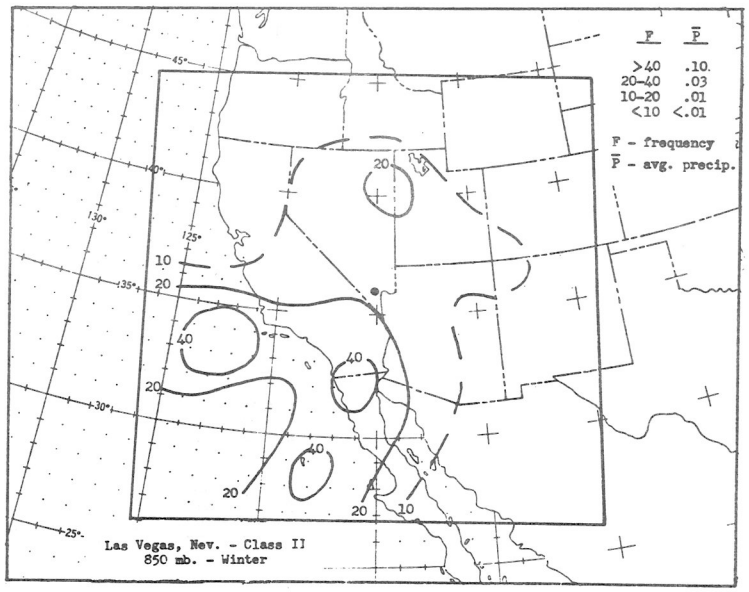

Chart 18 - IIa

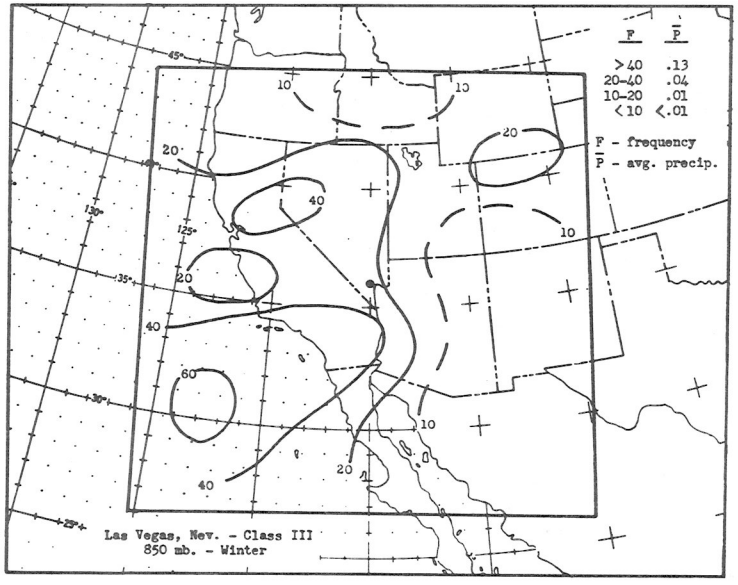

Chart 18 - IIIa

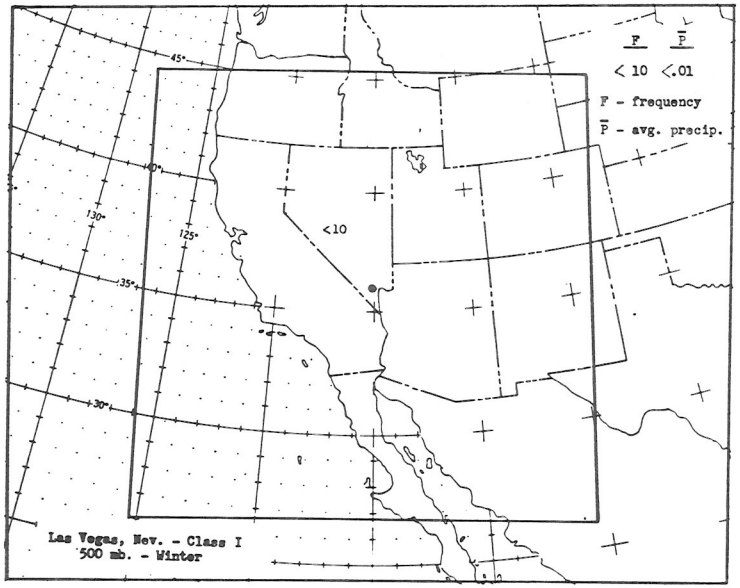

Chart 18 - Ib

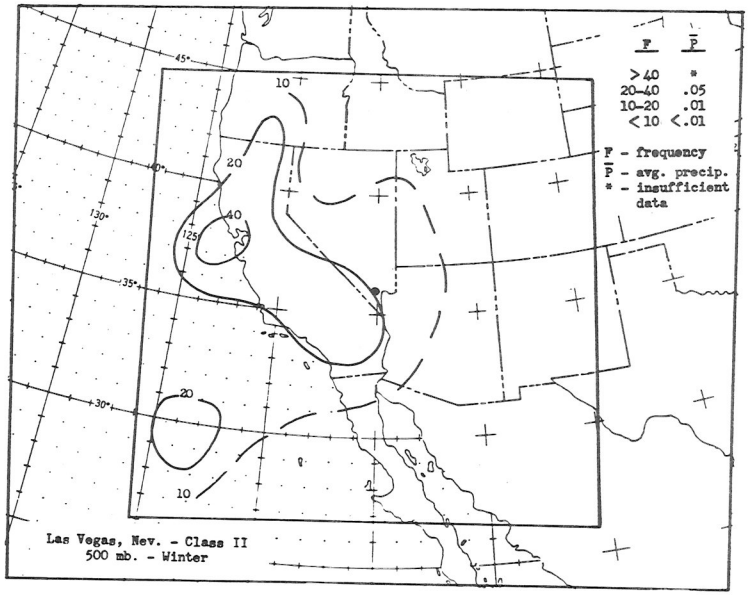

Chart 18 - IIb

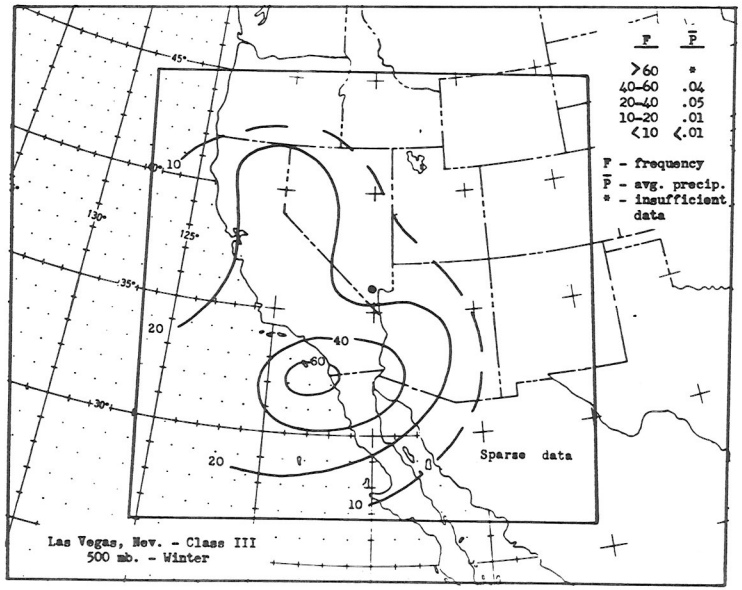

Chart 18 - IIIb

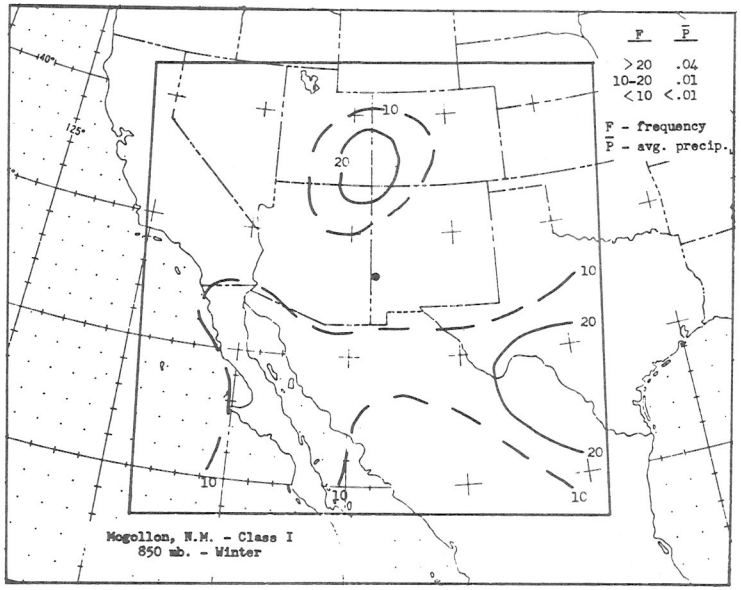

Chart 19 - Ia

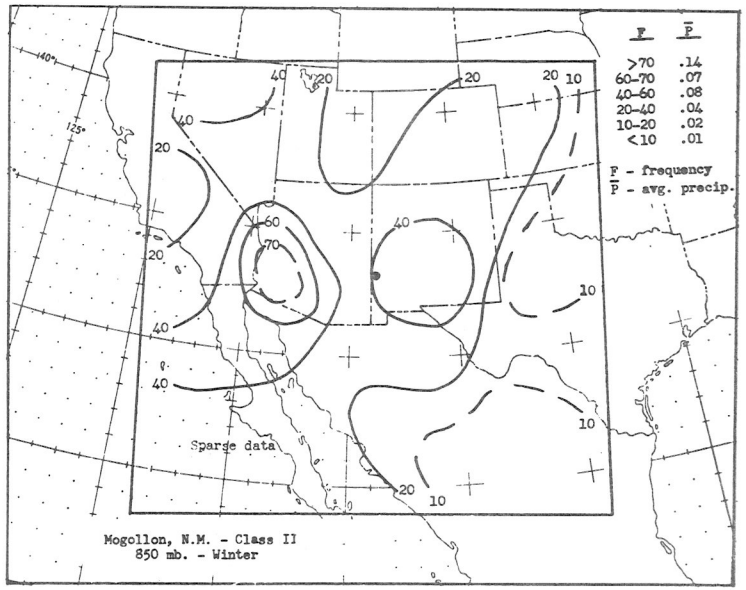

Chart 19 - IIa

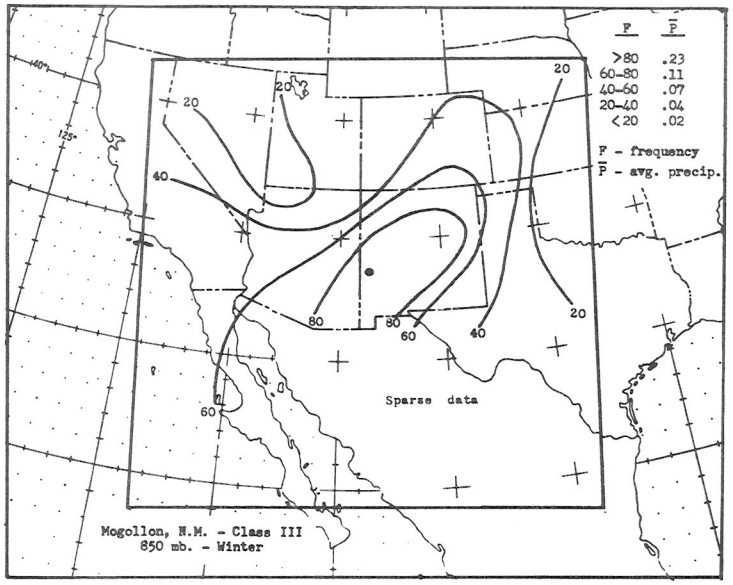

Chart 19 - IIIa

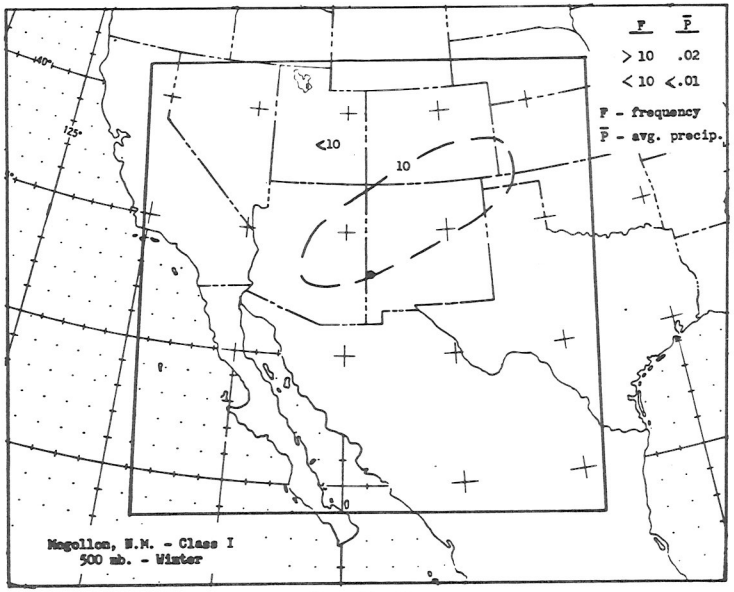

Chart 19 - Ib

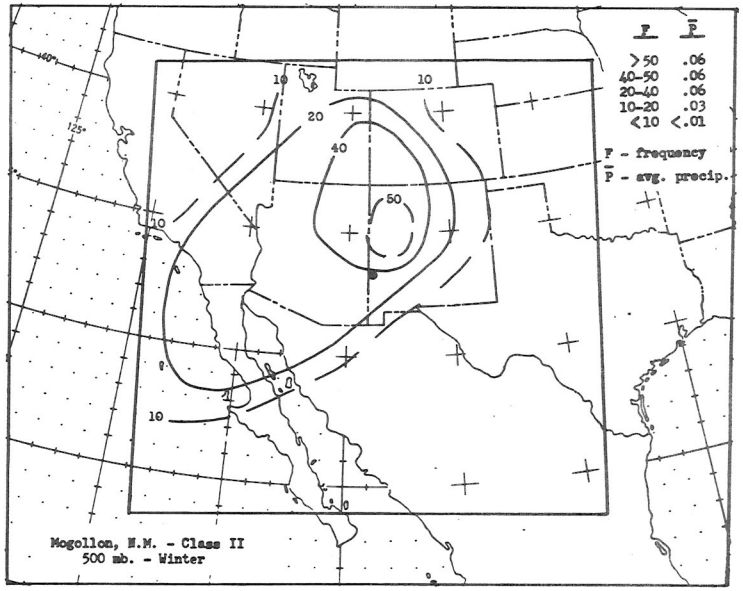

Chart 19 - IIb

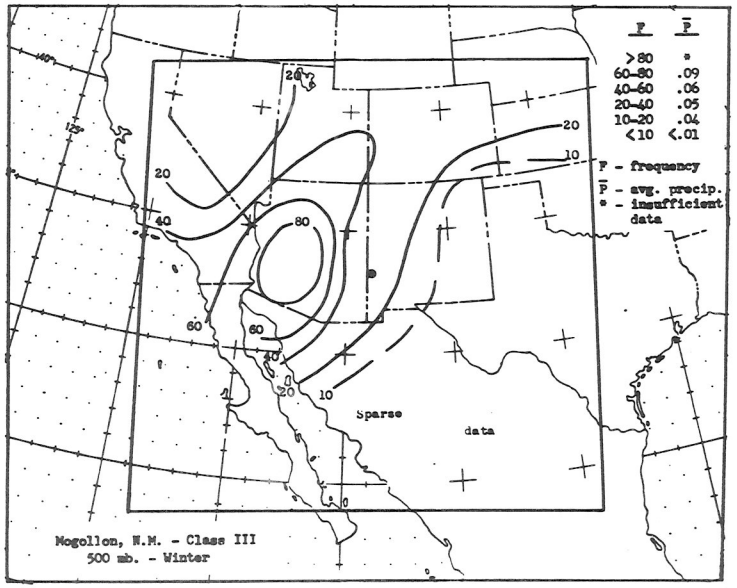

Chart 19 - IIIb

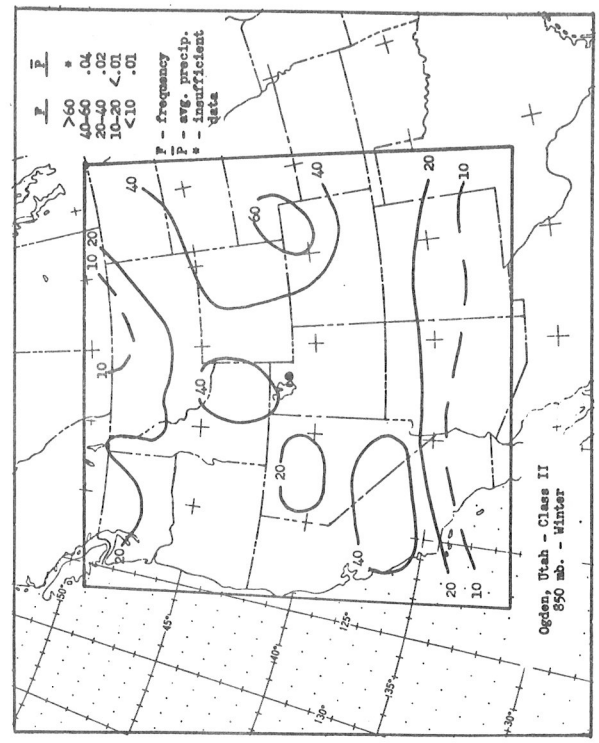

Chart 20 - IIa

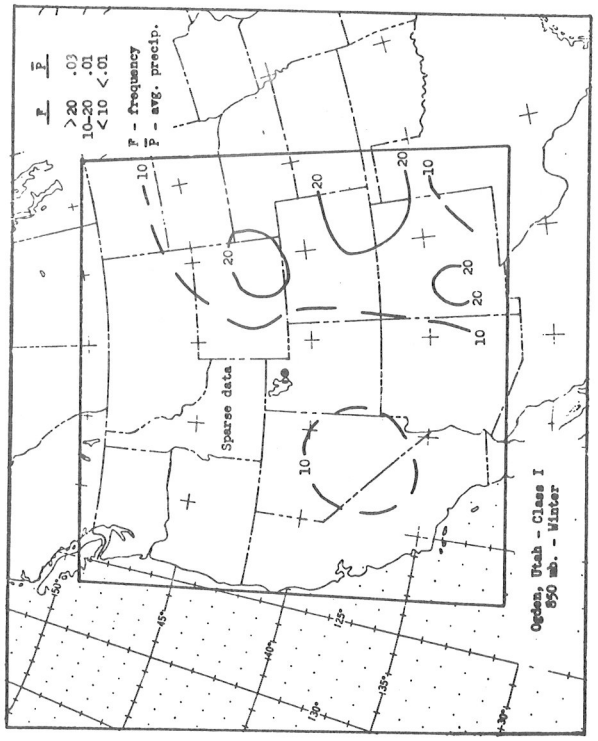

Chart 20 - Ia

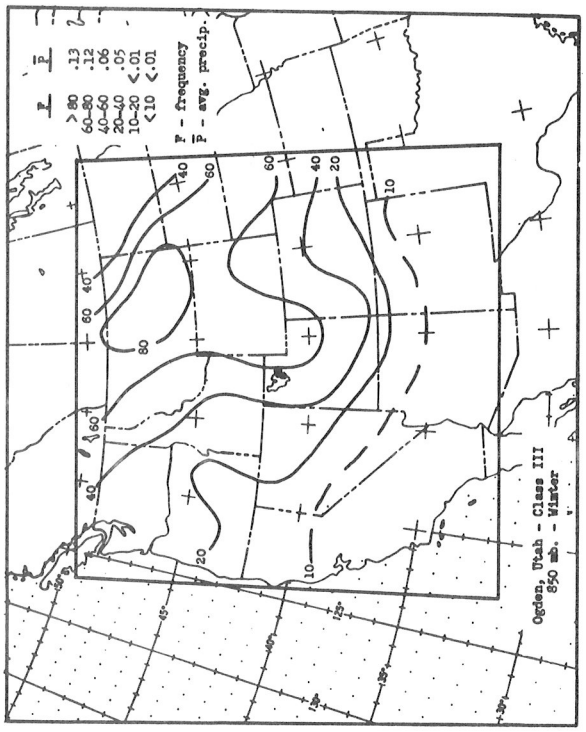

Chart 20 - IIIa

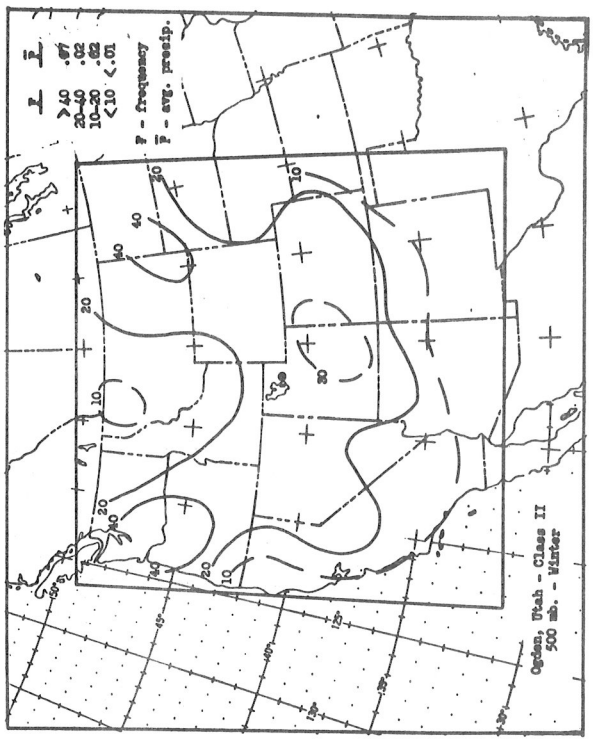

Chart 20 - IIb

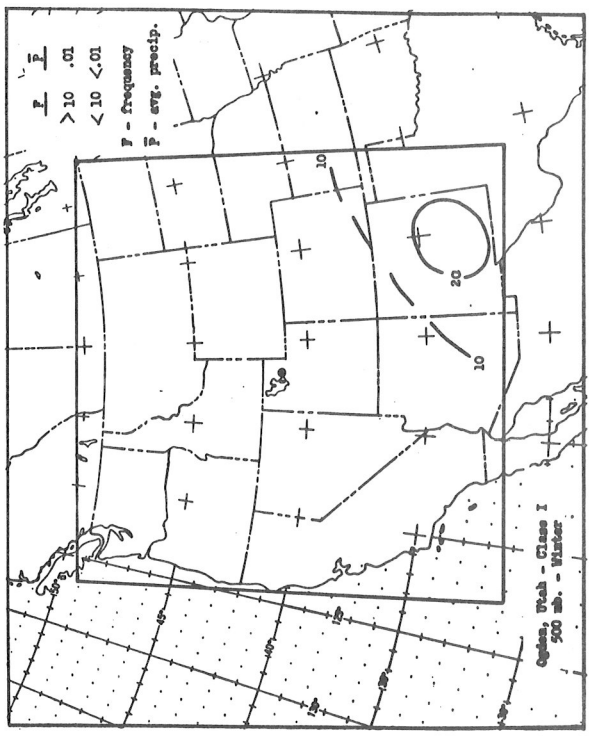

Chart 20 - Ib

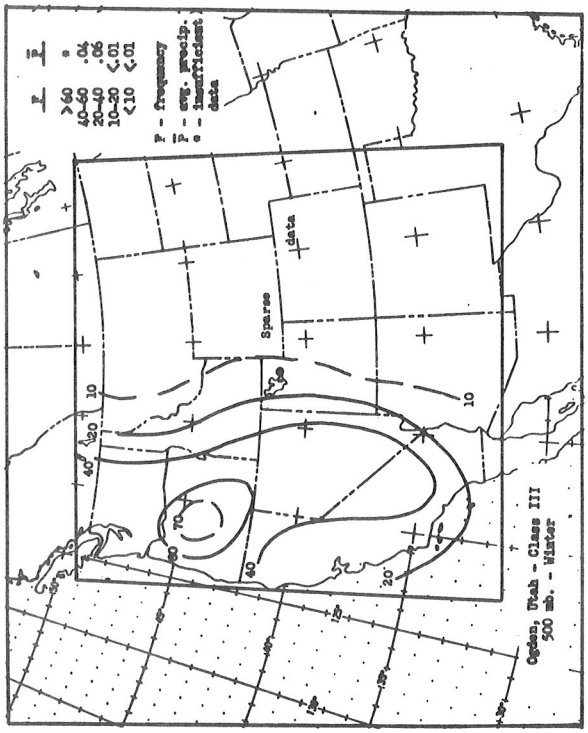

Chart 20 - IIIb

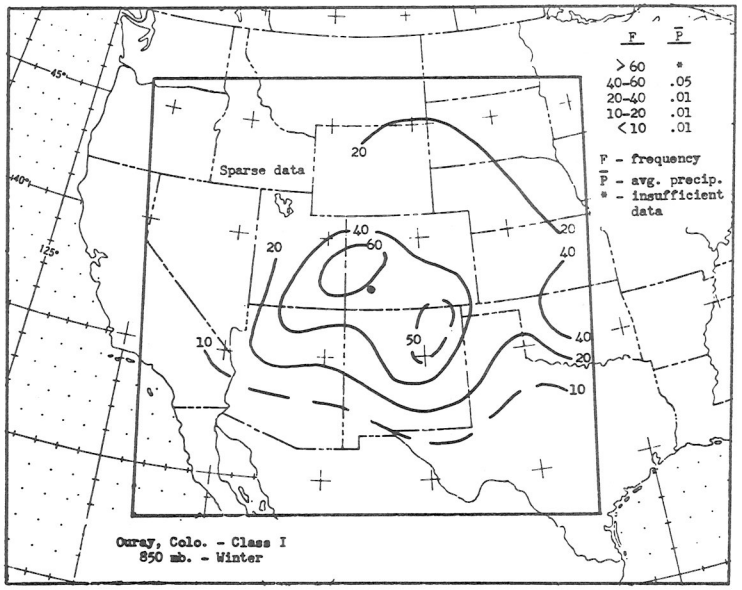

Chart 21 - Ia

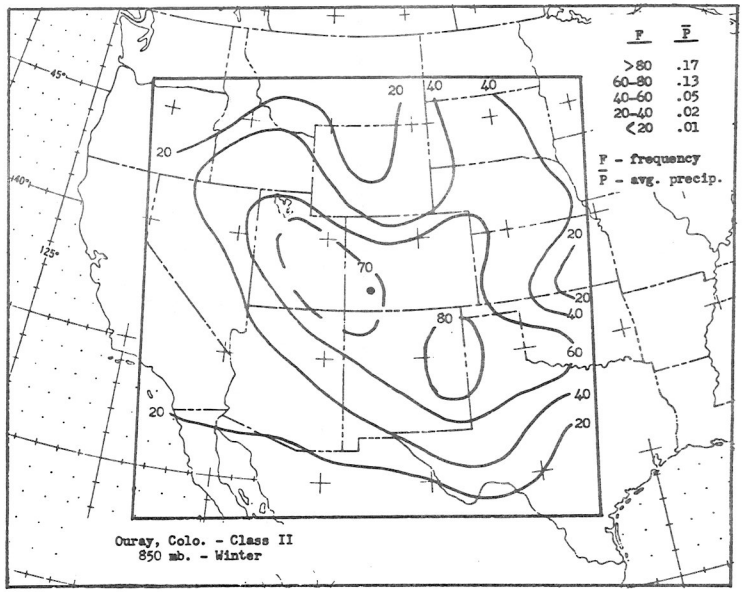

Chart 21 - IIa

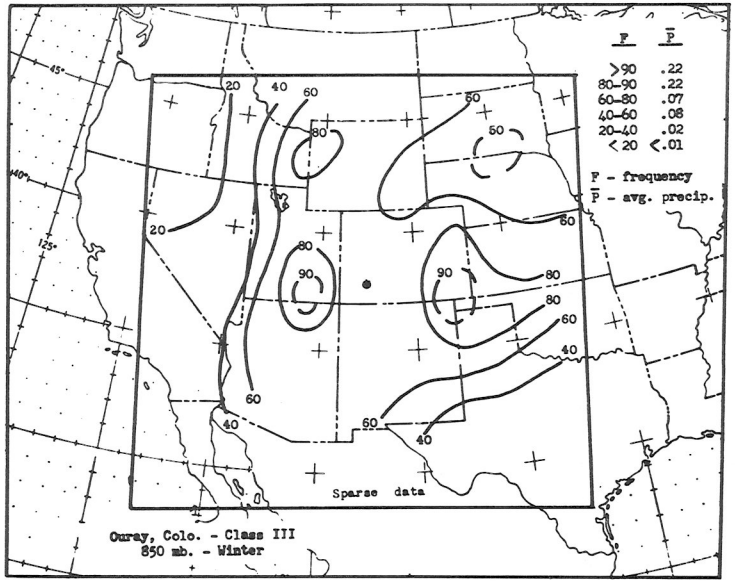

Chart 21 - IIIa

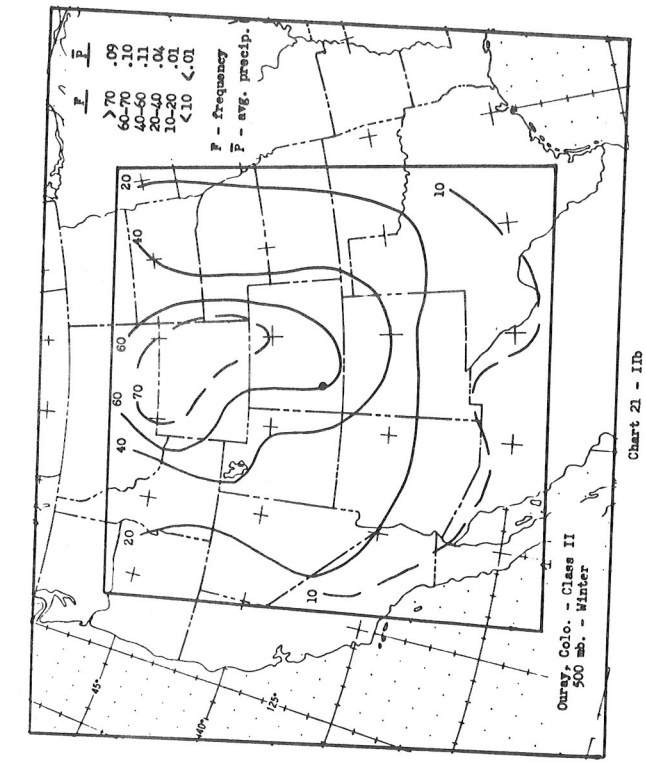

Chart 21 - IIb

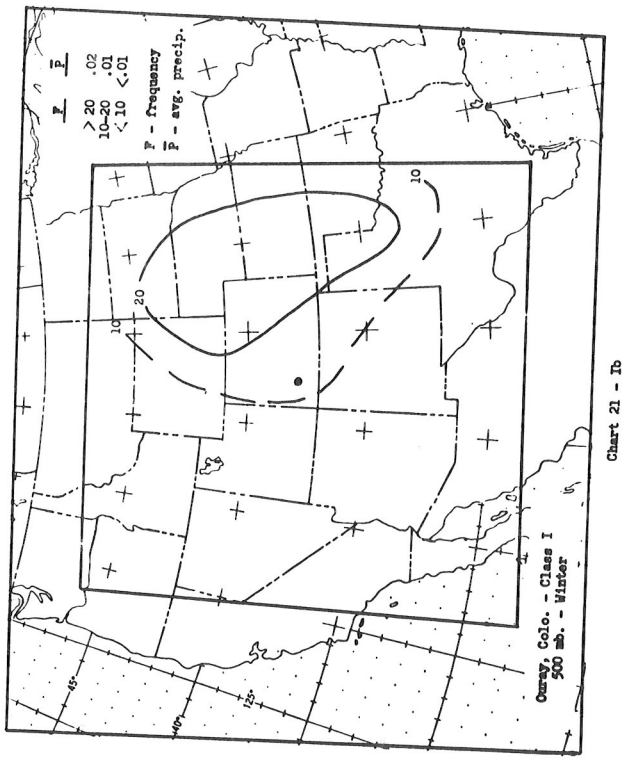

Chart 21 - Ib

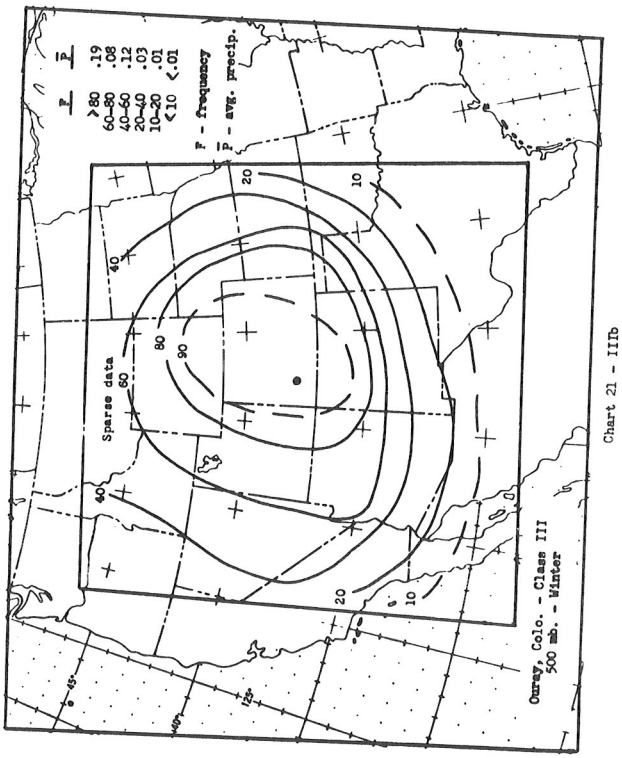

Chart 21 - IIIb

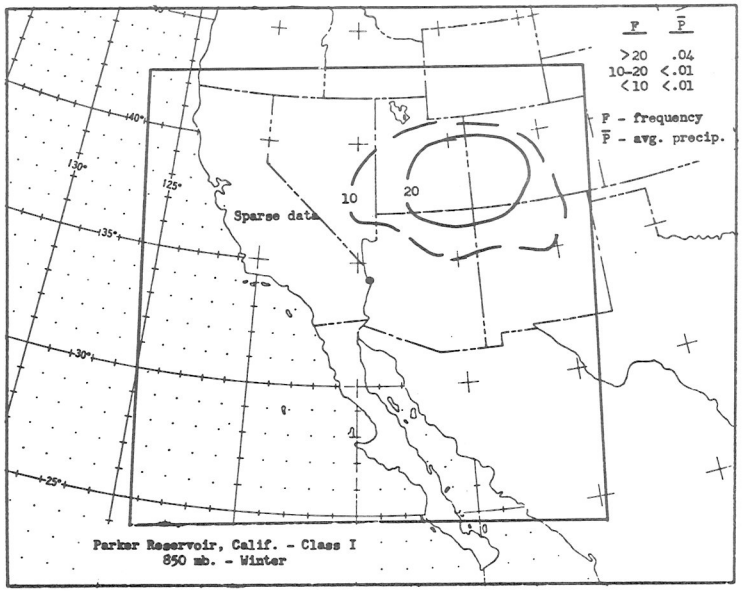

Chart 22 - Ia

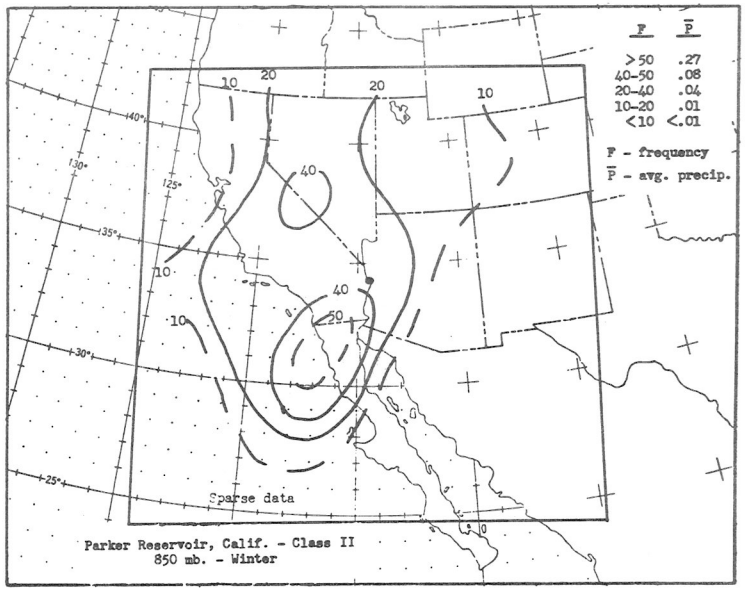

Chart 22 - IIa

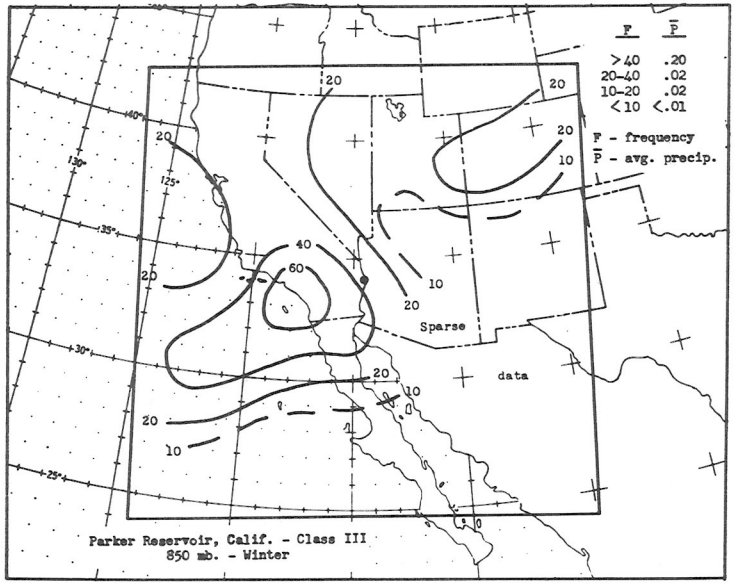

Chart 22 - IIIa

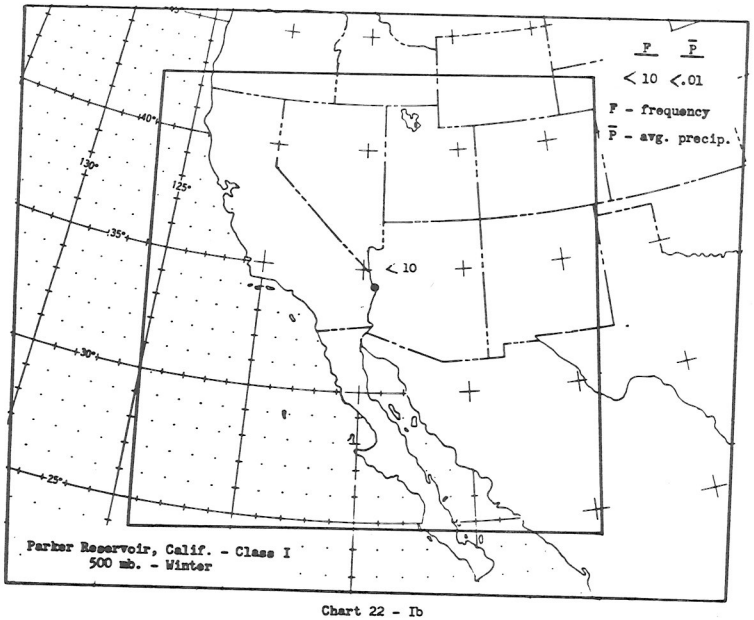

Chart 22 - Ib

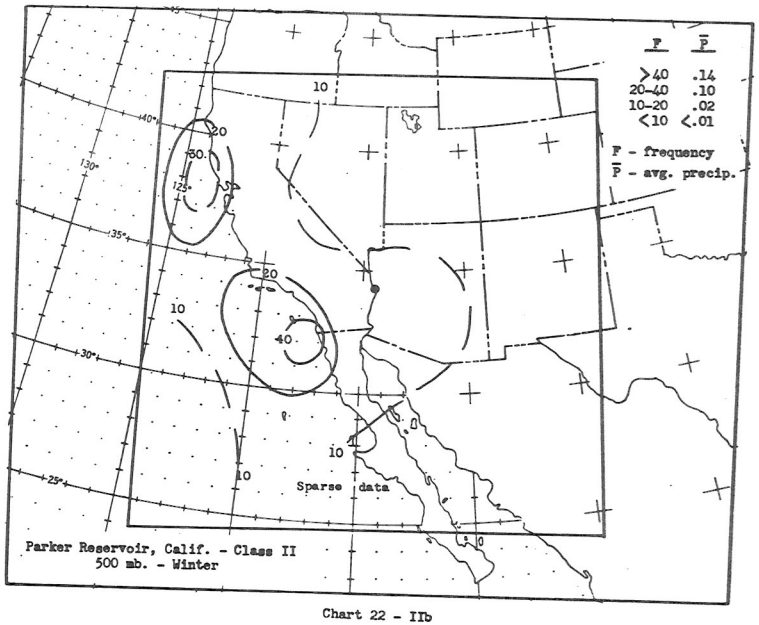

Chart 22 - IIb

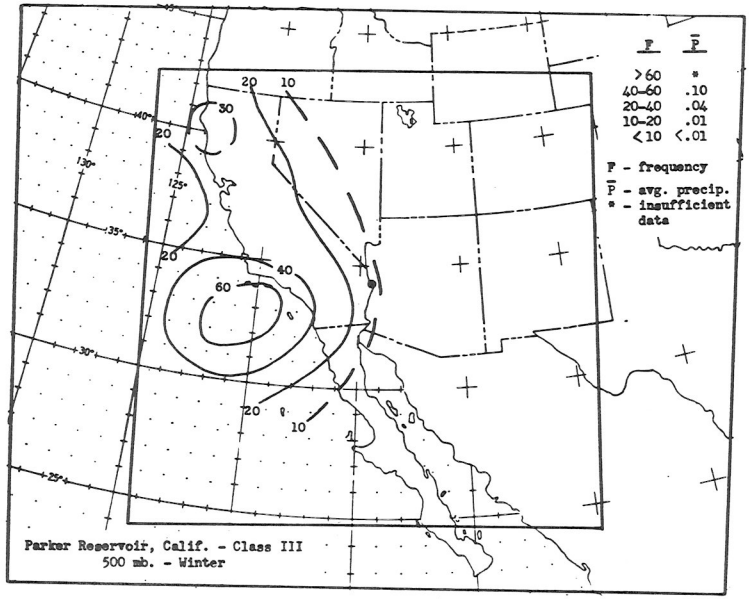

Chart 22 - IIIb

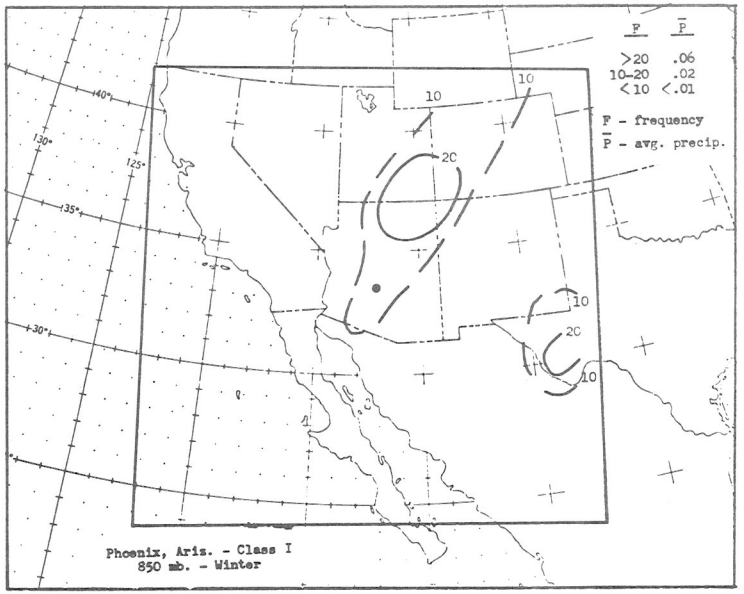

Chart 23 - Ia

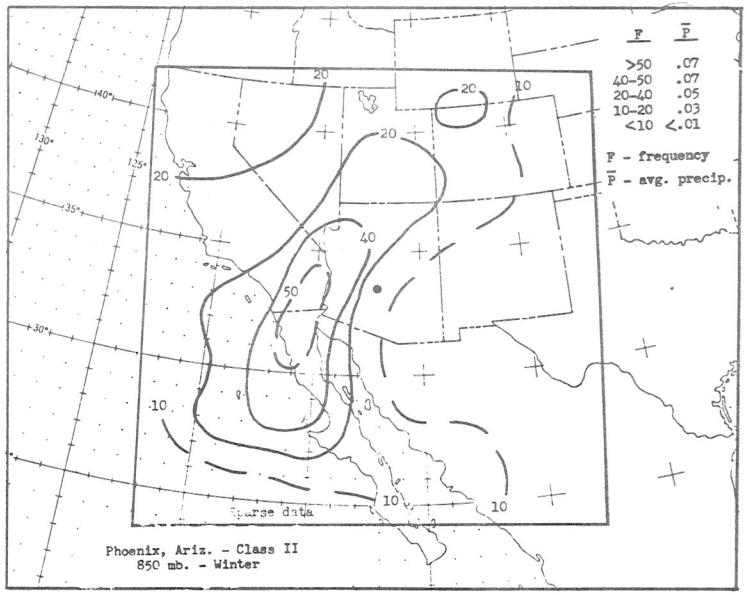

Chart 23 - IIa

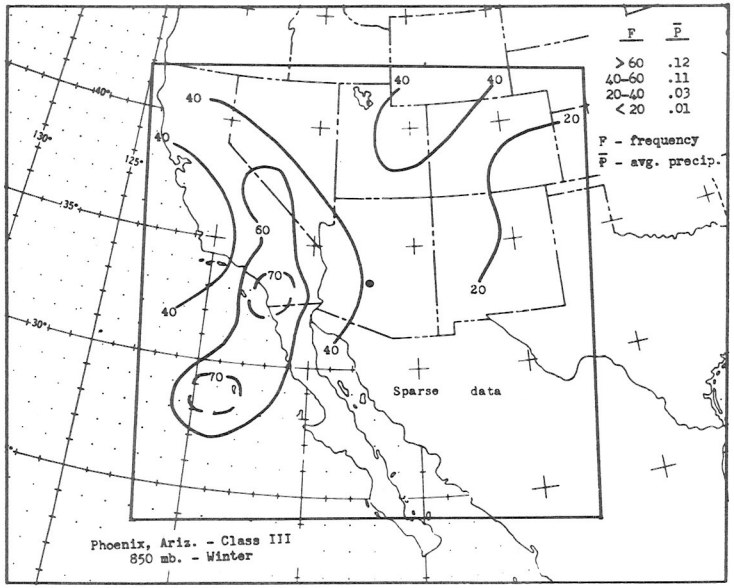

Chart 23 - IIIa

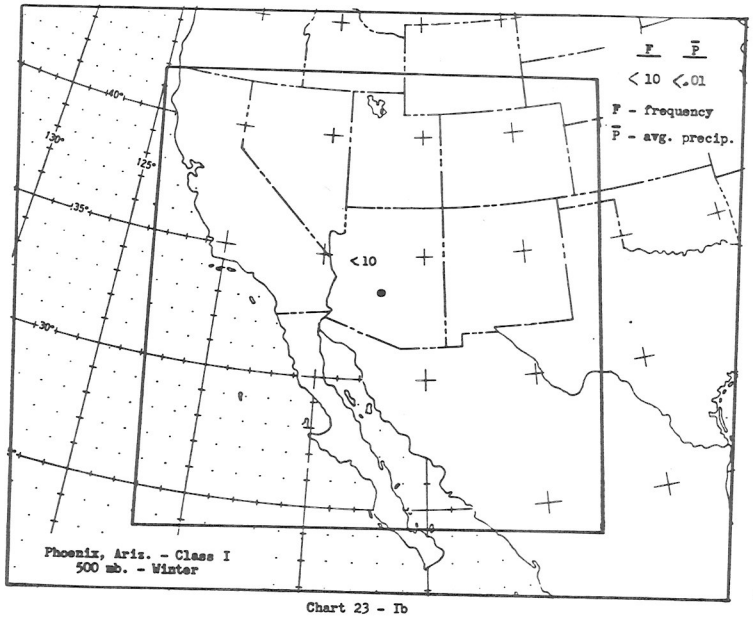

Chart 23 - Ib

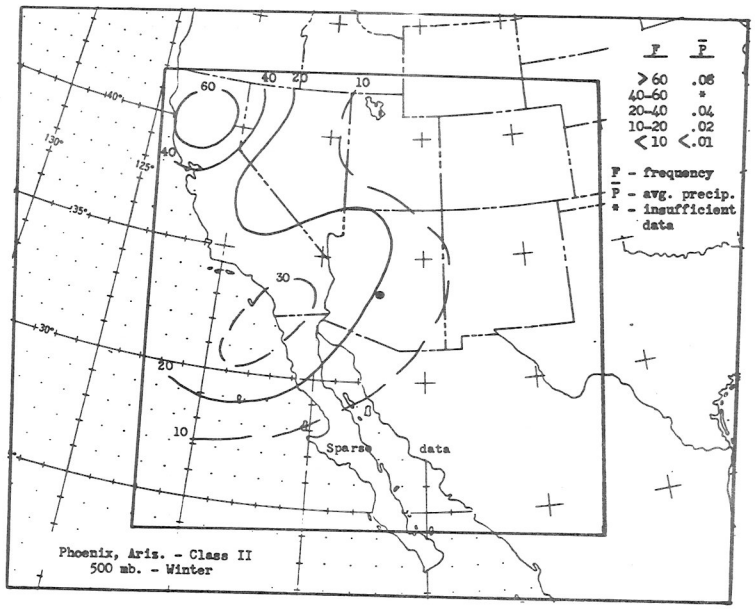

Chart 23 - IIb

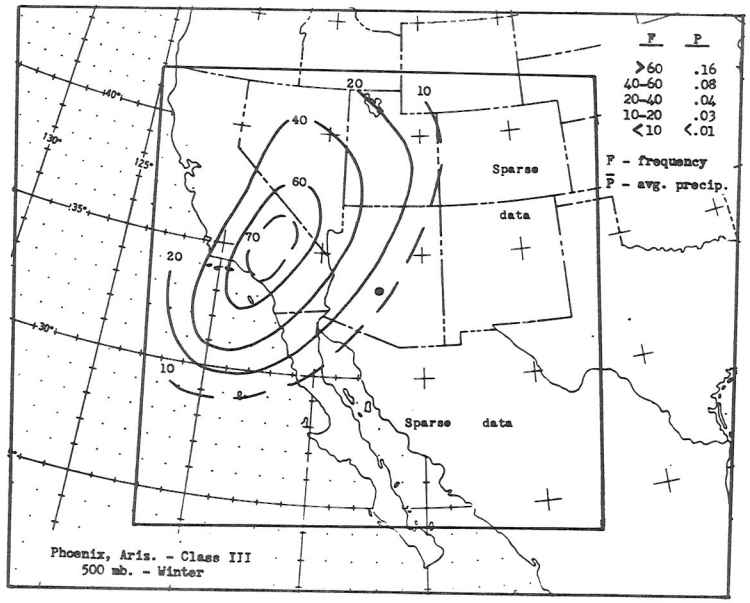

Chart 23 - IIIb

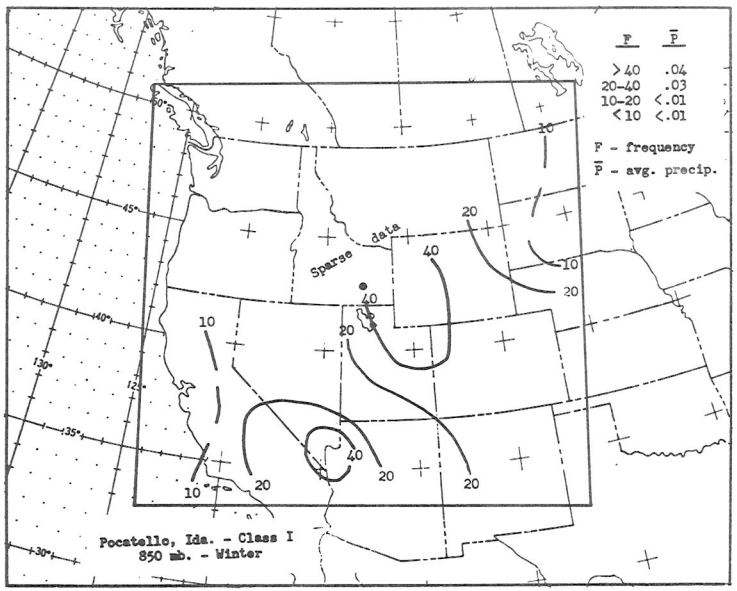

Chart 24 - Ia

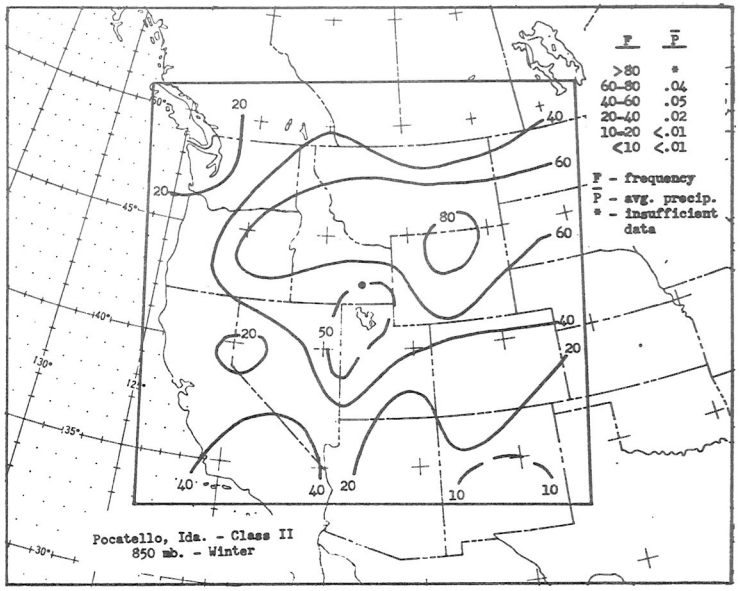

Chart 24 - IIa

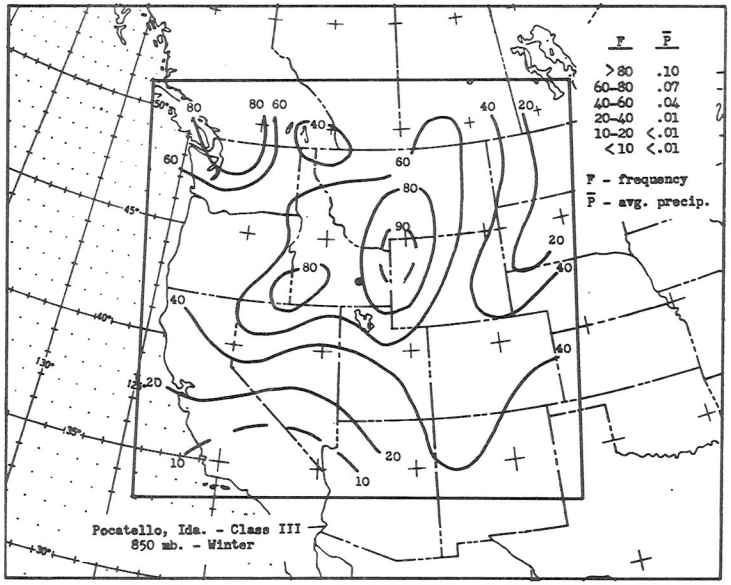

Chart 24 - IIIa

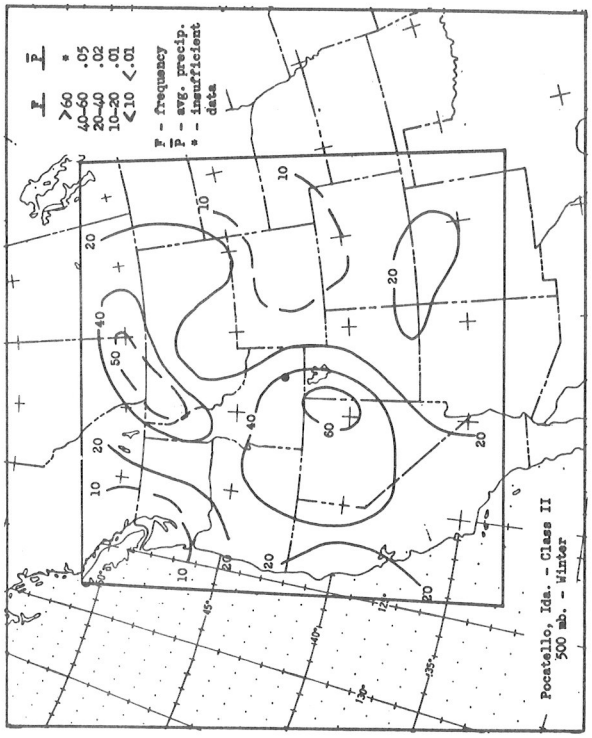

Chart 24 - IIb

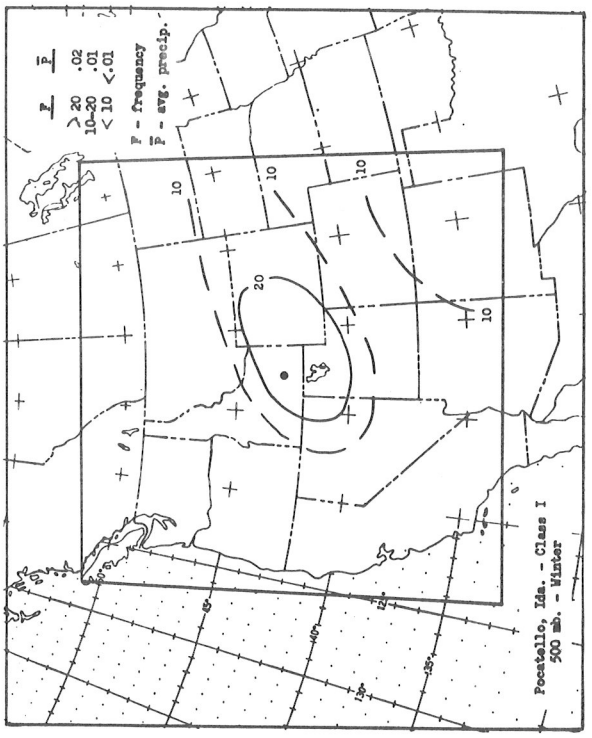

Chart 24 - Ib

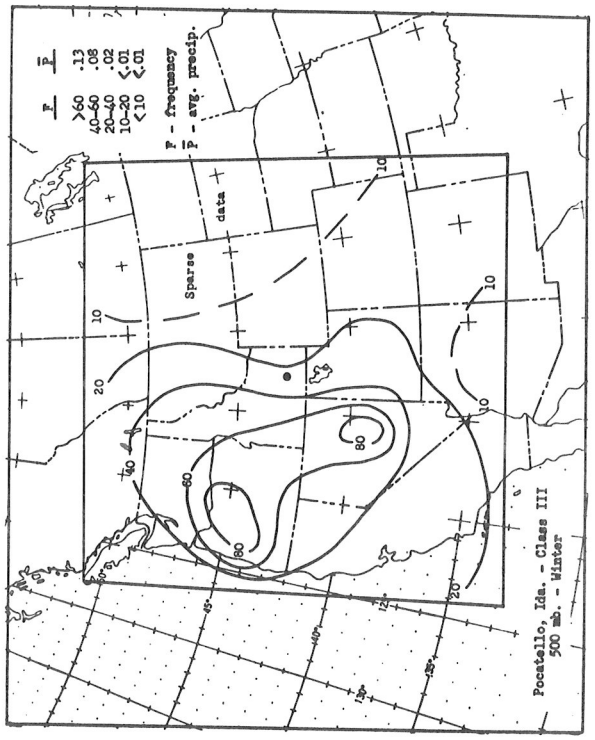

Chart 24 - IIIb

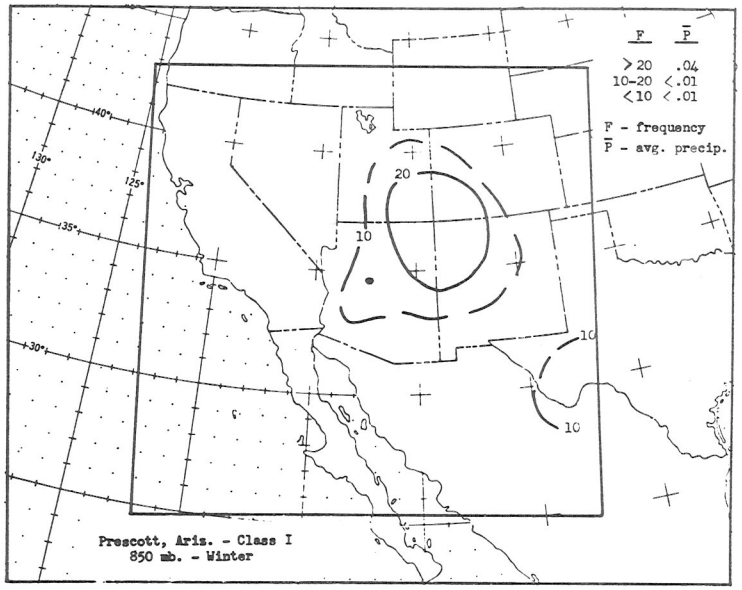

Chart 25 - Ia

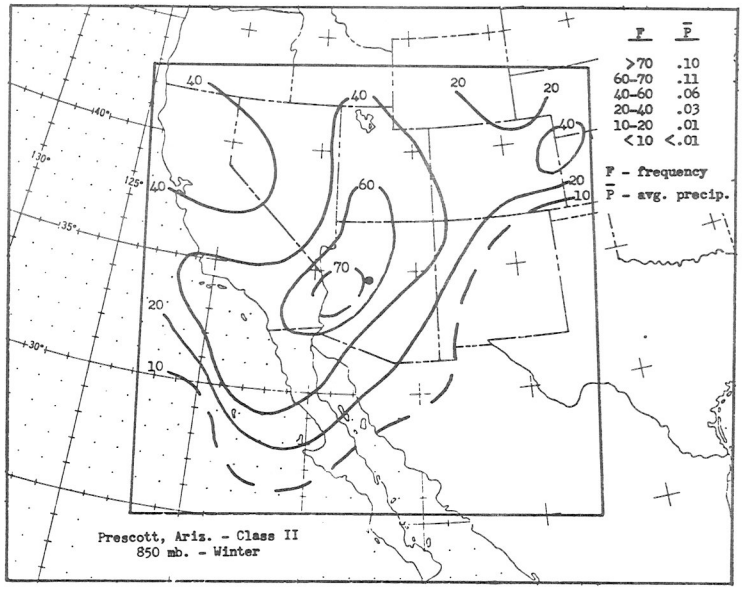

Chart 25 - IIa

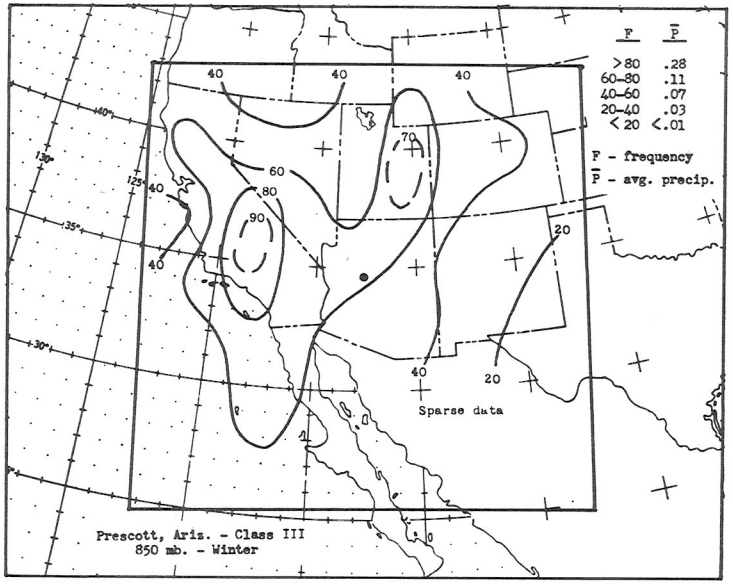

Chart 25 - IIIa

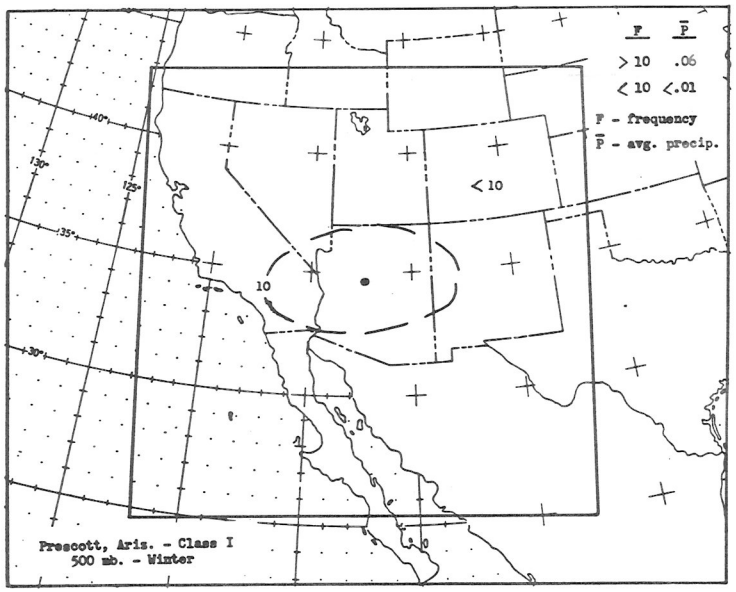

Chart 25 - Ib

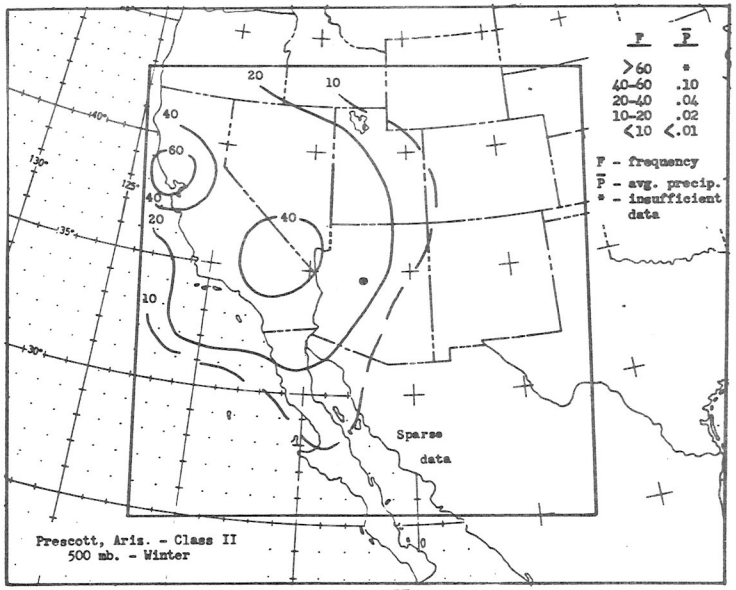

Chart 25 - IIb

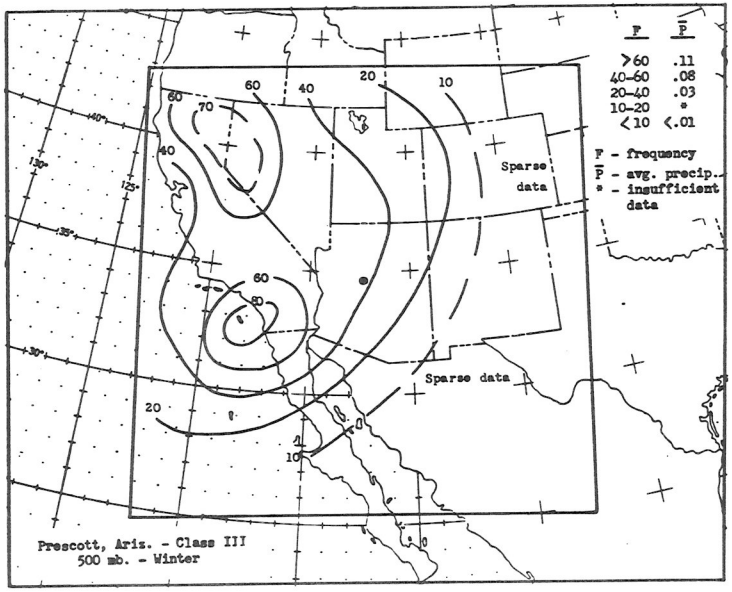

Chart 25 - IIIb

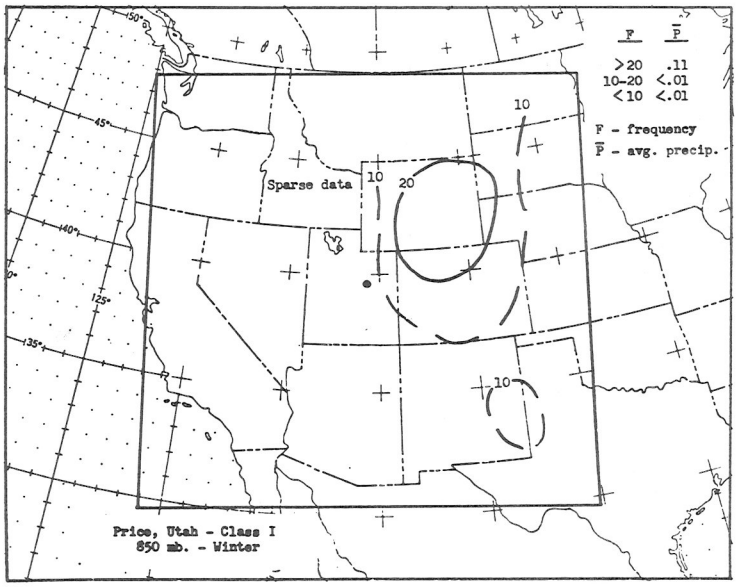

Chart 26 - Ia

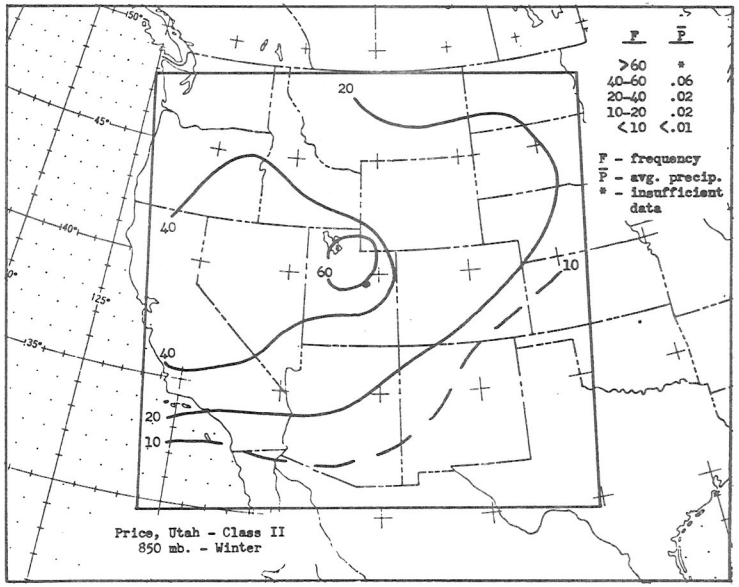

Chart 26 - IIa

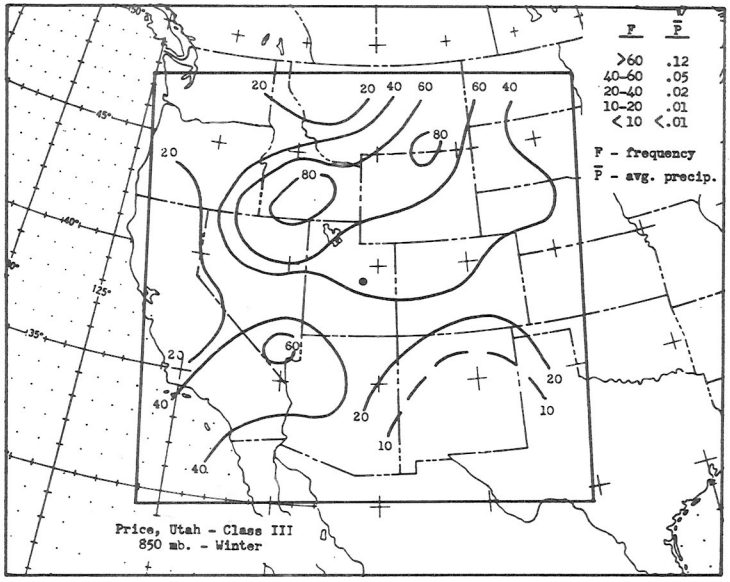

Chart 26 - IIIa

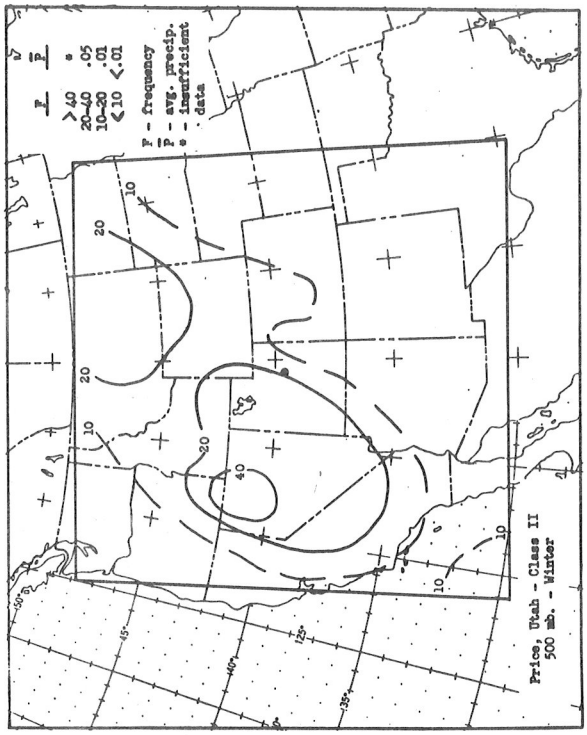

Chart 26 - IIb

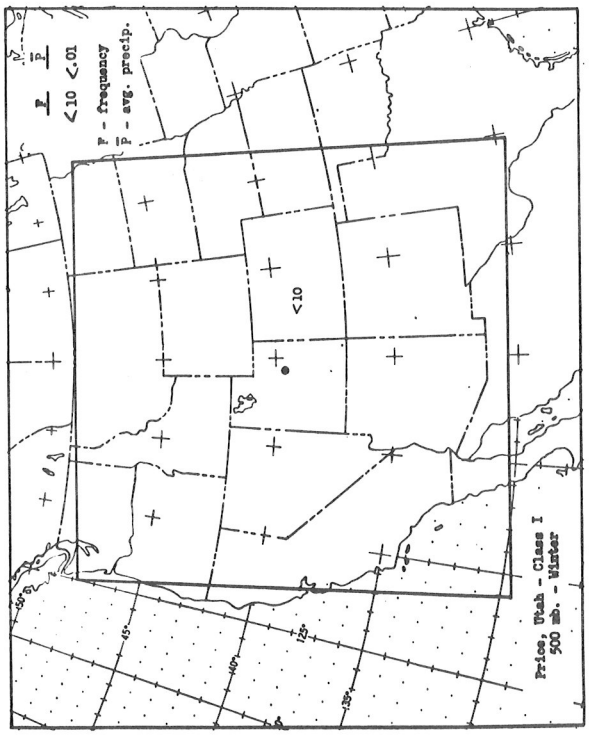

Chart 26 - Ib

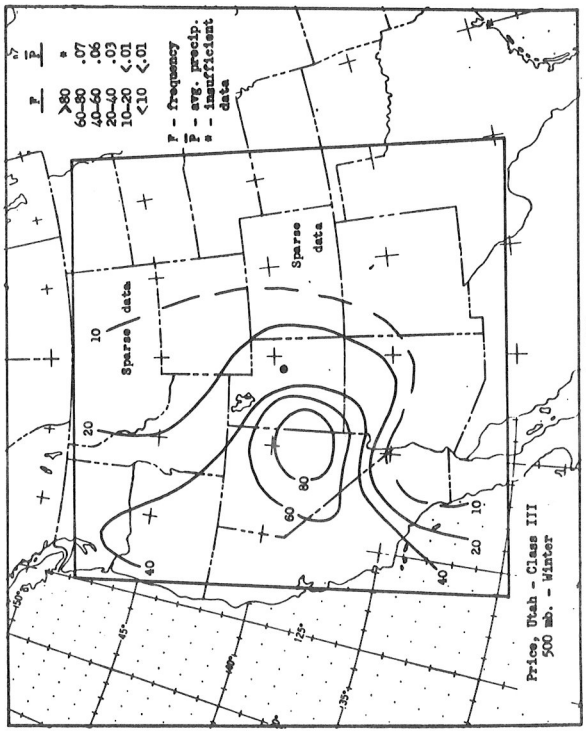

Chart 26 - IIIb

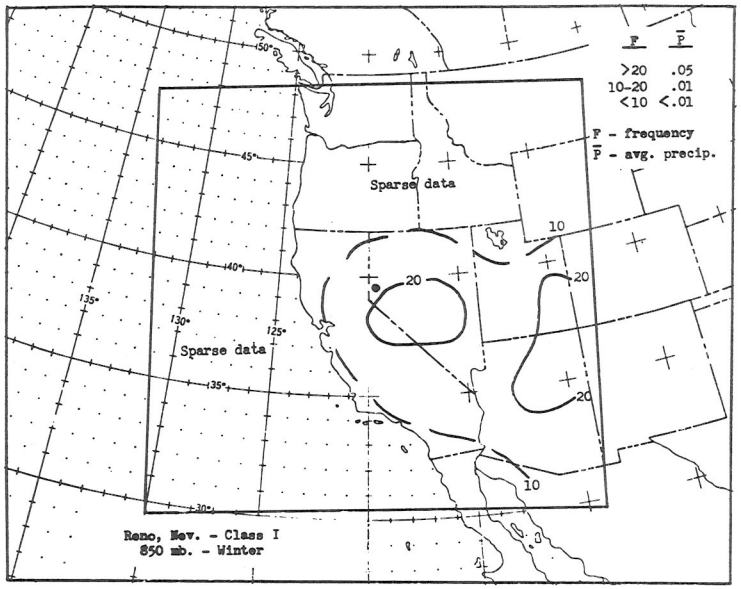

Chart 27 - Ia

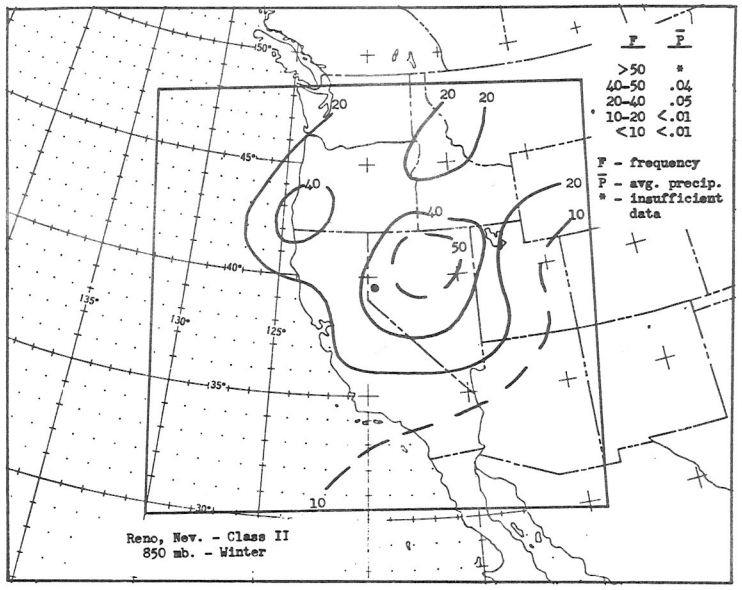

Chart 27 - IIa

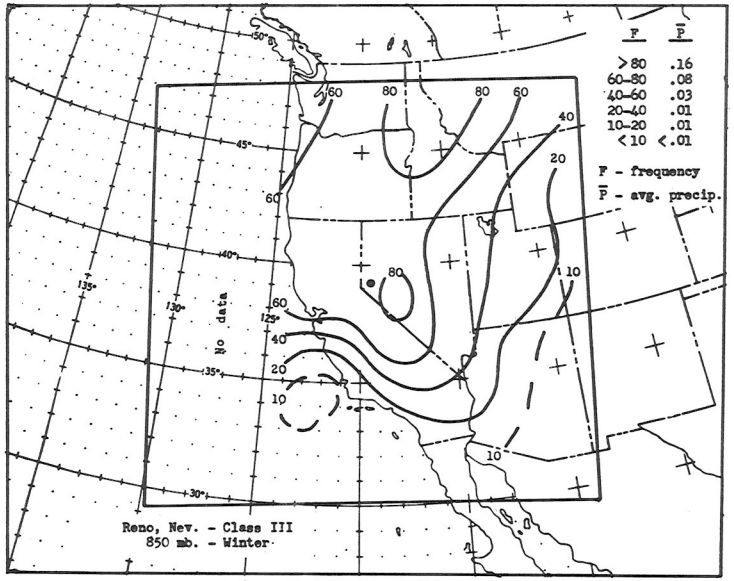

Chart 27 - IIIa

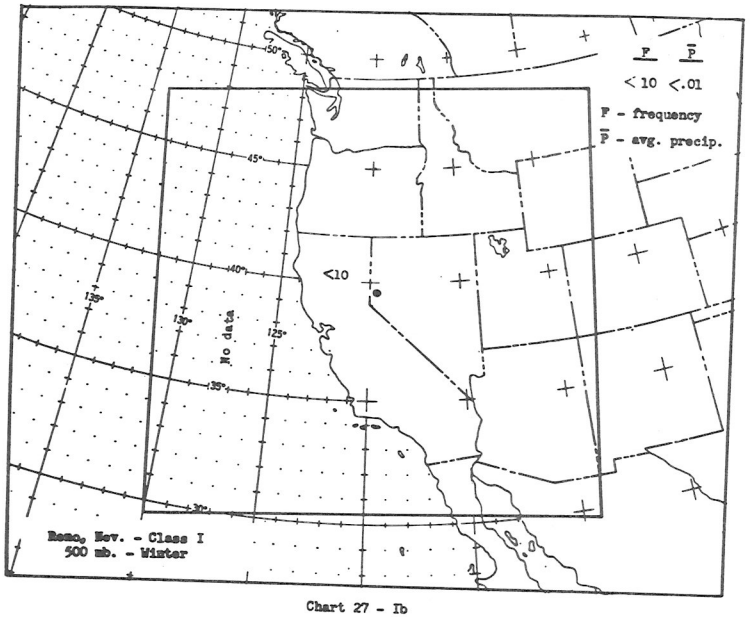

Chart 27 - Ib

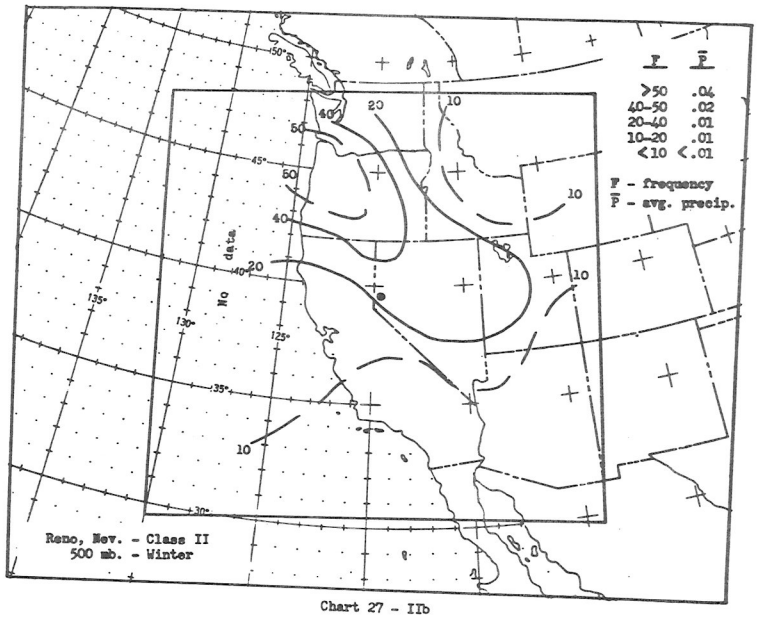

Chart 27 - IIb

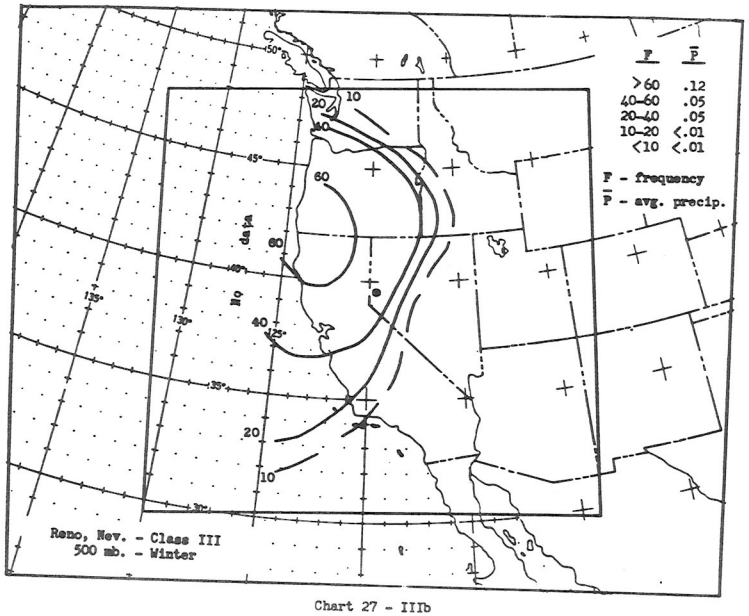

Chart 27 - IIIb

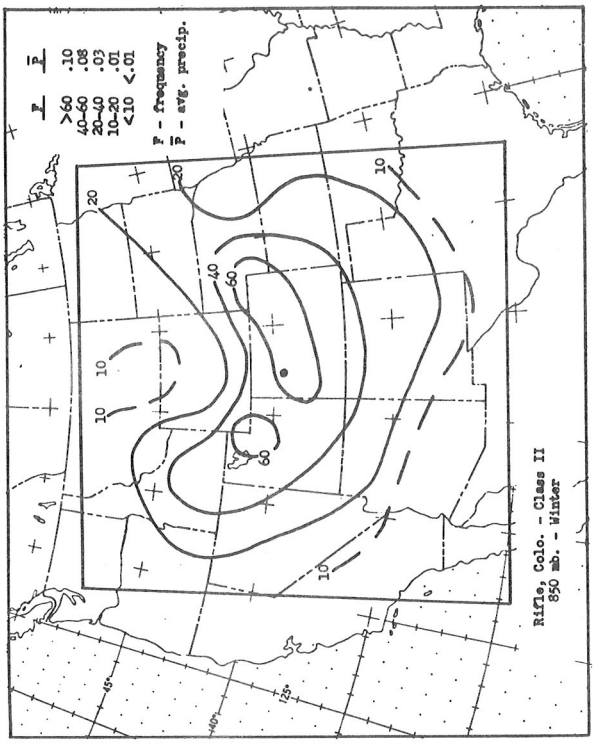

Chart 28 - IIa

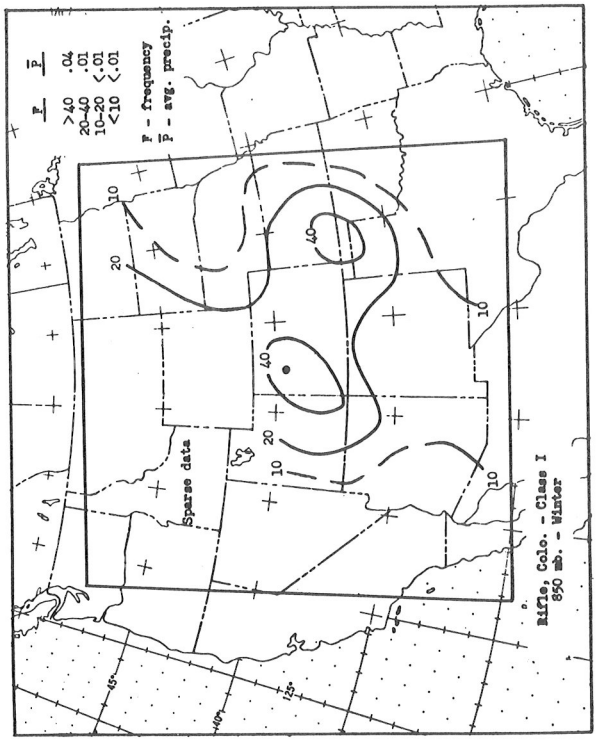

Chart 28 - Ia

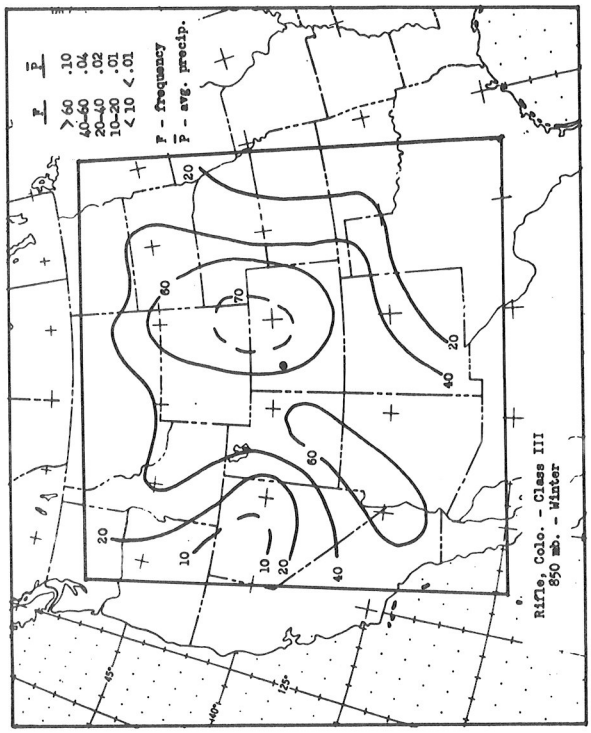

Chart 28 - IIIa

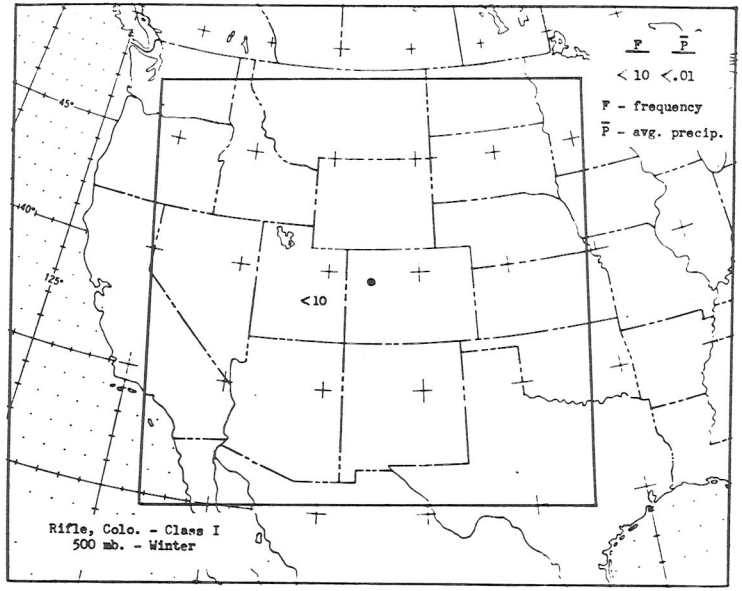

Chart 28 - Ib

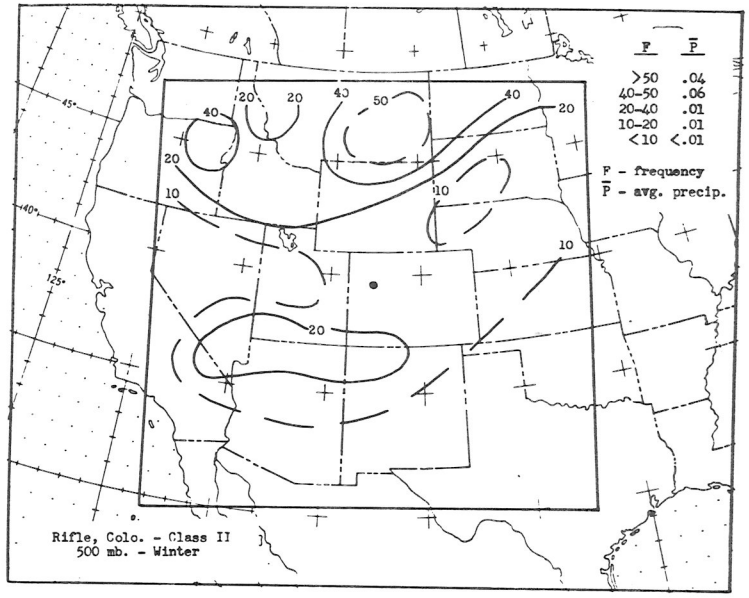

Chart 28 - IIb

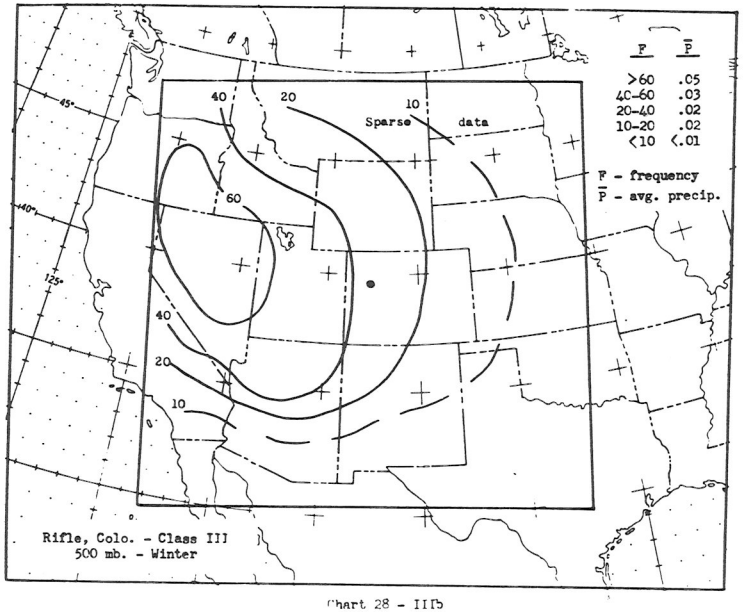

Chart 28 - IIIb

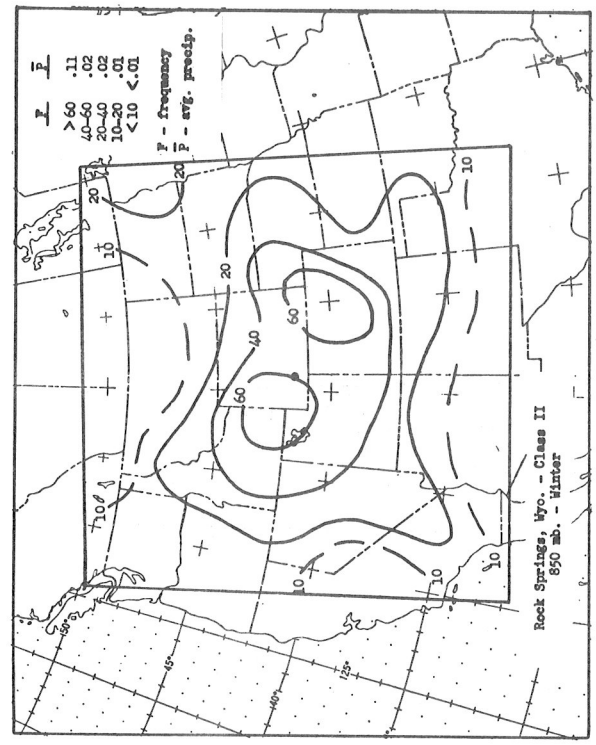

Chart 29 - IIa

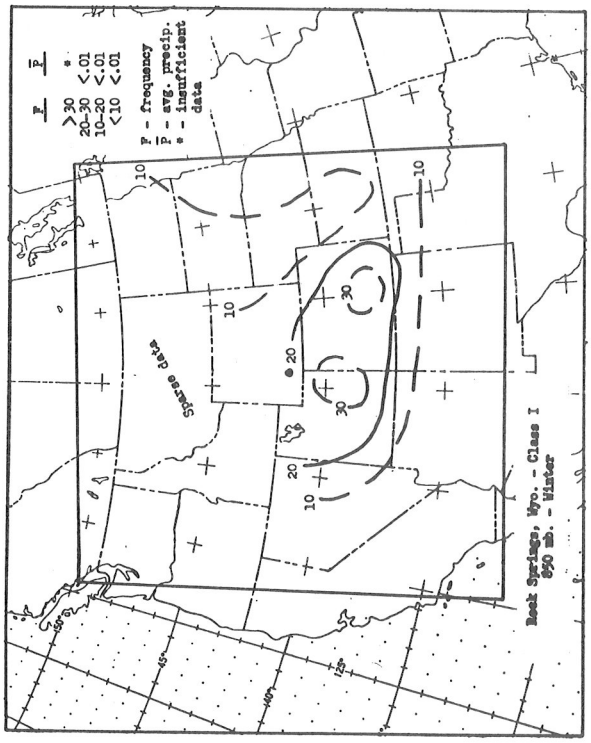

Chart 29 - Ia

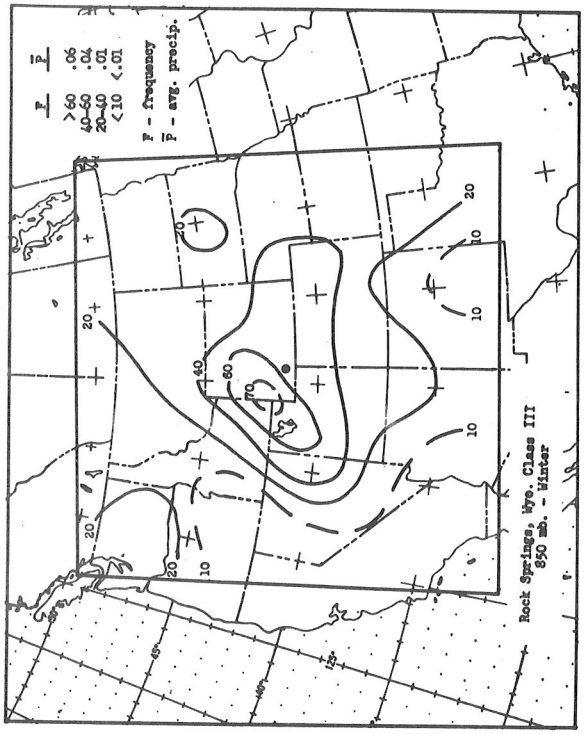

Chart 29 - IIIa

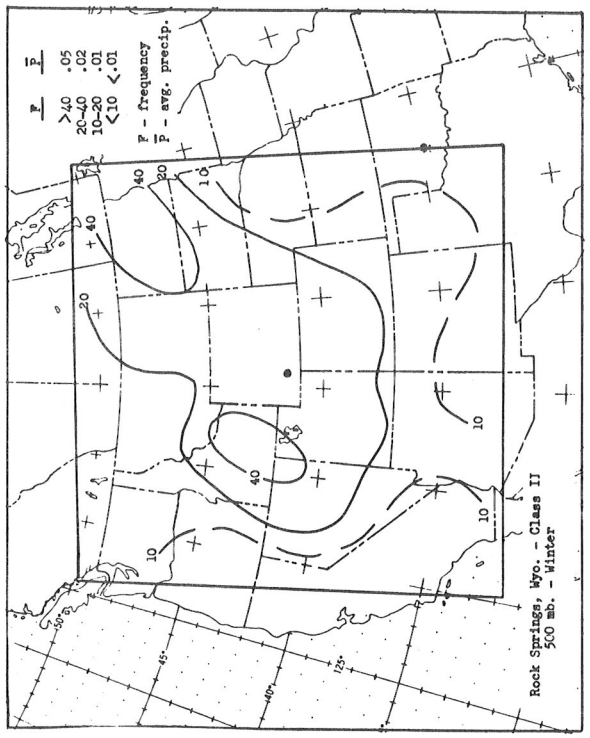

Chart 29 - IIb

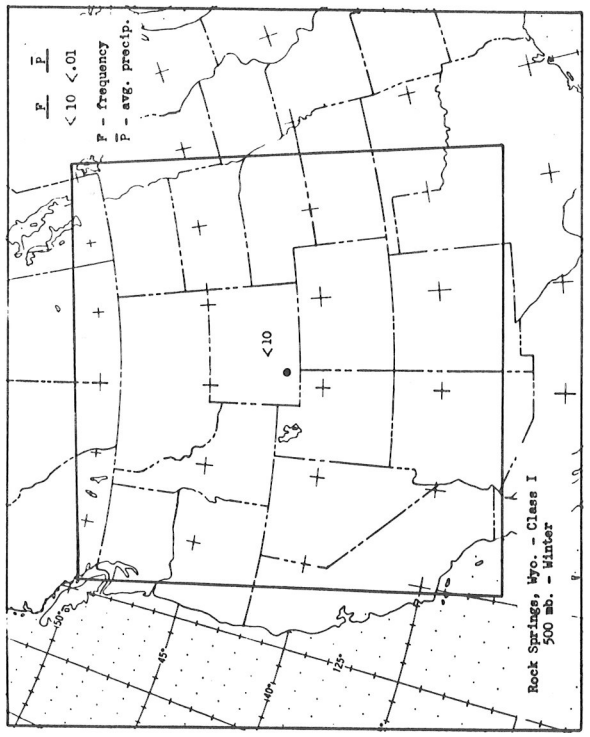

Chart 29 - Ib

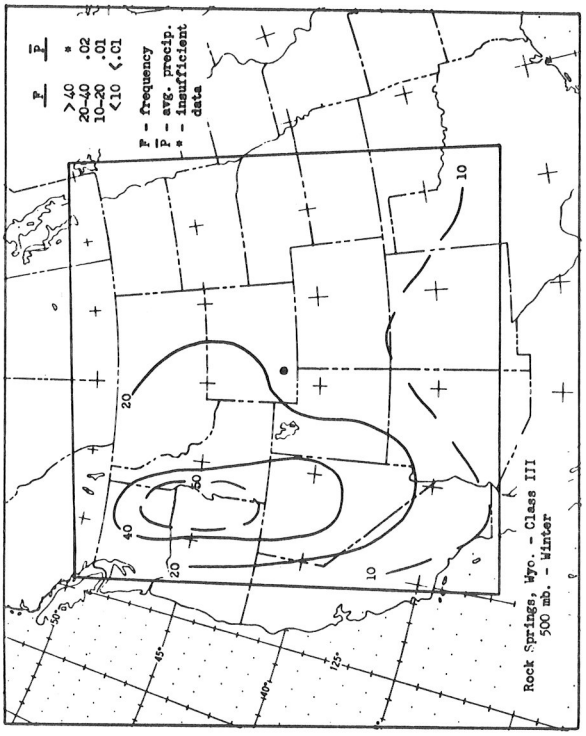

Chart 29 - IIIb

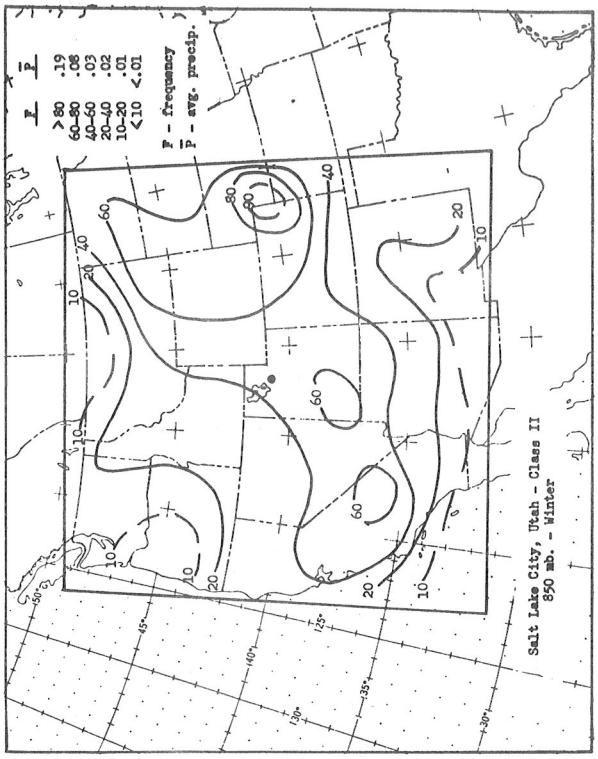

Chart 30 - IIa

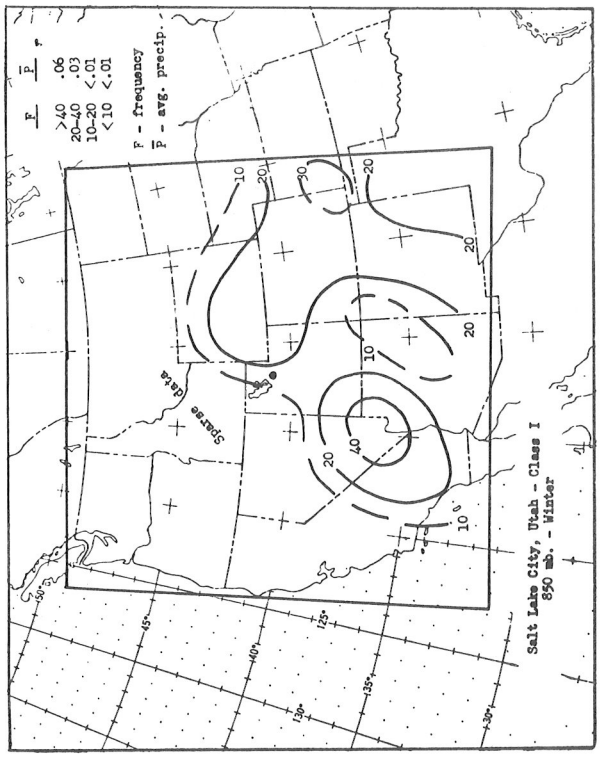

Chart 30 - Ia

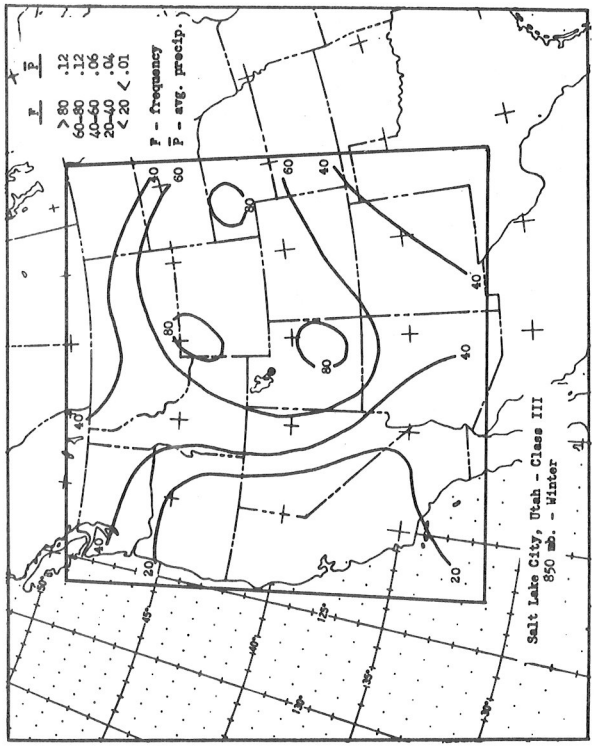

Chart 30 - IIIa

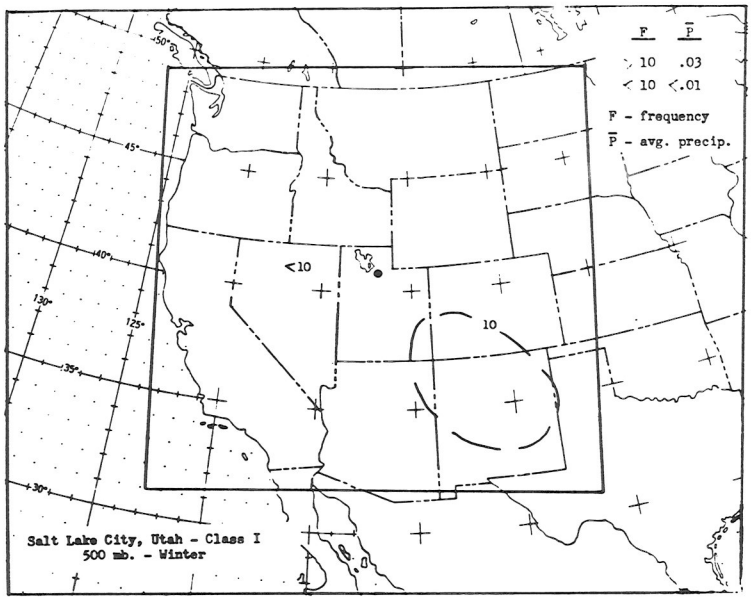

Chart 30 - Ib

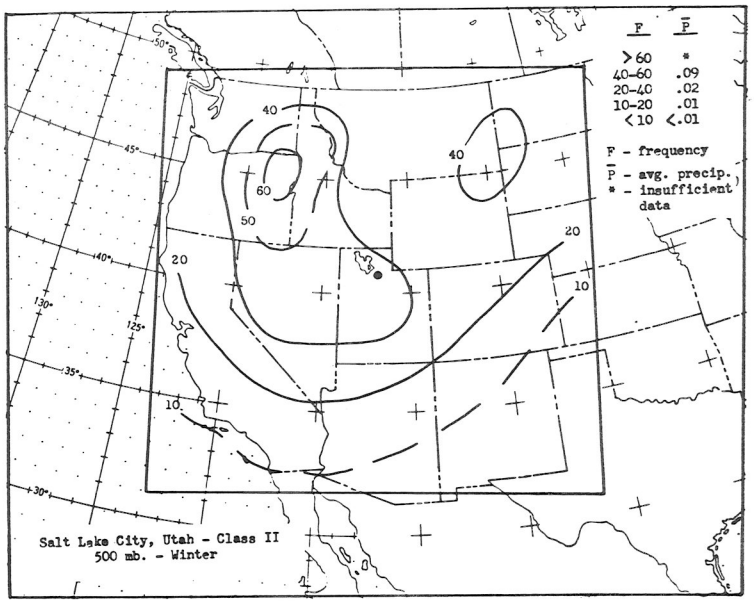

Chart 30 - IIb

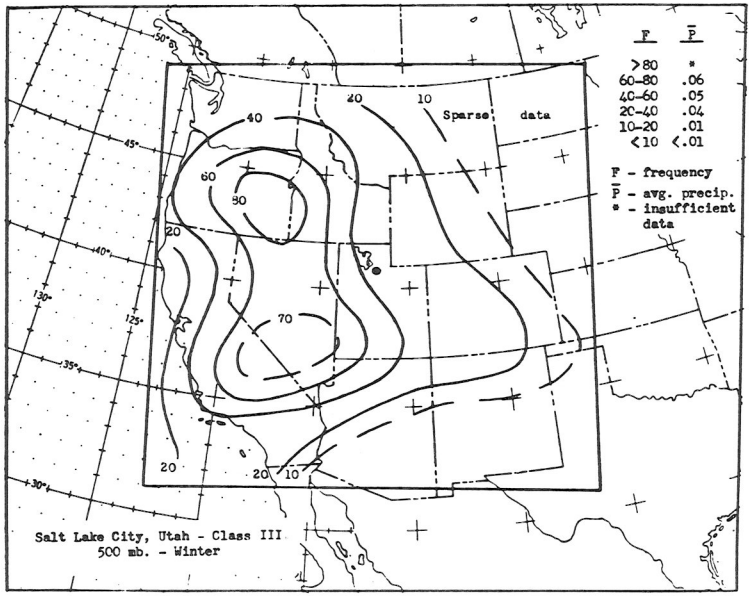

Chart 30 - IIIb

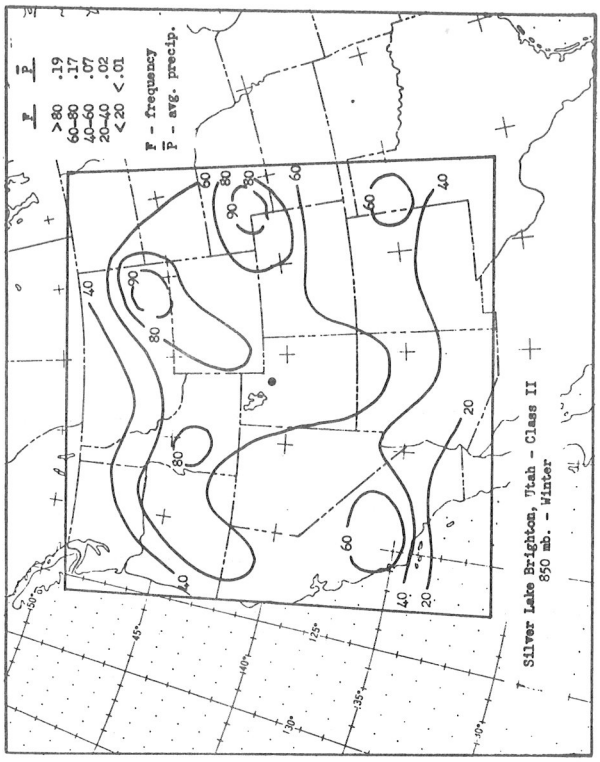

Chart 31 - IIa

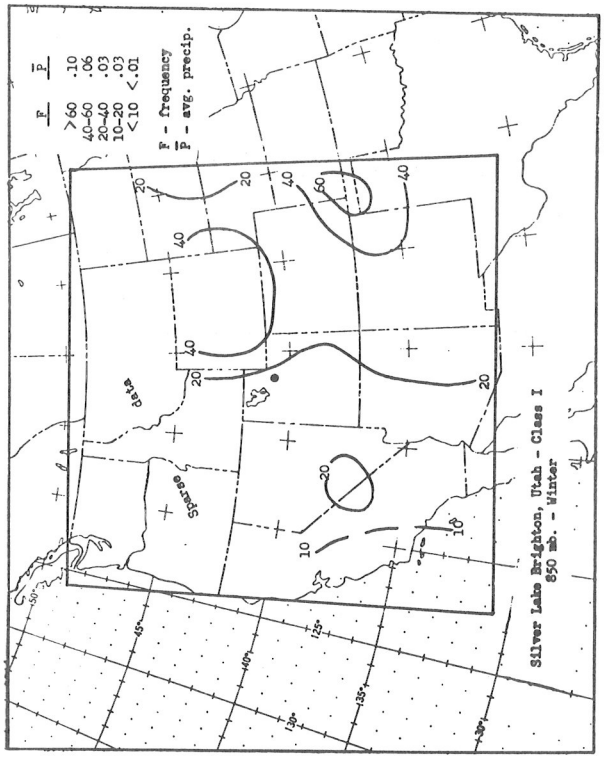

Chart 31 - Ia

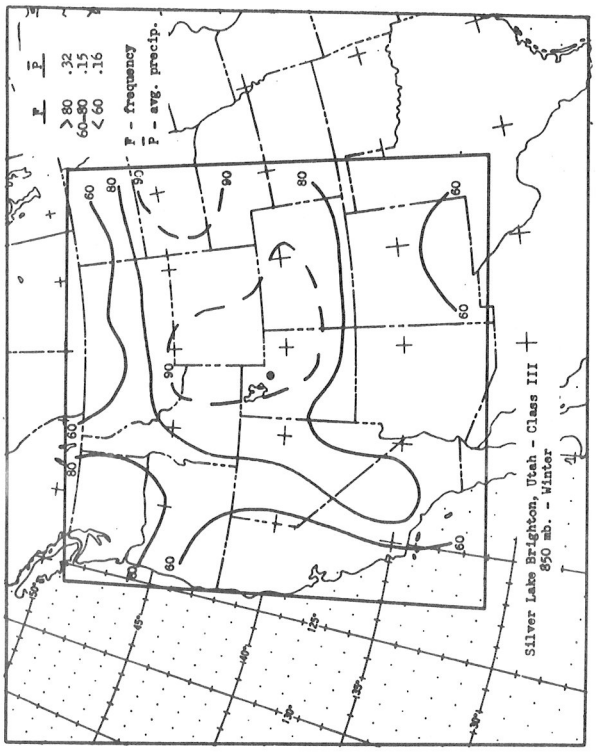

Chart 31 - IIIa

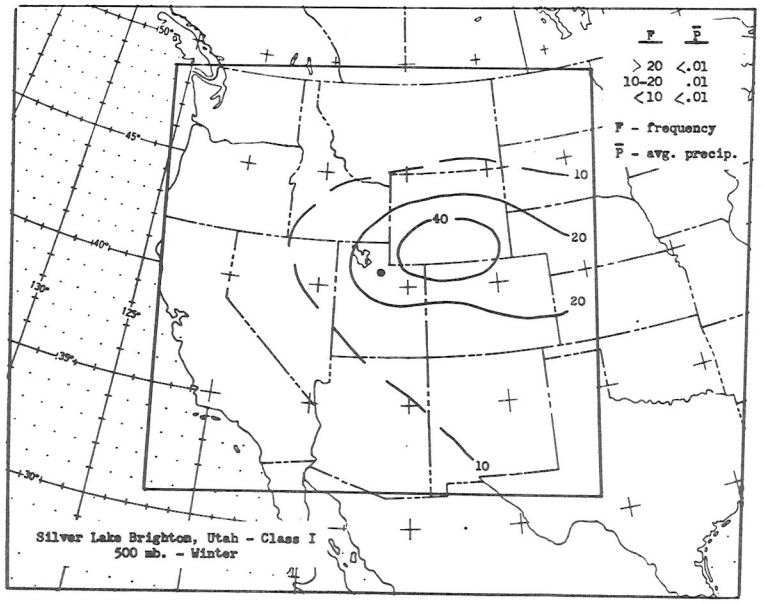

Chart 31 - Ib

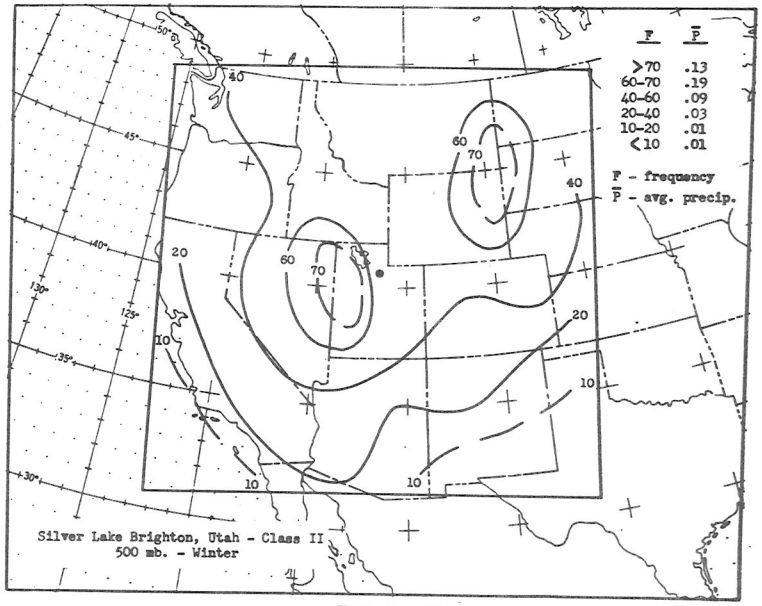

Chart 31 - IIb

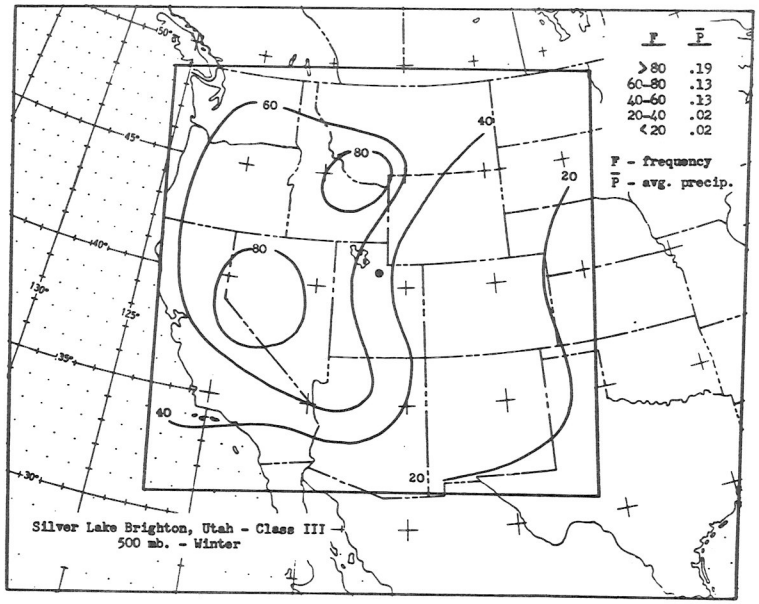

Chart 31 - IIIb

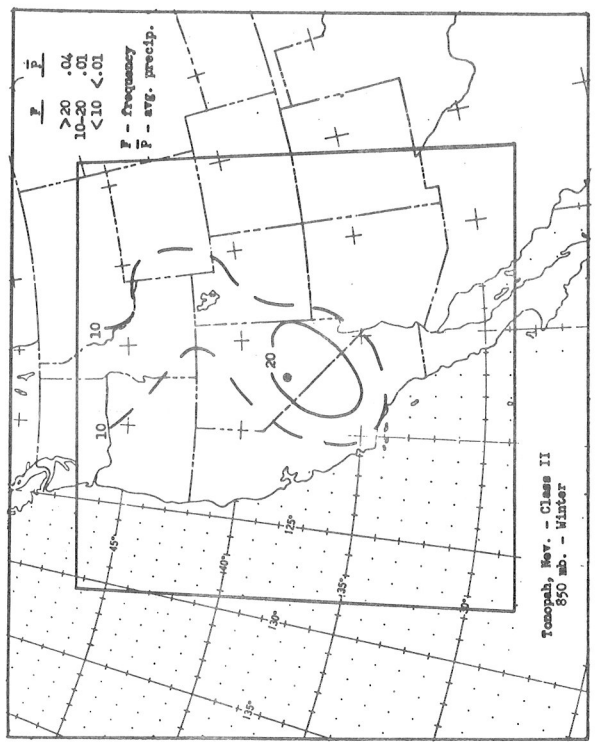

Chart 32 - IIa

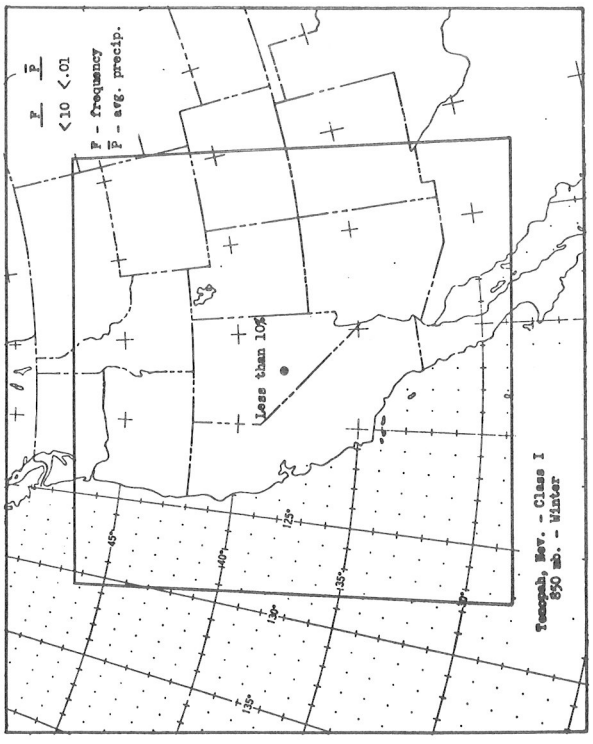

Chart 32 - Ia

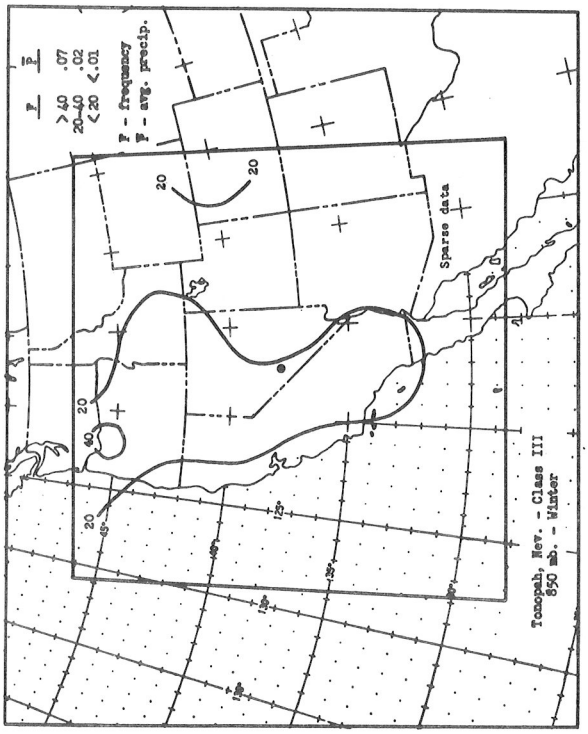

Chart 32 - IIIa

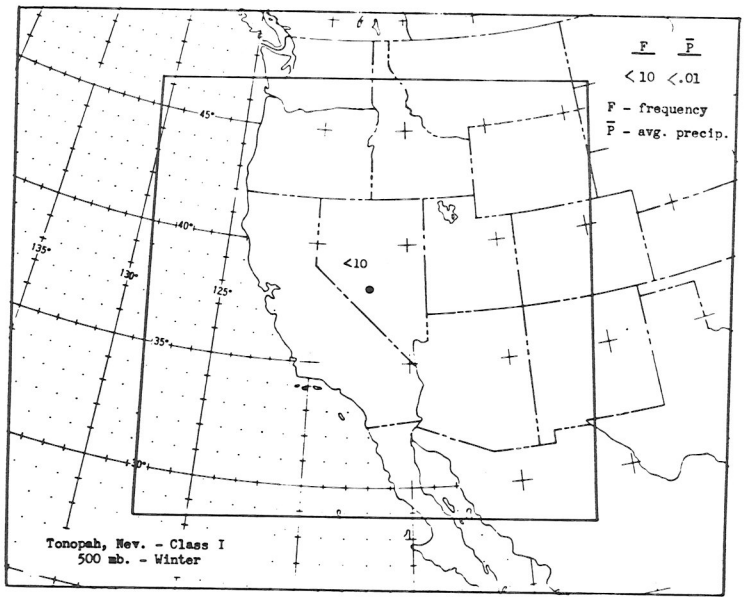

Chart 32 - Ib

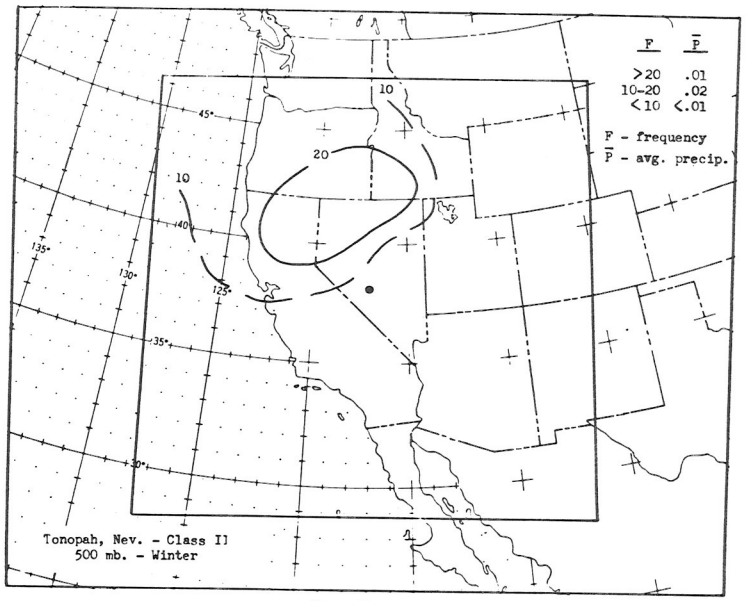

Chart 32 - IIb

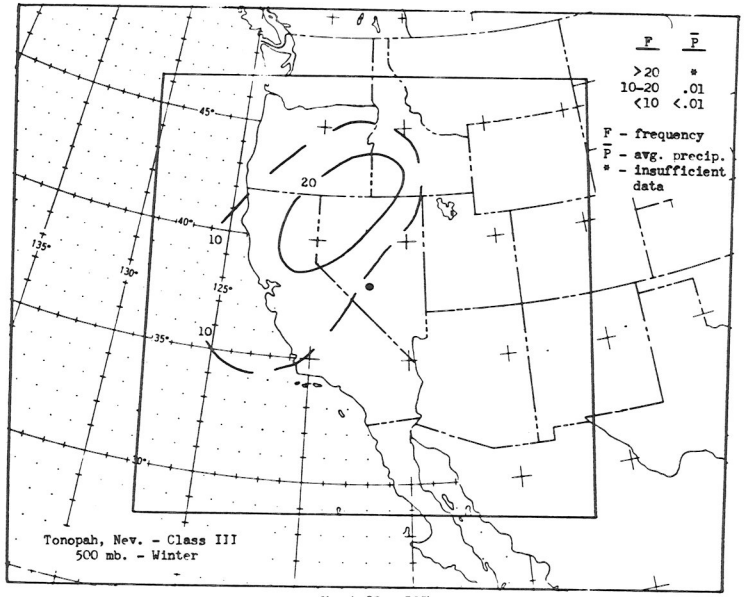

Chart 32 - IIIb

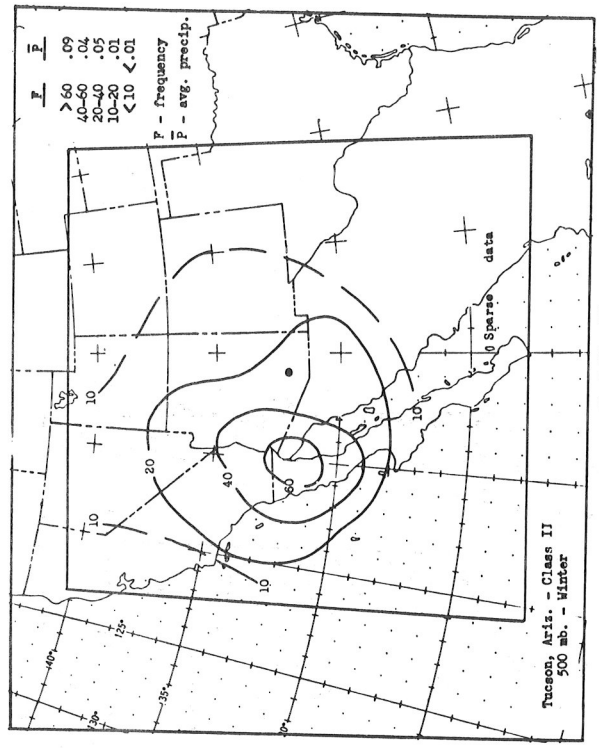

Chart 33 - IIb

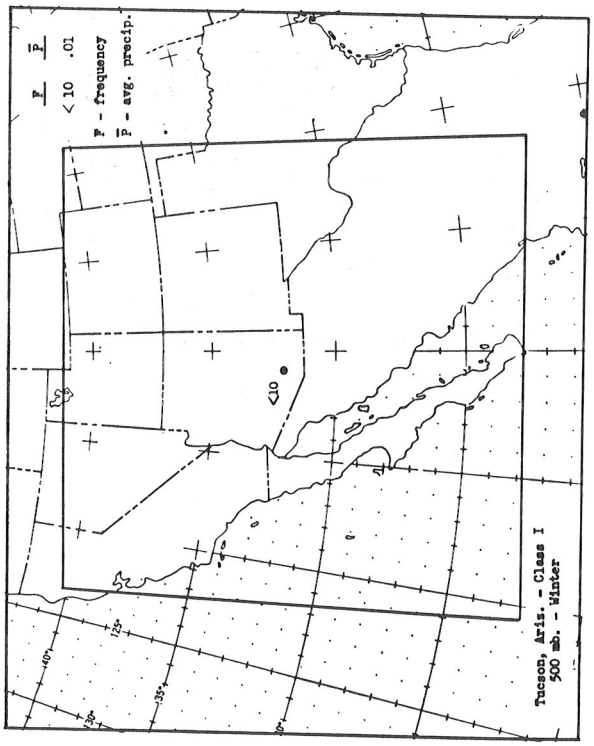

Chart 33 - Ib

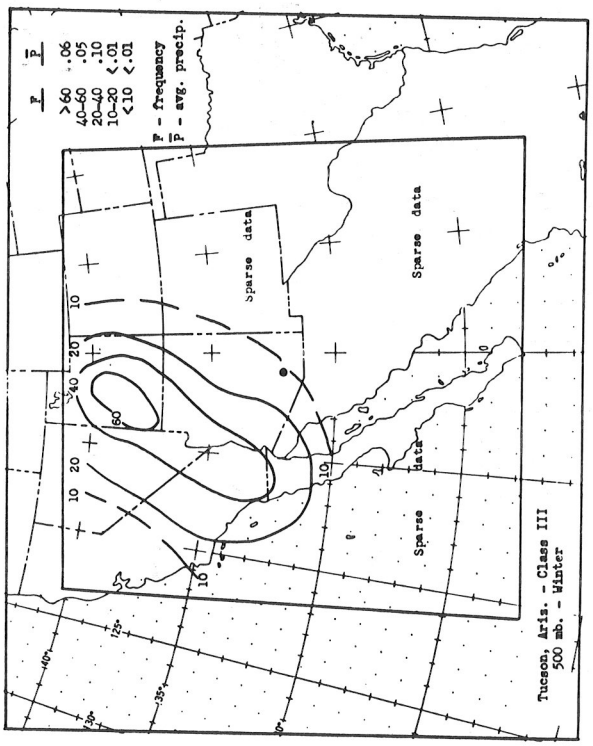

Chart 33 - IIIb

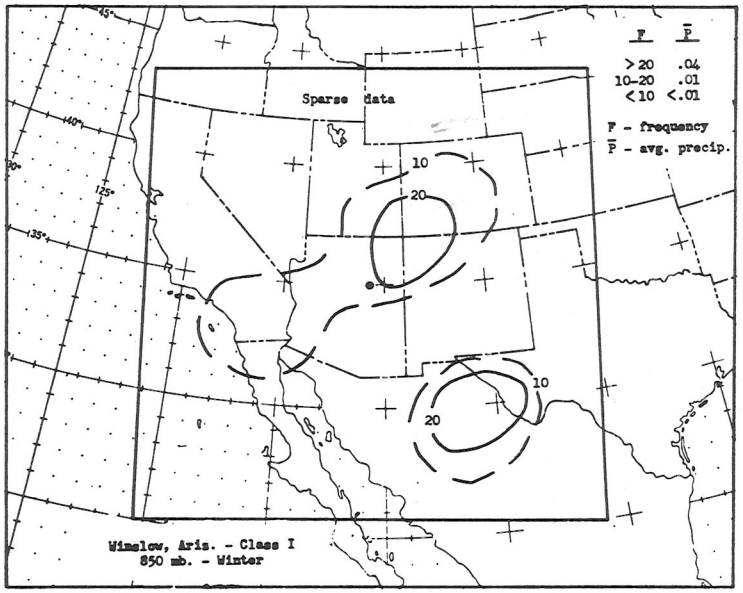

Chart 34 - Ia

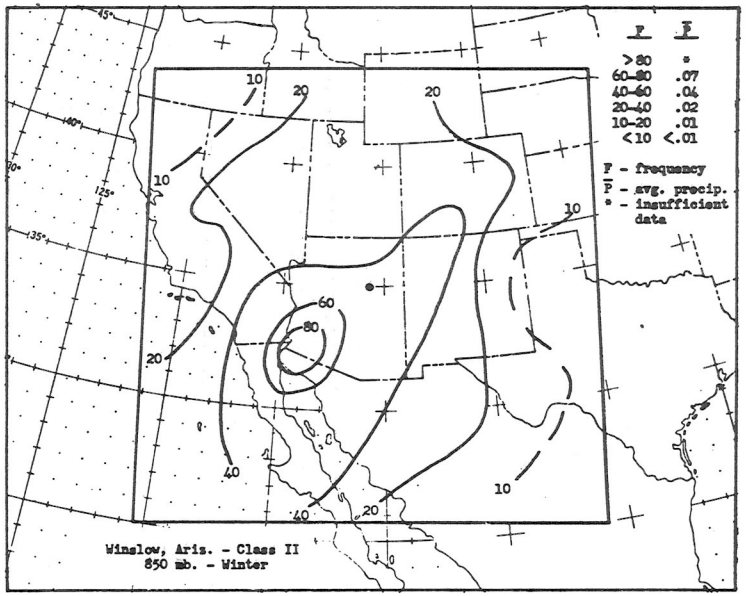

Chart 34 - IIa

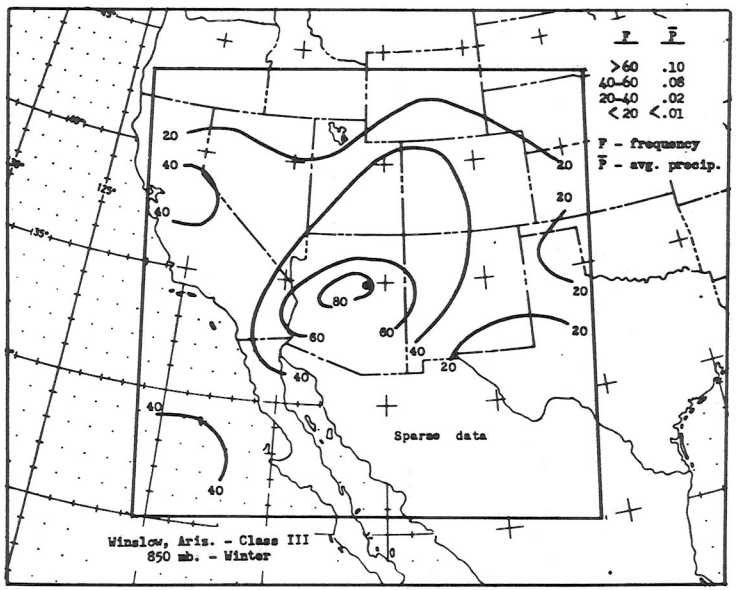

Chart 34 - IIIa

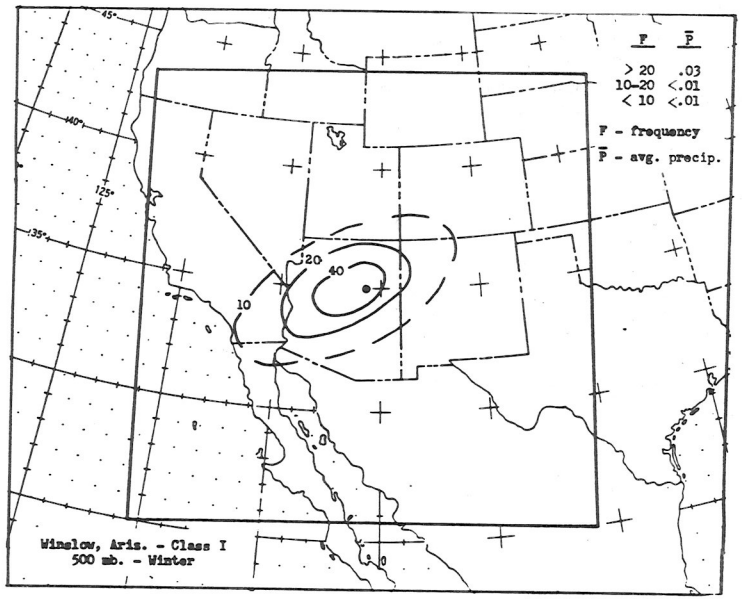

Chart 34 - Ib

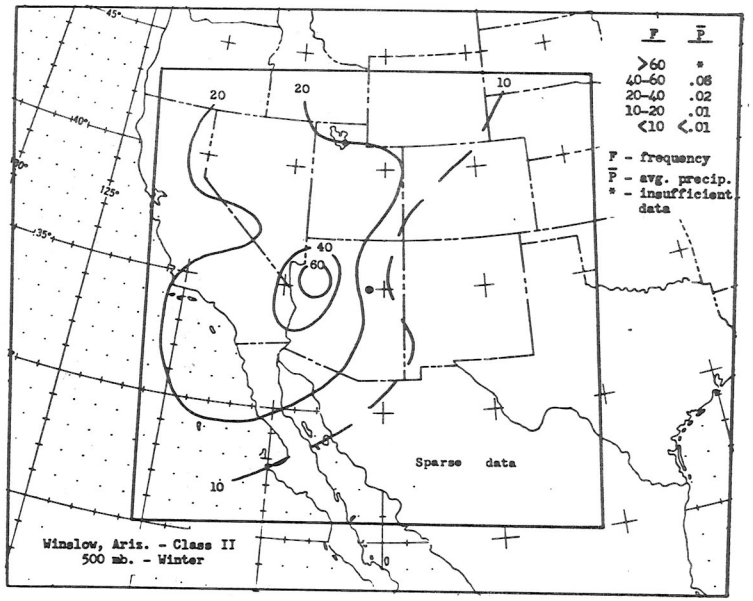

Chart 34 - IIb

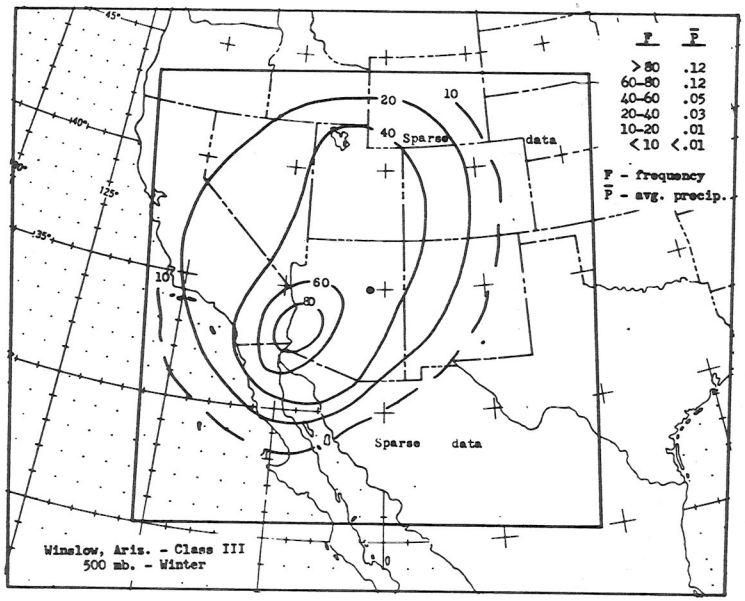

Chart 34 - IIIb

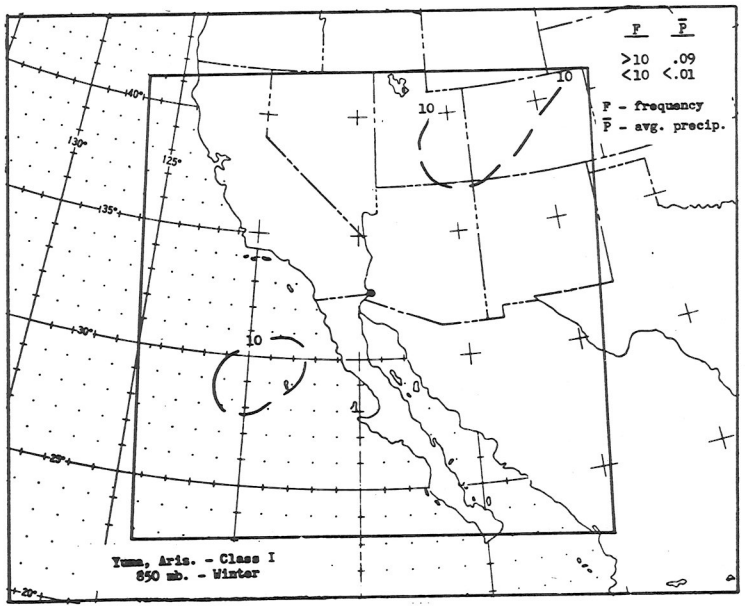

Chart 35 - Ia

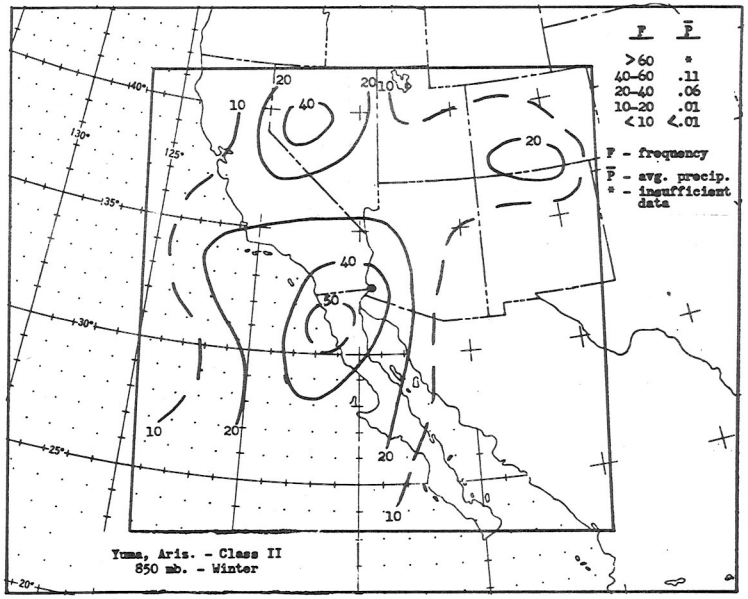

Chart 35 - IIa

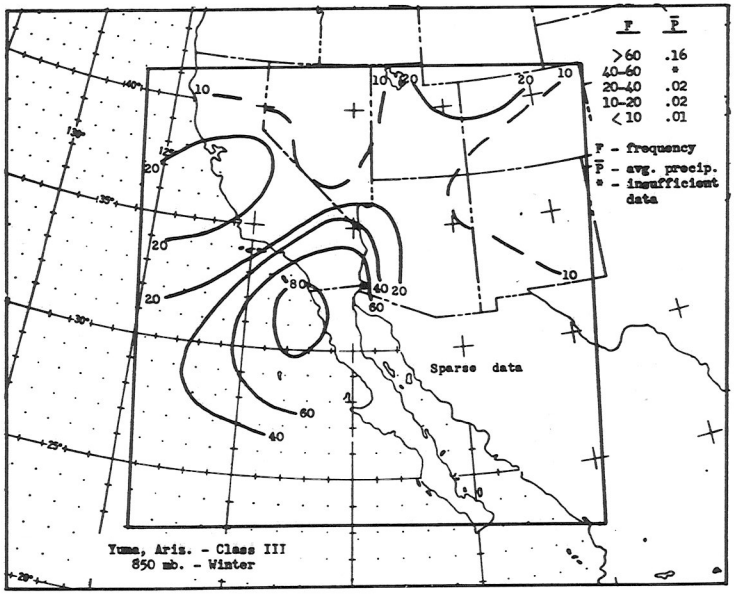

Chart 35 - IIIa

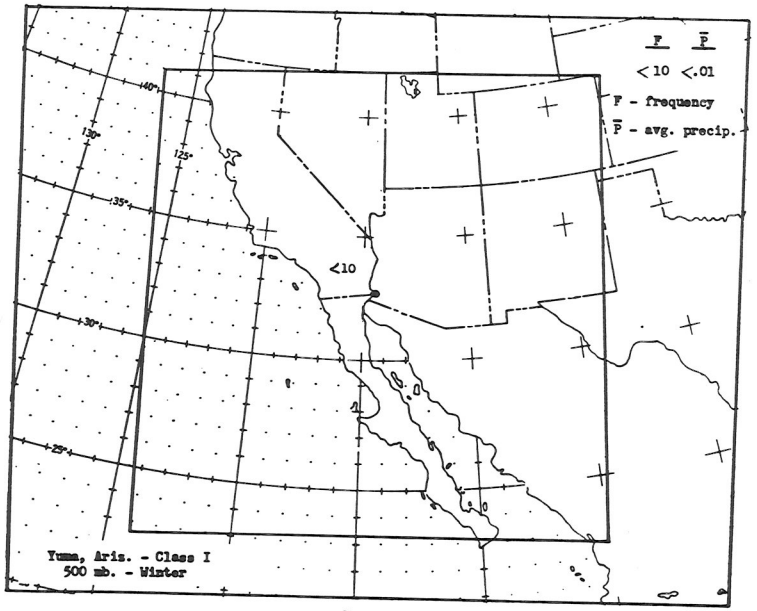

Chart 35 - Ib

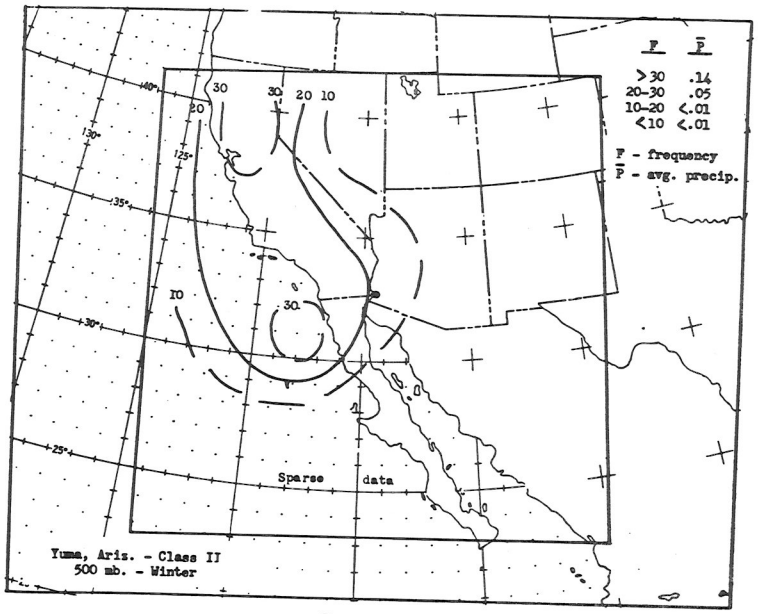

Chart 35 - IIb

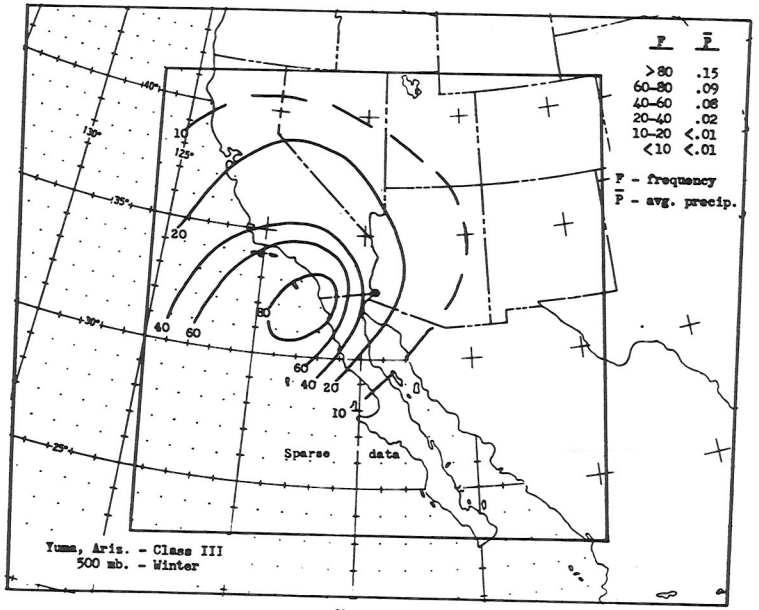

Chart 35 - IIIb

(Continued from inside front cover)

WBTM TDL 13 Interim Report on Sea and Swell Forecasting. N. A. Pore and W. S. Richardson, December 1967. (PB-177 038)

WBTM TDL 14 Meteorological Analysis of 1964-65 ICAO Turbulence Data. DeVer Colson, September 1968. (PB-180 268)

WBTM TDL 15 Prediction of Temperature and Dew Point by Three-Dimensional Trajectories. Ronald M. Reap, September 1968. (PB-180 727)

WBTM TDL 16 Objective Visibility Forecasting Techniques Based on Surface and Tower Observations. Donald M. Gales, October 1968. (PB-180 479)

WBTM TDL 17 Second Interim Report on Sea and Swell Forecasting. N. A. Pore and Lt. W. S. Richardson, USESSA, January 1969. (PB-182 273)

WBTM TDL 18 Conditional Probabilities of Precipitation Amounts in the Conterminous United States. Donald L. Jorgensen, William H. Klein, and Charles F. Roberts, March 1969. (PB-183 144)

WBTM TDL 19 An Operationally Oriented Small-Scale 500-Millibar Height Analysis. Harry R. Glahn and George W. Hollenbaugh, March 1969.

WBTM TDL 20 A Comparison of Two Methods of Reducing Truncation Error. Robert J. Bermowitz, May 1969. (PB-184 741)

WBTM TDL 21 Automatic Decoding of Hourly Weather Reports. George W. Hollenbaugh, Harry R. Glahn, and Dale A. Lowry, July 1969. (PB-185 806)

WBTM TDL 22 An Operationally Oriented Objective Analysis Program. Harry R. Glahn, George W. Hollenbaugh, and Dale A. Lowry, July 1969.

WBTM TDL 23 An Operational Subsynoptic Advection Model. Harry R. Glahn, Dale A. Lowry, and George W. Hollenbaugh, July 1969.

WBTM TDL 24 A Lake Erie Storm Surge Forecasting Technique. William S. Richardson and N. Arthur Pore, August 1969. (PB-185 778)